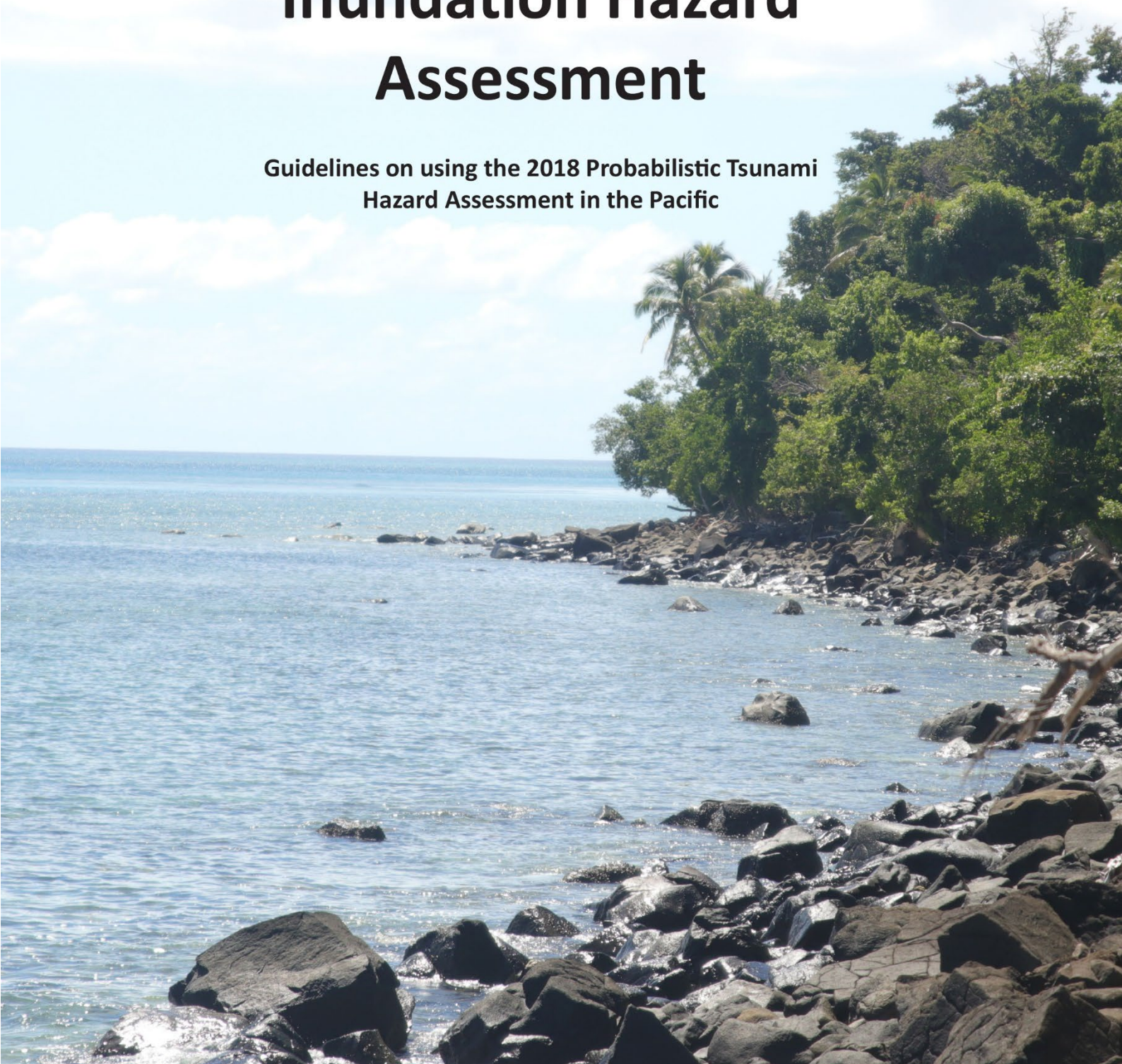




Pacific
Community
Communauté
du Pacifique

Earthquake Scenario Selection for Tsunami Inundation Hazard Assessment

Guidelines on using the 2018 Probabilistic Tsunami
Hazard Assessment in the Pacific



Earthquake Scenario Selection for Tsunami Inundation Hazard Assessment

Guidelines on using the 2018 Probabilistic Tsunami
Hazard Assessment in the Pacific



Australian Government
Geoscience Australia

Suva, Fiji, 2022

© Pacific Community (SPC) and the Commonwealth of Australia (Geoscience Australia), 2022

The text and illustrations in this document are available for reproduction under Creative Commons Attribution 4.0 International License (CC BY 4.0). This license does not extend to the use of any Pacific Community (SPC) or the Commonwealth of Australia (Geoscience Australia)'s coats of arms, marks, logos, icons or design elements.

Original text: English

Pacific Community Cataloguing-in-publication data

Earthquake scenario selection for tsunami inundation hazard assessment: guidelines on using the 2018 Probabilistic Tsunami Hazard Assessment in the Pacific

1. Natural disasters – Oceania.
2. Tsunamis – Oceania.
3. Tsunami damage – Oceania.
4. Tsunamis – Oceania – Handbooks, manuals, etc.
5. Earthquake prediction – Oceania – Handbooks, manuals, etc.
6. Earthquake hazard analysis – Oceania.
7. Earthquake hazard analysis – Oceania – Handbooks, manuals, etc.

I. Title II. Pacific Community

551.46370995

AACR2

ISBN: 978-982-00-1347-6



Rights and permissions AACR2

This publication is available under [Creative Commons Attribution 4.0 International License \(CC BY 4.0\)](https://creativecommons.org/licenses/by/4.0/).

Disclaimer: While efforts have been made to ensure the accuracy and reliability of the material contained in this manual, the Pacific Community and Geoscience Australia cannot guarantee that the information is free from errors or omissions. They do not accept any form of liability, contractual or otherwise, for the content of this manual or for any consequences arising from its use.

Attribution: Please cite this publication as follows –

Giblin, J., Damlamian, H., Davies, G., Weber, R. & Wilson, K. 2022. *Earthquake scenario selection for tsunami inundation hazard assessment: Guideline on using the 2018 Probabilistic Tsunami Hazard Assessment in the Pacific*. Joint publication by the Pacific Community (SPC) and Geoscience Australia. Noumea, New Caledonia.

Prepared for publication at SPC's Suva Regional Office, Private Mail Bag, Suva, Fiji, 2022

spc@spc.int | www.spc.int

Acknowledgements

The *Earthquake Scenario Selection for Tsunami Inundation Hazard Assessment: Guidelines on using the 2018 Probabilistic Tsunami Hazard Assessment (PTHA18) in the Pacific* is supported by the Australian Government (via the Australia Pacific Climate Partnership, APCP) and the World Bank (via the Pacific Catastrophe Risk Assessment and Financing Initiative, PCRAFI II).

The authors wish to thank the following reviewers for their contribution to this document:

Jerome Aucan, The Pacific Community (SPC)

Jose Borrero, eCoast

Cyprien Bosserelle, National Institute of Water and Atmospheric Research, New Zealand (NIWA)

Phil Cummins, Geoscience Australia (GA)

Jonathan Griffin, Geoscience Australia (GA)

Celina Smith, Department of Foreign Affairs and Trade, Australia (DFAT)

Shaun Williams, National Institute of Water and Atmospheric Research, New Zealand (NIWA)

Contents

Acknowledgements.....	i
Contents.....	ii
Executive Summary.....	1
Key Terms.....	2
1. Tsunami Risk in the Pacific.....	5
2. What is Probabilistic Tsunami Hazard Assessment?	7
3. Tsunami Frequency.....	8
4. Tsunami Hazard Uncertainty	10
4.1 Representing tsunami hazard uncertainty in PTHA	13
5. The 2018 Australian Probabilistic Tsunami Hazard Assessment (PTHA18).....	16
6. Tsunami Inundation Assessment Methods in the Pacific.....	18
6.1 Method 1: Scenario-based methodology and application in Samoa	20
6.2 Method 2: Monte Carlo sampling and application in PNG and Tonga.....	37
7 Summary and Conclusions.....	49
References	50
Appendix A: PTHA18 earthquake source details	57
Appendix B: Testing of the PTHA18	58
Appendix C: Inundation differences for tsunamis with similar offshore wave heights.	63
Appendix D: Synthetic catalogues	64
Appendix E: Stratified sampling by magnitude equations.....	65
Appendix F: Excluding small scenarios based on offshore wave heights.....	67
Appendix G: Procuring a tsunami inundation assessment.....	69

Executive Summary

Tsunamis can be a dangerous and destructive natural hazard. Pacific nations are particularly exposed and tsunami risk is a serious concern. Tsunami and disaster risk reduction is recognised as a cornerstone of sustainable development by the Australian Department of Foreign Affairs and Trade (DFAT) who co-funded this work with the World Bank.

This document provides guidance on how to assess earthquake-generated tsunami inundation hazards for Pacific Island nations. The methods described leverage the [2018 Probabilistic Tsunami Hazard Assessment](#) (PTHA18) developed by Geoscience Australia. The PTHA18 provides a global database of modelled earthquake-tsunami scenarios and frequencies that is shared under a Creative Commons License for the benefit of the global community. When used with tsunami inundation models, the PTHA18 can be used to assess the inundation hazard. The PTHA18 and these guidelines only consider tsunamis generated by undersea earthquakes, which cause the majority of tsunamis worldwide. Other geophysical processes such as landslides and volcanoes can also generate hazardous tsunamis, but require quite different modelling techniques beyond the scope of this work.

The intended audience for these guidelines includes scientists, academic institutions, and technical specialists responsible for assessing the tsunami hazard in the Pacific. Concepts are explained within the text and additional detail is provided in both the appendices and through links to online tutorials. We also encourage familiarisation with the relevant research.

Two methods are presented to assess the tsunami inundation hazard for a given location:

1. **Scenario-based:** This is a very flexible method that involves the selection of a subset of tsunami scenarios from the PTHA18. A variety of criteria can be used to guide the scenario selection, including the tsunami frequency estimates in the PTHA18. This method is less computationally intensive than the Monte Carlo sampling method.
2. **Monte Carlo sampling:** This method allows for rigorous translation of the tsunami frequencies and uncertainties in the PTHA18 to the **onshore** site of interest. It is less subjective than the scenario-based approach, and can give a more comprehensive representation of the hazard uncertainties implied by PTHA18. This method requires the modelling of hundreds of scenarios and can be very computationally demanding.

Both of these methods are widely applicable to the Pacific region, and case studies of tsunami hazard assessments from Pacific Island nations are included. We acknowledge that research into other methodologies is ongoing (e.g. Chock, 2016) and we expect the standards of best practice to evolve with advances in technology and science. We further encourage the open licensing of datasets used to support collective efforts towards community safety in the region.

An additional resource providing instruction on how to procure a tsunami hazard study is provided in Appendix G.

Key Terms

Key terms are bolded in the text at the first occurrence and definitions are provided below in alphabetical order. Definitions are provided in terms of their use in this document and relation to tsunami hazard science.

average recurrence intervals (ARIs)	The average time period in years between tsunami events that satisfy given criteria.
computational effort	The amount of computing resources required to carry out a task.
deaggregation	The separation of different source-zone contributions to the overall tsunami hazard.
deformation grids	A geographical xyz grid showing the amount of vertical movement due to an earthquake and the locations it occurs.
exceedance-rate curves	A graphical depiction of how frequently tsunamis that exceed a given parameter occur.
fault area	The area between two tectonic plates that slips during an earthquake.
Gutenberg–Richter b-value	A parameter of the Gutenberg–Richter earthquake frequency model that determines the relative frequency of large and small earthquakes.
hazard points	Location points that store tsunami wave and frequency data for the PTHA18.
high-performance computing (HPC)	Any computing system that enables much higher performance than with a standalone desktop or similar.
heterogeneous slip	Earthquake slip that varies spatially over the fault area (see Appendix A).
hydrodynamic modelling	The simulation and study of water motion such as tsunamis.
inundation	When the tsunami floods the land.
logic-tree mean	A quantity derived by averaging over all alternative models that are used to represent epistemic uncertainties.
magnitude–frequency	The relationship between an earthquake’s magnitude and its frequency.
maximum magnitude (M_{max})	The maximum possible magnitude of an earthquake for a given source zone. This is often poorly constrained.
maximum stage	The maximum tsunami water level above the background sea level.
non-parametric bootstrap	A resampling method used to compute confidence intervals.

non-uniform sampling	Sampling such that the sampling effort is deliberately varied in different parts of a population.
offshore	In the ocean some distance from the shore. In this document this often describes the locations of hazard points.
onshore	On land.
percentiles	Used to describe uncertainty in exceedance rate curves. For example, the 84th percentile curve gives an exceedance rate that we are 84% certain is larger than the true value.
probabilistic	Use of probability theory to represent randomness and uncertainty. Probabilistic tsunami hazard models provide estimates of the tsunami hazard, frequency and associated uncertainties.
Probabilistic Tsunami Hazard Assessment (PTHA)	A comprehensive tsunami hazard assessment that attempts to model all possible tsunami events and provide estimates on the tsunami hazard, frequency, and uncertainty.
PTHA18	The 2018 Australian Probabilistic Tsunami Hazard Assessment, developed by Geoscience Australia for public use. It can be used for local earthquake-tsunami hazard assessments in much of the Indian and Pacific Oceans.
risk	Risk is a combination of hazard, exposure, and vulnerability. How dangerous is the tsunami? How likely is it that a location will be affected? How likely is it that people and structures will be harmed?
root-mean-square error	The square root of the mean square of a set of errors.
scenario	One specific hypothetical earthquake and the resulting tsunami.
seismic coupling	The fraction of plate tectonic movements due to earthquakes (noting slow slip events are not classed as earthquakes).
sensitivity analysis	An analysis to determine how much a model output changes with changes in input variables.
slip	The amount of relative displacement between tectonic plates during an earthquake.
source zone	A region in which earthquakes occur.
stage	The water level above the background sea level.
stratified/importance sampling	Sampling within different magnitude bins with different importance criteria applied to reduce the overall number of scenarios required for modelling.

stratified sampling by magnitude	Sampling scenarios within different magnitude bins. For example, 30 scenarios for every 0.1 Mw bin.
subduction zones	A tectonic plate boundary where one plate is riding over the other. This is the type of plate boundary where most tsunamis are generated.
uncertainty	The degree to which the information is imperfect or unknown.
validation	An approach to check that a model achieves its intended purpose. This may involve comparing model results against real-world observations.
variable-area-uniform-slip	Representation of an earthquake that uses a constant slip across a randomly varying rupture area (see Appendix A).
wave train	The sequence of waves that make up a tsunami.
wave time series	A sequence of tsunami waves presented as time and water level data.
weighted mean	A mean where some values are weighted to contribute more than others.
random sampling with replacement	Sampling tsunami scenarios by randomly drawing from the available scenarios, recording that scenario, and then returning that scenario before drawing the next sample. Scenarios may be drawn multiple times but are always drawn from the same set of scenarios.

1. Tsunami Risk in the Pacific

The Pacific experiences more tsunamis than any other ocean in the world. Most tsunamis are generated by undersea earthquakes but they can also be caused by landslides, volcanoes, atmospheric pressure waves and asteroid impacts (NGDC/WDS, 2021). While a variety of mechanisms can generate hazardous tsunamis, these guidelines are limited to hazard assessment for earthquake-generated tsunamis on major **subduction zones**.

Earthquake-generated tsunamis represent an important fraction of the hazard; around 75% of historical tsunamis were generated by earthquakes (NGDC/WDS 2021). Historic earthquake tsunamis in the Pacific region include the 2007 Solomon Islands tsunami, which killed 52 people (Fritz and Kalligeris 2008), and the 1960 Chilean event, which killed over 1000 (Johnston et al., 2008) (Figure 1). The latter included over 200 deaths at distant locations in Japan, Hawaii, and the Philippines, highlighting that tsunamis can be hazardous even many thousands of kilometres from their source region (NGDC/WDS, 2021).

The methodologies in this document aim to facilitate the use of **Probabilistic Tsunami Hazard Assessment (PTHA)** in the Pacific, to assist Pacific Island countries and territories in understanding and mitigating their **risk**. PTHA is a family of methodologies used to estimate the average frequency of tsunamis matching criteria of relevance for risk management (Grezio et al. 2017). For example, we might want to estimate the average frequency of tsunami inundation exceeding some depth (such as >1m) at a specific coastal site of interest, where people or infrastructure will be located. Because tsunamis are rare, there is usually limited data available to constrain the hazard, and the frequency of inundation is often

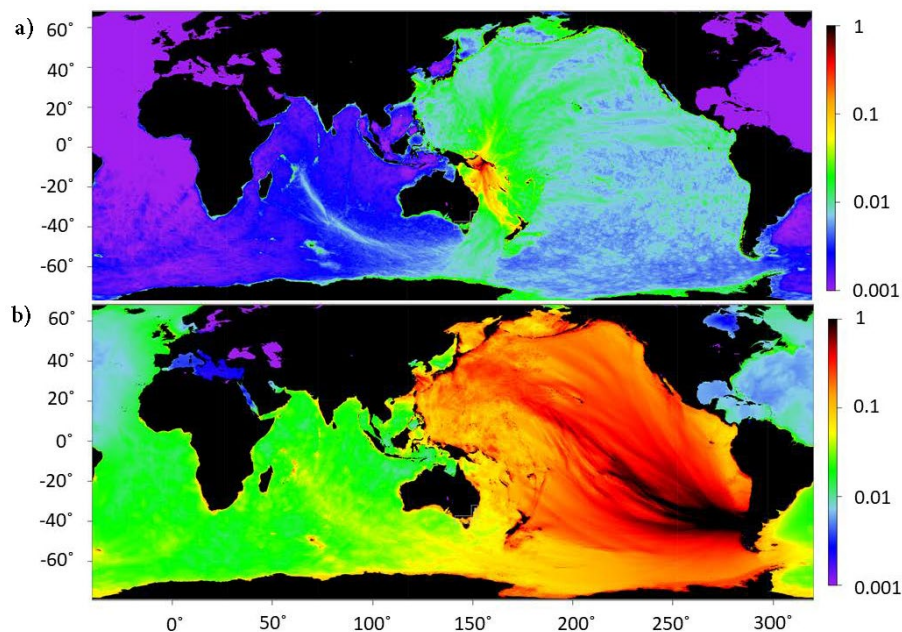


*Figure 1: Modelled tsunami wave heights above sea level similar to historic events: a) 2007 Solomon Islands earthquake tsunami; b) 1960 Chile earthquake tsunami. These events show how tsunamis can create an ocean-wide hazard. Both scenarios were sourced from the **PTHA18** (Davies and Griffin, 2018).*

uncertain. A benefit of PTHA methodologies is that there is scope to quantify these uncertainties and integrate them into the results, which is important because uncertainties should have an influence on robust risk-management decision-making (Behrens et al. 2021).

Methodologies for PTHA are much better established for earthquake tsunamis than for tsunamis from other sources (Behrens et al., 2021). That is why these guidelines are limited to earthquake sources. In particular, for earthquake tsunamis, large-scale PTHAs exist that provide a basis for earthquake-tsunami scenario design for site-specific tsunami inundation hazard assessments (e.g. Chock 2015; Power et al. 2017; Davies and Griffin 2018; Basili et al. 2021). The current guidelines focus on how to leverage large-scale PTHAs for site-specific earthquake tsunami inundation hazard studies.

Although not treated in this document, it is clear that landslides and volcanic processes are also significant sources of tsunami hazard in the Pacific. While apparently less common than earthquake tsunamis, they are also more prone to under-representation in historic databases (Goff, 2011). Notable examples include the 1998 Aitape tsunami in Papua New Guinea (generated by a landslide; Synolakis, 2002) and the 1888 Ritter Island tsunami (generated by a volcanic sector collapse; Ward and Day, 2003). More recently the Hunga Tonga–Hunga Ha'apai volcanic eruption generated a globally significant tsunami (15 January 2022). This was caused, in part, by a volcanic explosion that generated a horizontally propagating atmospheric pressure wave (Lamb wave), which applied a pressure force to the ocean as it travelled the globe at the speed of sound. The tsunami generated by the Lamb wave was observed globally, even in the Mediterranean Ocean. In addition the volcanic eruption generated a local tsunami that travelled through the ocean, causing inundation in Tonga. At the time of writing, details of the local tsunami generation mechanisms remain unclear, but may reflect water displacement by the explosion, associated volcanic mass movements, or some combination of factors.

PTHA methodologies for such non-earthquake sources are much less advanced than for earthquakes (Lovholt et al., 2019; Behrens et al., 2021). Some progress in this area has been made for landslides (Power et al., 2016; Lane et al., 2016; Clarke et al., 2019) and for some volcanic mechanisms (Paris et al., 2019; Pakoksung et al., 2021). But to the authors' knowledge there are no corresponding large-scale PTHA databases that can support tsunami scenario design for inundation hazard assessments. Many Pacific nations are of volcanic origin, such that landslide and volcanic processes are expected to significantly contribute to the tsunami hazards in many cases (Goff 2011; Goff and Terry 2016). Although beyond the scope of this report, we encourage further research on methodologies for assessing those hazards.

2. What is Probabilistic Tsunami Hazard Assessment?

Probabilistic Tsunami Hazard Assessments (PTHAs) are designed to estimate the frequency with which tsunamis of any given size may occur in the future. Although we cannot predict the timing of future tsunamis, nor precisely how often they occur, PTHA enables their average frequency to be estimated with quantified uncertainties. This is useful to support emergency management planning and risk mitigation.

It is known that the largest and most destructive tsunamis occur with the lowest frequency and as they are rare, coastlines with significant tsunami hazard may not have a historical record of tsunamis comparable to a credible worst case (e.g. Atwater et al., 1995; Jankaew, 2008; Lovholt et al., 2014). Because tsunamis are often not well represented historically, the tsunami hazard is often very uncertain (Grezio et al., 2017; Behrens et al., 2021). For example, prior to the 2004 Sumatra–Andaman earthquake which generated the Indian Ocean tsunami, the historical record did not suggest that such large earthquake tsunamis were possible in the Sumatra–Andaman region (Satake and Atwater, 2007). However, there had been some speculation that very large earthquakes and tsunamis *might* be possible, based on consideration of uncertainties in the regional historical record (Cummins, 2004). PTHA provides a framework where such uncertainties can be integrated into the analysis. This is advantageous because it can facilitate more robust hazard assessment to inform risk mitigation (Grezio et al., 2017; Behrens et al., 2021).

In principle, PTHAs involve the simulation of a large set of tsunami **scenarios** that are intended to represent the full diversity of tsunamis that may occur in the future. This is a significant undertaking and in practice, PTHAs may limit the scope to regionally significant earthquake sources (e.g. Burbidge et al., 2008; Li et al., 2016), or to major earthquake sources at ocean-basin or global scales (e.g. Chock et al., 2015; Davies et al., 2017; Yuan et al., 2021; Basili et al., 2021).

The intention of PTHA is to estimate the frequency of tsunamis of any given size, and to represent the **uncertainty** in these frequencies.

These guidelines focus on using **offshore** PTHAs to support site-specific tsunami inundation hazard assessments in the Pacific. Offshore PTHAs are concerned with the size and frequency of tsunamis in the deep ocean. For earthquake-generated tsunamis, several existing offshore PTHAs provide databases of modelled deep ocean tsunami scenarios and frequencies (Chock, 2015; Power et al., 2017; Davies and Griffin, 2018, 2020). These offshore PTHAs cannot be used directly to represent tsunami inundation because they represent tsunamis at relatively coarse spatial scales (several kilometres). By combining their tsunami scenarios and frequencies with a site-specific tsunami inundation model, the tsunami inundation hazards can be assessed at specific sites of interest.

The advantage of leveraging offshore PTHAs for **onshore** hazard assessment is that the site-specific studies do not need to re-implement their own analysis of tsunami scenarios and

frequencies. This saves time and promotes greater consistency between different studies. In these guidelines the offshore PTHA we focus on is the 2018 Australian Probabilistic Tsunami Hazard Assessment (PTHA18). The advice provided is also relevant to other offshore PTHAs.

Below we provide further information on how tsunami frequencies and uncertainties are represented in PTHA, followed by a brief overview of PTHA18.

3. Tsunami Frequency

In PTHA, tsunami frequency information is often represented using **exceedance-rate curves**. These model the average frequency (events/year) of tsunamis for which some quantity of interest, such as a maximum water level, exceeds a threshold (Behrens et al., 2021). In the context of tsunami inundation, the quantity of interest might be the water depth at a particular site. When considering deep-ocean tsunami sizes in offshore PTHAs, the maximum water level above sea level is more often used (e.g. Figure 2).

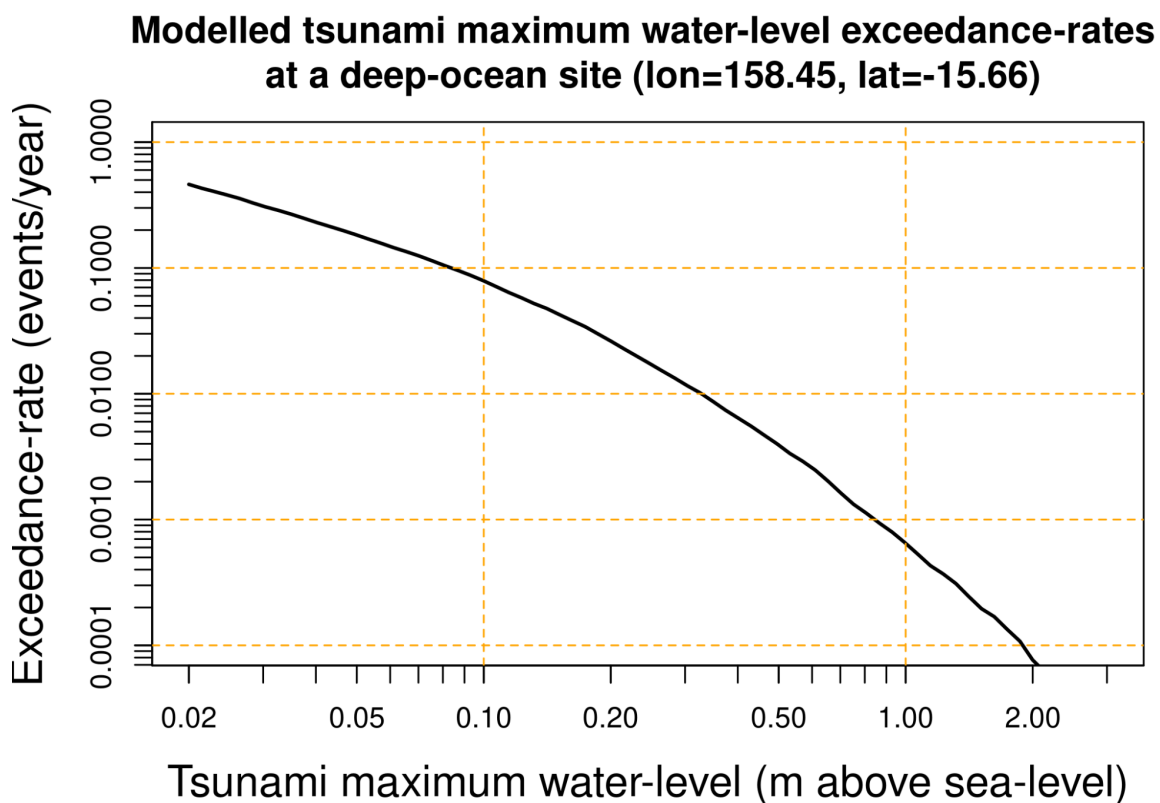


Figure 2: Exceedance rate curve example: Exceedance rates for tsunami maximum water-level above sea-level at a given location (sourced from the PTHA18).

In these guidelines when equations are presented, exceedance-rate curves are denoted as $\lambda(Q > Q^T)$. Here Q is the quantity of interest, Q^T is the threshold, and λ is the exceedance-rate. Calculation of exceedance-rate curves in PTHAs requires that:

- The tsunami has been simulated for each scenario e in the set of all PTHA scenarios E .
 - for each scenario one can determine whether the quantity of interest exceeds the threshold ($Q(e) > Q^T$).
- The scenario occurrence rates $r(e)$ (events/year) have been modelled for all PTHA scenarios $e \in E$.
 - in large-scale earthquake-tsunami hazard assessments, this is often achieved by first modelling earthquake **magnitude–frequency** relations for each **source zone**, and then partitioning the occurrence rates among the modelled scenarios from that source (e.g. Power et al., 2017; Davies and Griffin, 2018; Basili et al., 2021).

The modelled exceedance-rate curve $\lambda(Q > Q^T)$ is then:

$$\lambda(Q > Q^T) = \sum_{e \in E} r(e) 1_{(Q(e) > Q^T)}$$

where $1_{(Q(e) > Q^T)}$ is an indicator function which takes the value 1 if $Q(e) > Q^T$, and 0 otherwise.

Exceedance rates are often transformed into alternative representations of the tsunami frequency. Below we present several representations that are particularly common in PTHA:

- **Average recurrence intervals** $ARI(Q > Q^T)$ give the average time between repeated exceedances of the threshold in units of years. These are also often called “Return Periods”, and are computed as:

$$ARI(Q > Q^T) = \frac{1}{\lambda(Q > Q^T)}$$

- **Annual exceedance probabilities** $AEP(Q > Q^T)$ give the chance of one or more exceedances in any year. The following equation assumes the events occur independently:

$$AEP(Q > Q^T) = 1 - \exp[-\lambda(Q > Q^T)]$$

- The **exceedance probability over a specified time-frame** τ , denoted $EP(Q > Q^T | \tau)$, is similar to the AEP but uses a different time period (e.g. $\tau = 50$ years). The following equation assumes the events occur independently:

$$EP(Q > Q^T | \tau) = 1 - \exp[-\lambda(Q > Q^T) \tau].$$

All these different representations of tsunami frequency are widely used in PTHA. For calculation purposes it is often mathematically easier to work directly with exceedance rates, rather than the alternatives, because exceedance rates are additive.

4. Tsunami Hazard Uncertainty

Tsunami hazards can in principle be modelled at any site, even if few nearby tsunami observations exist, assuming sufficient elevation data is available for **hydrodynamic modelling**. However, the results will inherit any uncertainties in the representation of tsunamis, their source processes and frequencies.

For example, models of earthquake tsunamis must represent the earthquake scenario magnitude, geometry, rigidity, rupture area and **slip**. If exceedance-rate information is desired, then decisions must also be made on the representation of earthquake frequencies. These modelling decisions are not standardised, and different choices can have a large impact on tsunami hazard assessments (e.g. Cardno, 2013; Li et al., 2016; Sepulveda et al. 2019; Behrens et al. 2021). It is useful to distinguish between two kinds of uncertainty affecting tsunami hazard assessment.

Epistemic uncertainties reflect our knowledge gaps and may be reduced with future scientific advances.

Aleatory uncertainties reflect irreducible randomness that will not be reduced with future scientific advances.

A key epistemic uncertainty affecting earthquake-tsunami hazards is the **maximum magnitude** earthquake possible on a given fault (M_{max}). Current-day scientific knowledge offers little consensus on how M_{max} should be estimated, and surveys of expert opinion suggest large uncertainty on many subduction zones (Berryman et al., 2015). These uncertainties are epistemic because, in future, they might be reduced by advances in paleo-tsunami research or earthquake mechanics (e.g. England, 2018; Pilarczyk et al., 2021).

To illustrate the significance of present-day M_{max} uncertainties for tsunami hazard assessment in the Pacific, consider the case of the Kermadec–Tonga subduction zone, a key south-west Pacific earthquake source:

- The Global Earthquake Model’s Faulted Earth Subduction Interface Characterisation Project Version 2 suggests M_{max} could be anywhere in the range 8.1–9.6 (Berryman et al., 2015)
- A survey of experts at the *2018 Expert meeting on tsunami sources, hazards, risk and uncertainties associated with the Tonga–Kermadec Subduction Zone* found that experts’ preferred M_{max} values were in the range 8.7–9.8, with an average of 9.4 (UNESCO/IOC, 2020).

These M_{max} values suggest the largest earthquake tsunamis generated on the Kermadec–Tonga trench might vary anywhere between:

- (Lower limit) An event comparable in size to the recent 2009 Samoa earthquake tsunami (Mw 8.1)
- (Upper limit) An event larger than the 1960 Chile earthquake tsunami (Mw 9.5).

In this circumstance a “worst-case” earthquake tsunami scenario cannot be defined with any confidence, and it is similarly difficult to estimate tsunami frequencies. Large uncertainties in M_{max} exist on many other subduction zones (Berryman et al., 2015). Figure 3 shows how this epistemic uncertainty is represented on different source zones in the 2018 Australian Probabilistic Tsunami Hazard Assessment (Davies and Griffin 2018).

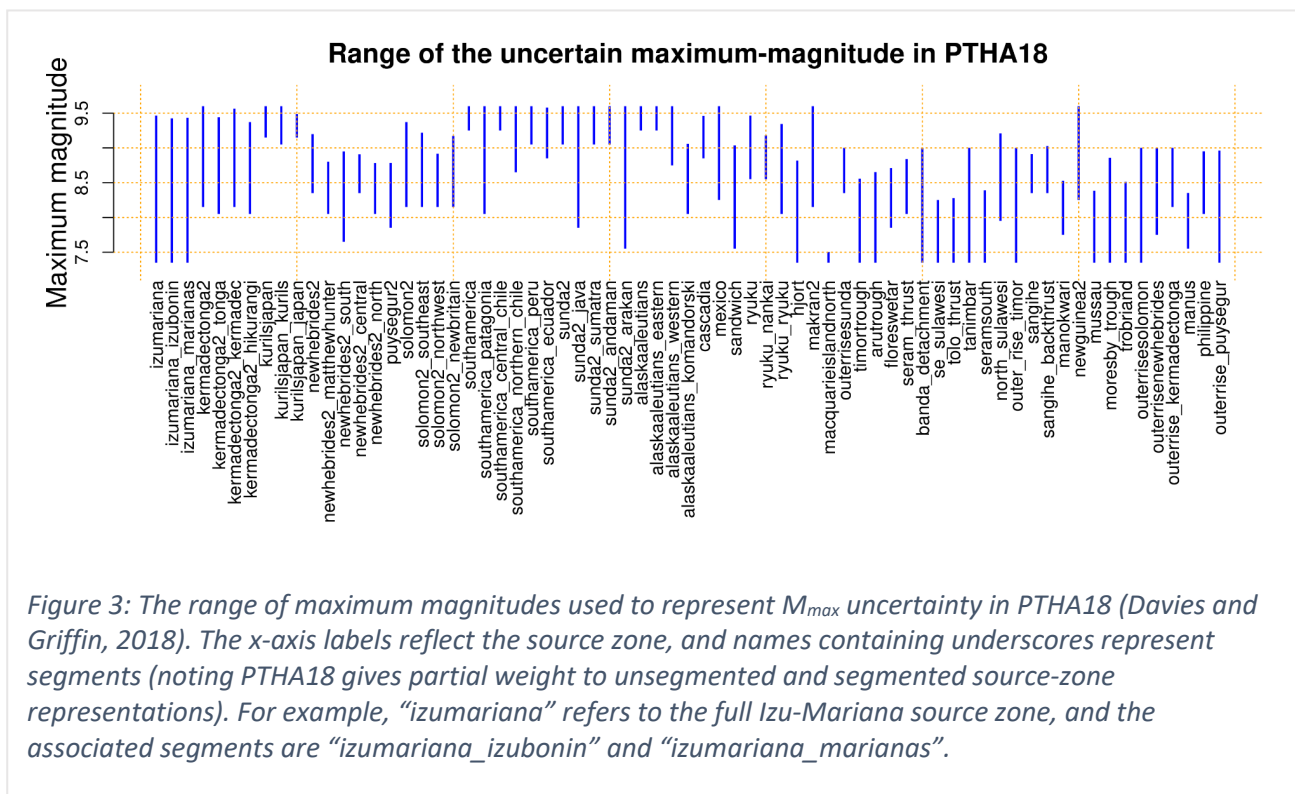


Figure 3: The range of maximum magnitudes used to represent M_{max} uncertainty in PTHA18 (Davies and Griffin, 2018). The x-axis labels reflect the source zone, and names containing underscores represent segments (noting PTHA18 gives partial weight to unsegmented and segmented source-zone representations). For example, “izumariana” refers to the full Izu-Mariana source zone, and the associated segments are “izumariana_izubonin” and “izumariana_marianas”.

Maximum magnitudes are not the only epistemic uncertainty affecting tsunami hazard assessments. Modelled exceedance rates are also affected by epistemic uncertainties in the **seismic coupling** and **Gutenberg–Richter b-value**, and these uncertainties are substantial on many subduction zones (Berryman et al., 2015).

Another class of uncertainties affects the relationship between the earthquake magnitude and the resulting tsunami. In general this is modulated by the earthquake geometry. For example, although a general positive correlation exists between the magnitude and **fault area** of historical earthquakes, it is only approximate (Allen and Hayes, 2017). Figure 4 highlights that some earthquakes exhibit a relatively compact fault area for their magnitude (e.g. Tohoku 2011) while others cover a relatively large fault area (e.g. Sumatra 2004). This affects the average earthquake slip, and thus the size of the resulting tsunami (Butler et al., 2017; An et al., 2018). Natural variations in the spatial distribution of earthquake slip over the fault can

have a similar effect on the tsunami. These effects are important both near to the tsunami source (e.g. Mueller et al., 2015; Melgar et al., 2019; Sannikova et al., 2021) and at trans-oceanic distances (e.g. Gica et al., 2007; Li et al., 2016; Butler et al., 2017; Davies, 2019; Sannikova et al., 2021).

Hazard assessments often represent this geometric variability as an **aleatory** uncertainty. In practice, this is achieved by simulating a large number of random scenarios to represent the intrinsic variability of earthquakes (Geist and Oglesby, 2014). The hazard results will also depend on how these random scenarios are generated, which is an epistemic uncertainty (e.g. Geist et al., 2007; Murphy et al., 2016; Scala et al., 2019).

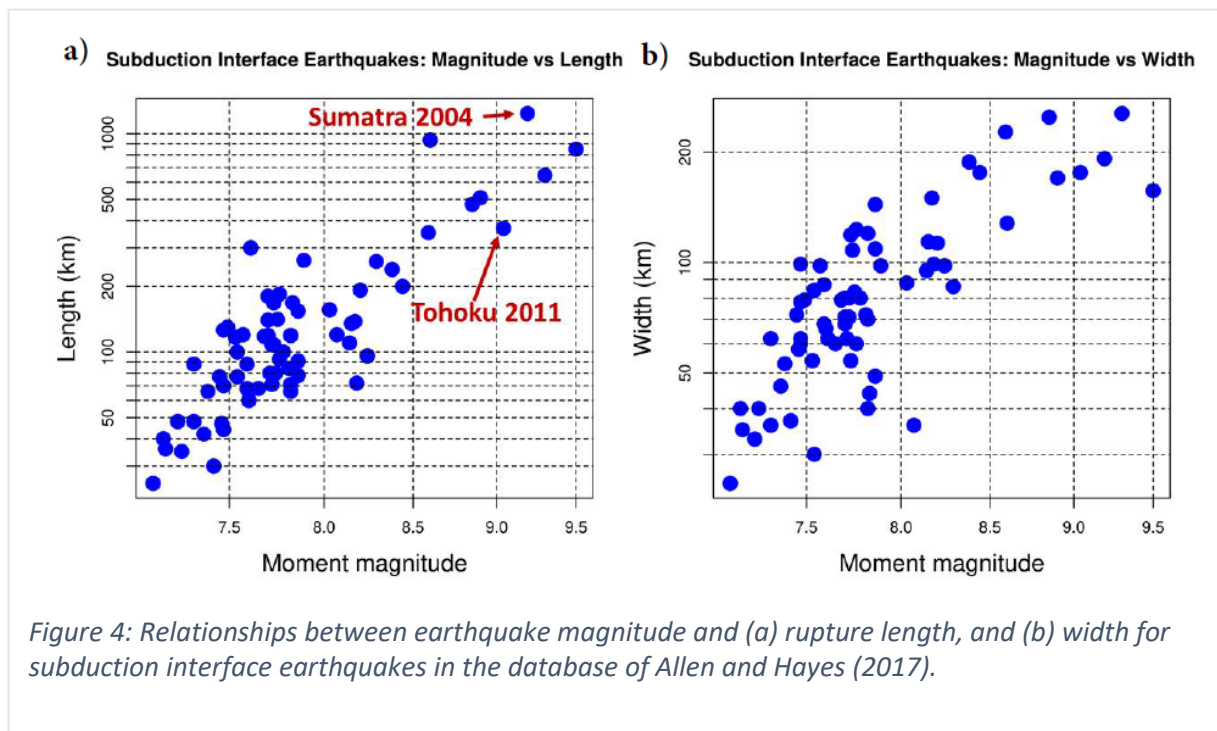


Figure 4: Relationships between earthquake magnitude and (a) rupture length, and (b) width for subduction interface earthquakes in the database of Allen and Hayes (2017).

Tsunami risk-management actions should aim to robustly account for these uncertainties. One strategy is to use hazard assessments that focus only on extreme scenarios, such as Mw 9.6–9.8 earthquakes on the Kermadec–Tonga trench (based on the higher end of expert-opinion estimates above). If this is done while using earthquake properties optimised to produce inundation at the site of interest, the results will provide a “probable upper-bound” on future tsunami inundation from near-field earthquakes. While potentially useful, this approach suffers the shortcoming of being very conservative. Furthermore, uncertain decisions will still be required; for example, how concentrated is the earthquake slip permitted to be?

An opposing alternative is to simulate a range of tsunamis with magnitude and geometry comparable to known nearby historical events. These scenarios are credible and may give a useful indication of the most exposed regions. However, this approach discounts the possibility that future tsunamis could be much larger. Recent history illustrates the danger: in the Honshu region of Japan, prior to the 2011 Tohoku tsunami, most hazard assessments used M_{max} of 7.9–8.5, based on imperfect knowledge of historical earthquakes (Kagan and Jackson,

2013). These hazard assessments substantially under-estimated the size of the 2011 earthquake (magnitude 9.1) and resulting tsunami. It is likely that consideration of larger scenarios could have prevented the Fukushima nuclear accident and reduced the 19,000 fatalities (Koshimura and Shuto, 2015; Okal, 2015; Synolakis and Kanoglu, 2015).

4.1 Representing tsunami hazard uncertainty in PTHA

PTHA offers a framework for finding the middle ground between the “extreme” and the “historically derived” types of scenarios discussed above, while accounting for epistemic and aleatory uncertainties that affect the hazard information produced. A key benefit of PTHA is that it provides a structured approach to including “known unknowns” in tsunami hazard assessment. In risk management applications, judgments need to be made about how the uncertainties should influence risk-mitigation measures. These decisions will involve trade-offs that depend on the criticality of the application at hand; they are not simply modelling decisions. Although this can be approached without formal reasoning (e.g. using expert judgement to select scenarios appropriate to the application of interest) PTHA has the potential to make the reasoning explicit. Furthermore, as compared with ad hoc scenario construction, the assumptions underlying PTHA methodologies can be tested (at least partially) by comparing the statistical properties of model predictions with observations for multiple tsunamis. This is feasible at sufficiently large spatial scales (e.g. Davies, 2019; Davies and Griffin, 2020; Selva et al., 2021).

To represent uncertainties in hazard calculations, PTHAs can use a set I of scenario occurrence-rate models $r_i(e), i \in I$, rather than relying on a single scenario occurrence-rate model $r(e)$ (used to define the exceedance rate in Equation 1). These alternative models make different assumptions about the scenario occurrence rates. For example, one model might assume a maximum magnitude of 8.1 on the Kermadec–Tonga source zone, resulting in a zero occurrence rate for scenarios with higher magnitudes, while another model might use the value 9.6, and thus assign a positive occurrence rate to the same scenarios. The alternative occurrence-rate models can similarly represent other uncertain parameters, like the seismic coupling or Gutenberg–Richter b-value, or even the way that earthquake scenarios should be generated.

In PTHA these alternatives can be weighted within a probabilistic framework (Grezio et al., 2017; Behrens et al., 2021). This provides a structured way to represent the epistemic uncertainties. Different PTHAs vary greatly in the number of alternative models used. For example, Li et al. (2016) considered 2 alternative models on the Manila trench, whereas Davies and Griffin (2018) used at least 32,000 alternatives per source zone. The exact number of models is not particularly important; rather it is important that they give a reasonable description of the uncertainties that exist.

Because PTHAs use multiple scenario occurrence-rate models $r_i(e)$, they also produce multiple exceedance-rate curves λ_i :

Equation 1

$$\lambda_i(Q > Q^T) = \sum_{e \in E} r_i(e) 1_{(Q(e) > Q^T)}$$

where each model $i \in I$ has an associated weight w_i ; more likely models will have higher weights and the weights sum to one. The set of models and their weights lead to a distribution of exceedance-rate curves which represents uncertainties in the true exceedance rate. The latter distribution can be summarised, for example by using the **weighted mean** or a set of **percentiles** (Power et al., 2017; Davies and Griffin, 2020). The model derived from the weighted mean is often also called the **logic-tree-mean** exceedance-rate model, and is computed as:

$$\bar{\lambda} = \sum_{i \in I} w_i \lambda_i(Q > Q^T)$$

assuming weights w_i are normalised to sum to one. An example depicting uncertainties in the exceedance-rate curves using the logic-tree mean and a set of percentiles is shown in Figure 5.

Using the approach above, PTHA provides a framework in which observations, theory and expert opinion can inform how scenarios are modelled and how alternatives are weighted. Expert opinion has a particularly important role in data-limited situations that often characterise tsunami hazard assessment (e.g. Basili et al., 2021). For example the Global Earthquake Model's Faulted Earth Subduction Interface Characterisation Project (Berryman et al., 2015) suggests lower, preferred and upper limits for a range of parameters relevant to magnitude–frequency estimation on subduction zones. Using PTHA the analyst can simultaneously consider extreme scenarios, scenarios comparable to historical events, and those in between, while quantitatively keeping track of the scenario credibility.

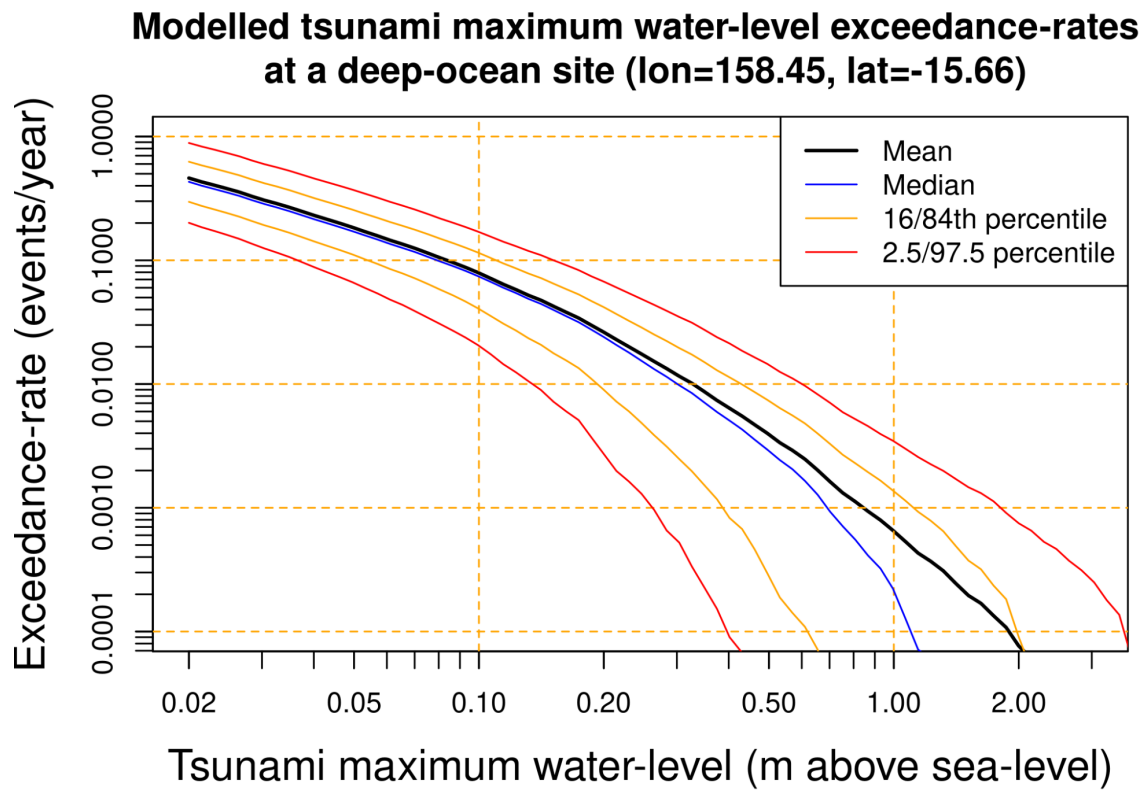


Figure 5: Representation of epistemic uncertainties in exceedance-rate curves by using the mean and a set of percentiles. A key feature of PTHA is that these uncertainties can be integrated into the analysis in a structured way.

5. The 2018 Australian Probabilistic Tsunami Hazard Assessment (PTHA18)

PTHA18 is a large-scale PTHA that simulates earthquake-generated tsunamis from major earthquake source zones in the Pacific and Indian Oceans, with a focus on Australia (Figure 6). It estimates the frequency that earthquake tsunamis of any given size occur at approximately 20,000 offshore locations referred to as **hazard points**. The hazard points are globally distributed, including around large land masses in the Pacific. Major Pacific Ocean earthquake sources are represented (Figure 6). PTHA18 models tsunamis with a relatively coarse resolution (1 arcmin²) and so does not provide information on tsunami inundation. However the PTHA18 offers a regionally consistent resource to support earthquake-tsunami scenario design for hazard assessment.

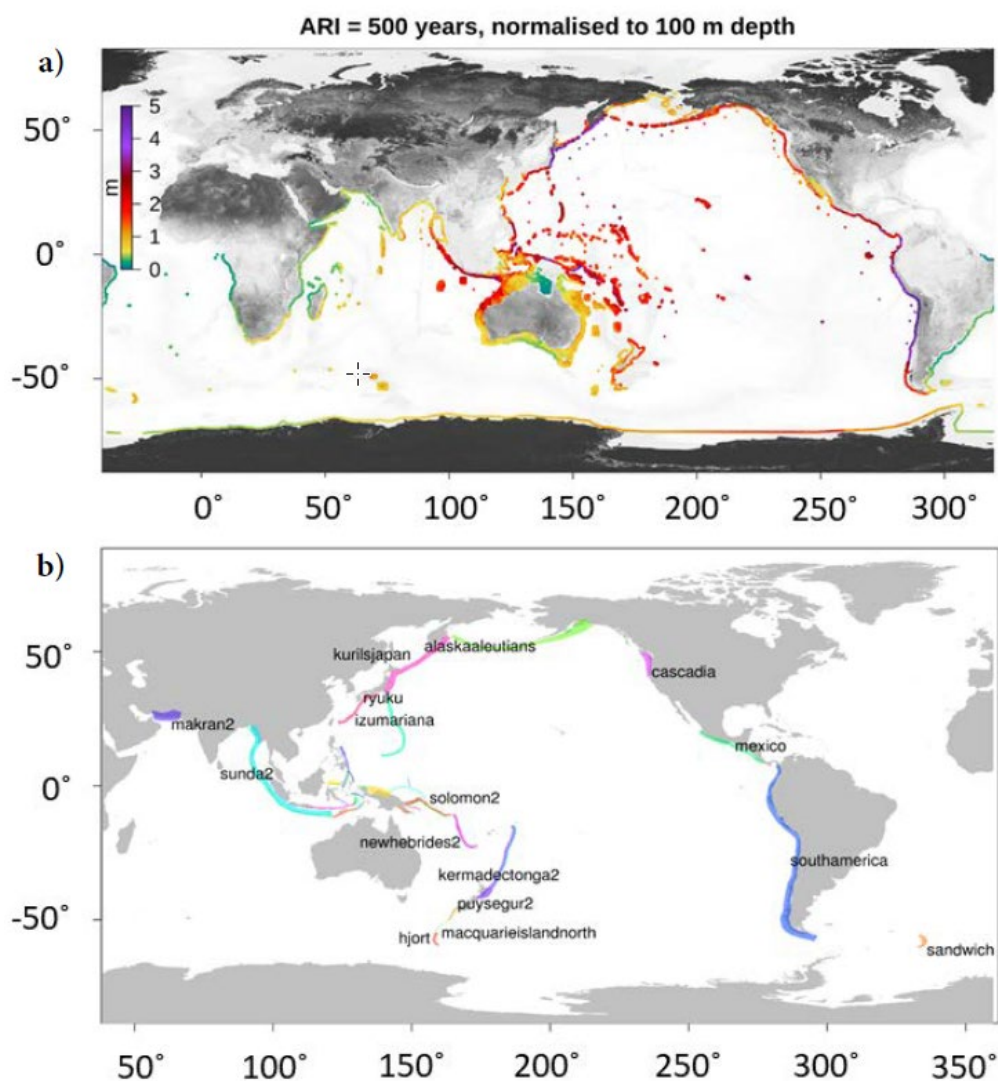


Figure 6: PTHA18 hazard points and earthquake source zones: (a) Hazard points where tsunami size and frequency information are stored. Hazard points are coloured according to tsunami maxima (normalised to 100 m depth using Green's law) with an Average Recurrence Interval (ARI) of 500 years; (b) The earthquake source zones used in the PTHA18 (Davies and Griffin, 2018, 2020).

Detailed information on the PTHA18 is available in the [project report](#) (Davies and Griffin, 2018) and subsequent publications (Davies, 2019; Davies and Griffin, 2020). The [source code](#) and associated [tutorials](#) are available under a permissive open-source licence. The PTHA18 database is openly available and can be interrogated in many ways to extract earthquake scenario initial conditions, **wave time series** at hazard points, exceedance-rate curves with quantified uncertainties, and hazard **deaggregation** information (Figure 7). Specific tutorials will be referred to throughout this document.

Further information on the PTHA18 is provided in the Appendices. Appendix A provides earthquake source details and Appendix B provides a summary of PTHA18 testing.

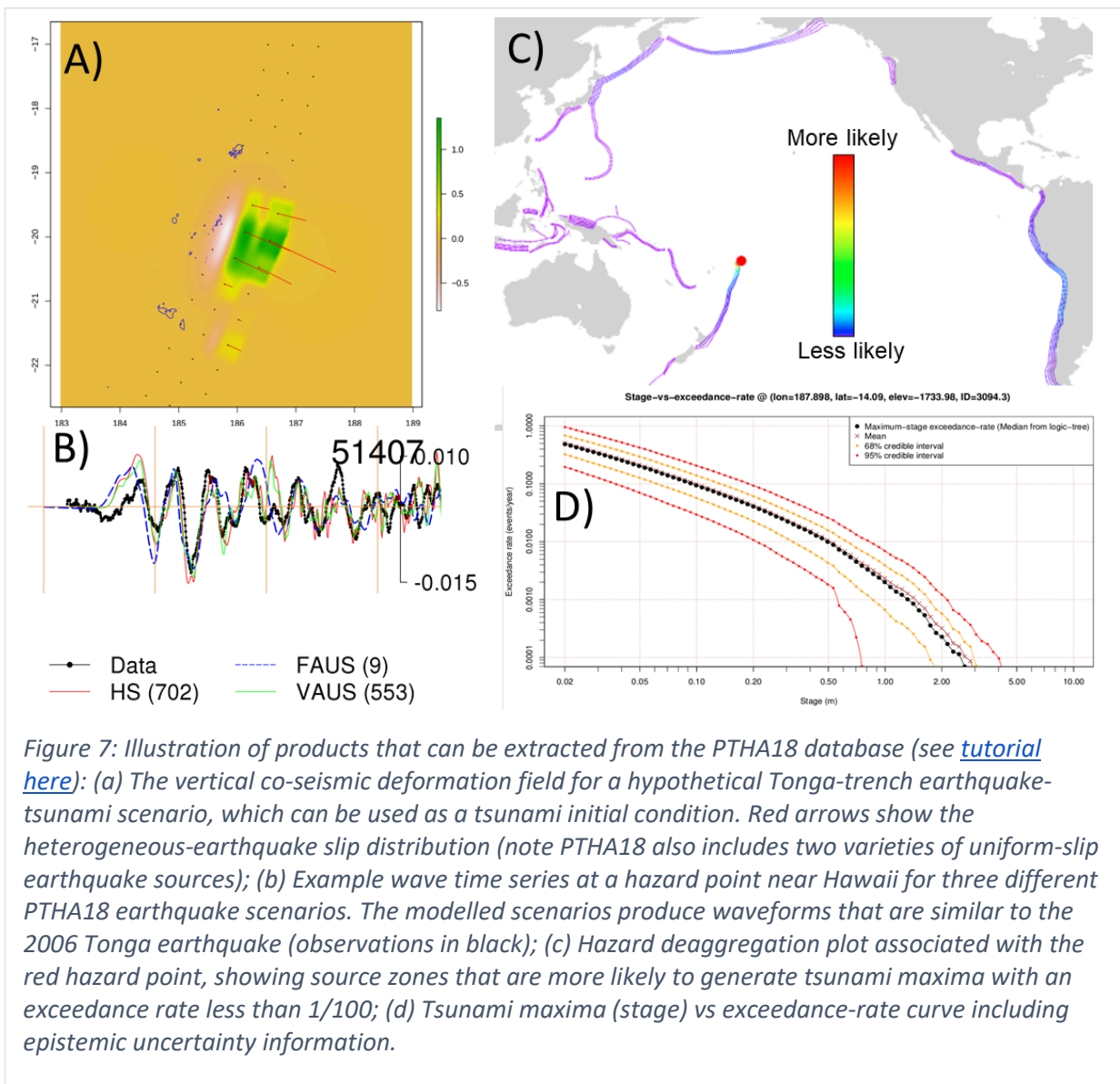


Figure 7: Illustration of products that can be extracted from the PTHA18 database (see [tutorial here](#)): (a) The vertical co-seismic deformation field for a hypothetical Tonga-trench earthquake-tsunami scenario, which can be used as a tsunami initial condition. Red arrows show the heterogeneous-earthquake slip distribution (note PTHA18 also includes two varieties of uniform-slip earthquake sources); (b) Example wave time series at a hazard point near Hawaii for three different PTHA18 earthquake scenarios. The modelled scenarios produce waveforms that are similar to the 2006 Tonga earthquake (observations in black); (c) Hazard deaggregation plot associated with the red hazard point, showing source zones that are more likely to generate tsunami maxima with an exceedance rate less than 1/100; (d) Tsunami maxima (stage) vs exceedance-rate curve including epistemic uncertainty information.

Although these guidelines focus on use of the PTHA18, much of the advice is also directly applicable to other offshore PTHAs. Modellers are encouraged to use such alternatives if judged appropriate for their application.

- For example in the western USA, the ASCE tsunami standard provides a PTHA that is mandated for use in certain design processes (Chock, 2015).
- In New Zealand, the development of much evacuation mapping has been based on a separate national-scale PTHA (Power et al., 2017).

At any site, scientists should also consider the consistency of whatever large-scale PTHA they use with other locally available information (such as historical and paleo-tsunami observations). Although large-scale PTHAs use observations to constrain the modelled hazard, there are technical challenges in comprehensively integrating all available information. For example, direct use of onshore tsunami observations is difficult when models do not explicitly resolve inundation (although subjective approaches exist; Butler et al., 2016). If the offshore PTHA implies a hazard that is substantially inconsistent with inferences from local data, then modellers should carefully consider whether it is appropriate to rely on that offshore PTHA for their study. Furthermore, any such issues should be clearly communicated with end users.

6. Tsunami Inundation Assessment Methods in the Pacific

Tsunamis are generally most destructive when they inundate the land. Tsunami inundation hazard assessments are designed to estimate how deep the water may get, and how often this might be expected to occur.

Offshore PTHAs, including the PTHA18, only provide information about the **offshore** tsunami hazard (i.e. wave heights and frequencies). This document describes two methods to leverage the offshore PTHA18 data to determine the **onshore** inundation hazard, by combining scenarios and frequencies from the offshore PTHA with an inundation model.

The most complete way to understand the implications of the offshore PTHA18 for the onshore hazard at any site would be to simulate inundation for every single offshore PTHA18 scenario. By combining these modelled onshore depths with the scenario frequencies in the offshore PTHA, one could compute exceedance-rate curves at any site in the inundation model domain.

Unfortunately, it is usually impractical to simulate inundation for all tsunami scenarios in the offshore PTHA, because it requires too many high resolution inundation simulations, which are computationally costly. As a practical alternative we suggest two different methods that enable the number of scenarios to be significantly reduced. The two methods presented in this document are as follows, with pros and cons summarised in Table 1:

1. **Scenario-based**: Simulation of a limited number of tsunami scenarios with nominal return periods, which are inferred from offshore PTHA results at one or more nearby hazard points.

2. **Monte Carlo sampling:** Simulation of a large number of tsunami scenarios (>100) in a manner that can approximate the results that would be obtained by modelling all PTHA18 scenarios, and fully represent the associated uncertainties.

Table 1: Pros and cons of the scenario-based and Monte Carlo sampling methods.

Pros	Cons
Scenario-based	
<ul style="list-style-type: none"> • Is flexible • Can target specific events • User judgement can easily influence the scenario selection. • The number of scenarios can be kept low and reduce computational costs. 	<ul style="list-style-type: none"> • Involves subjective judgement • Does not formally approximate the inundation hazard that would be obtained by simulating all offshore PTHA scenarios. • Uncertainties are not rigorously represented.
Monte Carlo sampling	
<ul style="list-style-type: none"> • Formally approximates the inundation hazard that would be obtained by simulating all offshore PTHA scenarios. • Uncertainties can be represented in the same way as in the offshore PTHA. • Is less subjective than the scenario-based approach. 	<ul style="list-style-type: none"> • Has high computational cost because many scenarios must be modelled. • Is more technically challenging to implement than scenario-based approach. • Is more difficult to integrate user judgement into the methodology.

6.1 Method 1: Scenario-based methodology and application in Samoa

Scenario-based approaches to tsunami hazard assessment involve simulating inundation for a limited set of scenarios. Of the two methods in this document, the scenario-based approach is the easier to implement. It also allows for greater control over which scenarios are selected for modelling. For example:

- Knowledge of the local tsunami history can be incorporated into the scenario selection, by ensuring that scenarios comparable to historical events are selected.
- The modelling team might focus on scenarios consistent with their own judgements about the most plausible earthquake magnitudes (irrespective of the PTHA18 predictions).

These decisions involve some subjectivity and so should be implemented with care. We highly recommend they are made in consultation with key end-users. But so long as they are carefully justified and communicated, this flexibility represents a great strength of the scenario-based approach.

In the scenario-based methodology, the scenario source zone(s) are first specified by the user, with the PTHA18 source deaggregation helping to guide this choice. The user also specifies a range of exceedance rates of interest for their study. For each source zone, tsunami scenarios with **maximum stage** values corresponding to these exceedance rates at one or more **hazard points** are identified. For each exceedance rate, multiple scenarios are selected. These will produce different inundation footprints because the offshore wave heights used to identify the scenarios are an imperfect predictor of inundation. By using multiple scenarios, we reduce the chance of this leading to underestimation of the hazard.

A feature of this approach is that we simultaneously use offshore wave height information at multiple PTHA18 hazard points. This makes it easier to apply the method to small regions (islands or groups of islands) where multiple relevant hazard points are affected by similar scenarios. This situation holds for many small Pacific Island nations, such as in Samoa, where we are interested in tsunami hazards all around the islands. If only a single hazard point could be used to select scenarios, then we would need to select different scenarios for each hazard point. We would also need to decide which set of scenarios should be used to create the final inundation maps (and this might vary for each onshore location). The latter decision might not be obvious and could introduce artificial discontinuities into the inundation maps. To circumvent this issue, we search for PTHA18 scenarios that individually satisfy the exceedance-rate criteria at one or more selected hazard points, while always producing smaller waves at the others. By combining multiple such scenarios, we create a set of scenarios for which the largest waves meet the exceedance-rate criteria at every hazard point of interest. We then simulate inundation for this set of scenarios and use their maxima to create the nominal inundation map with the specified exceedance rate.

An advantage of the use of multiple hazard points is the reduction in computational cost that arises when the same scenarios are applicable to multiple hazard points. However, if very large areas are to be modelled, then this benefit will no longer hold, and different scenarios will be appropriate in different regions. In such cases it is preferable to partition the region of interest into well-separated zones (e.g. distinct island groups) and apply the method separately to each zone.

Checklist – what do I need?

- [PTHA18 report](#)
- [PTHA18 source code](#)
- An understanding of the relevant source zones for my area of interest (see PTHA18 report)
- [Tsunami history](#) for the area
- PTHA18 global [hazard point locations](#)
- The source deaggregation plot [code](#) to see which sources contribute most to the hazard at the selected hazard points
- The [multi-hazard point scenario selection script](#), which implements the workflow
- High performance computing resources are helpful

Outcomes – what will this method provide me with?

- Inundation depth maps for a composite of scenarios with selected ARIs.

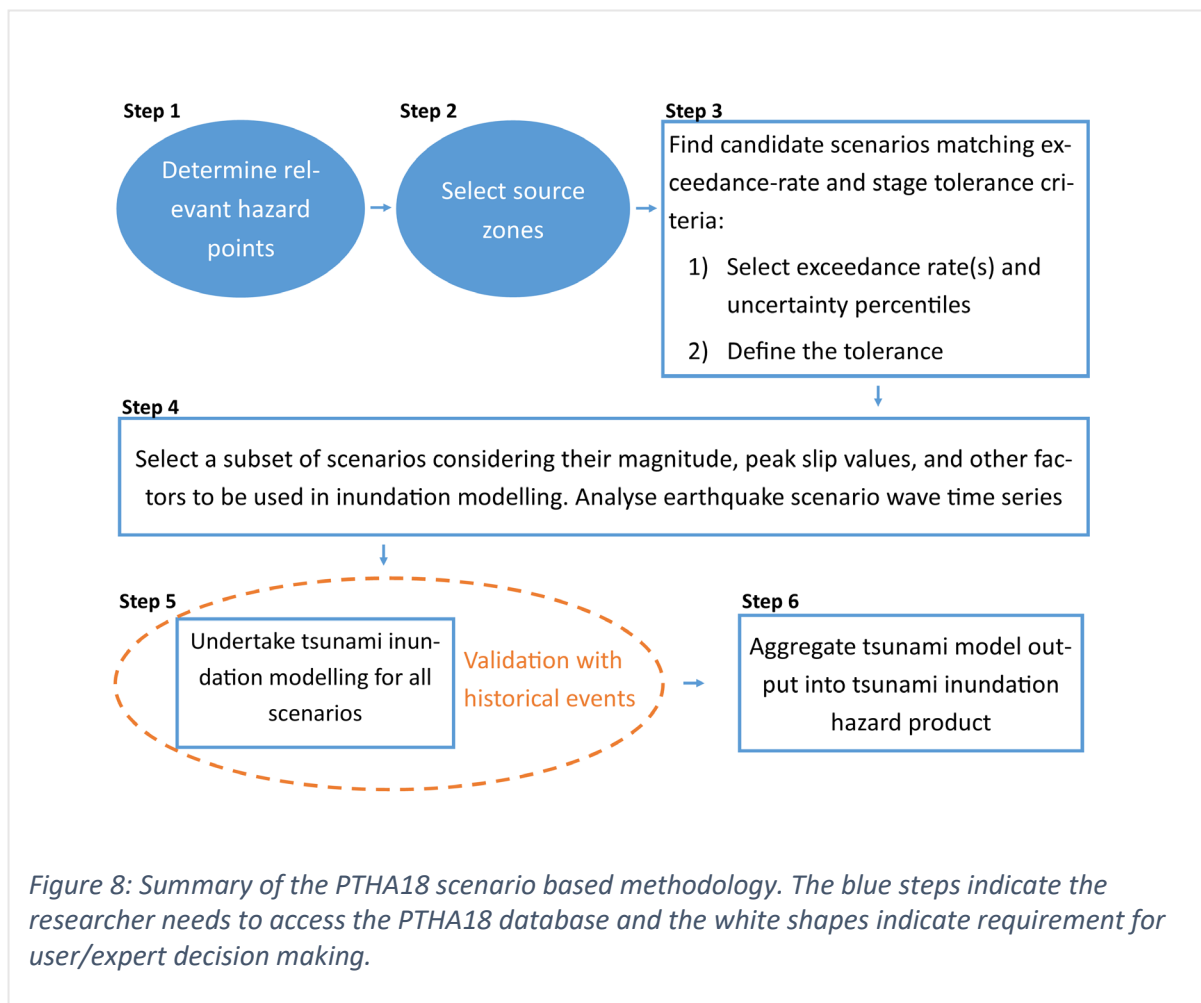
Limitations

- The onshore hazard results do not formally approximate the results that would be obtained by simulating all scenarios in the offshore PTHA.
- Due to the need for subjective judgement, different users are likely to obtain different answers when applying the technique.
- Uncertainties that are represented in the offshore PTHA are not comprehensively represented in the onshore hazard results.

Steps – how to do it

The workflow is similar to that presented in [this tutorial on multi-gauge-scenario-selection](#) using the PTHA18 database. Modellers applying this methodology are encouraged to consult the tutorial to aid the practical implementation of each step.

A summary of the scenario-based approach is provided in Figure 8. This section describes the steps below in further detail alongside the Samoan case study. A separate report for the Samoa tsunami hazard assessment is also available (Giblin et al. 2022).



Step 1: Hazard point selection

The PTHA18 **hazard points** store site-specific information including tsunami **wave time series** for every earthquake **scenario**. The modeller should identify the PTHA18 hazard points near to their study site (e.g. Figure 9). The number of hazard points to be considered will depend on the scale of the assessment. Even for very localised studies where only one hazard point *could* be considered, it is worth including multiple nearby hazard points (if they exist) so the scenario selection is not unduly reliant on a single site. We suggest avoiding points in shallow water (e.g. less than 100 m) or points that are very close to the coast, because the coarse-grid linear tsunami solver used in PTHA18 is not well suited for modelling waves at such sites.

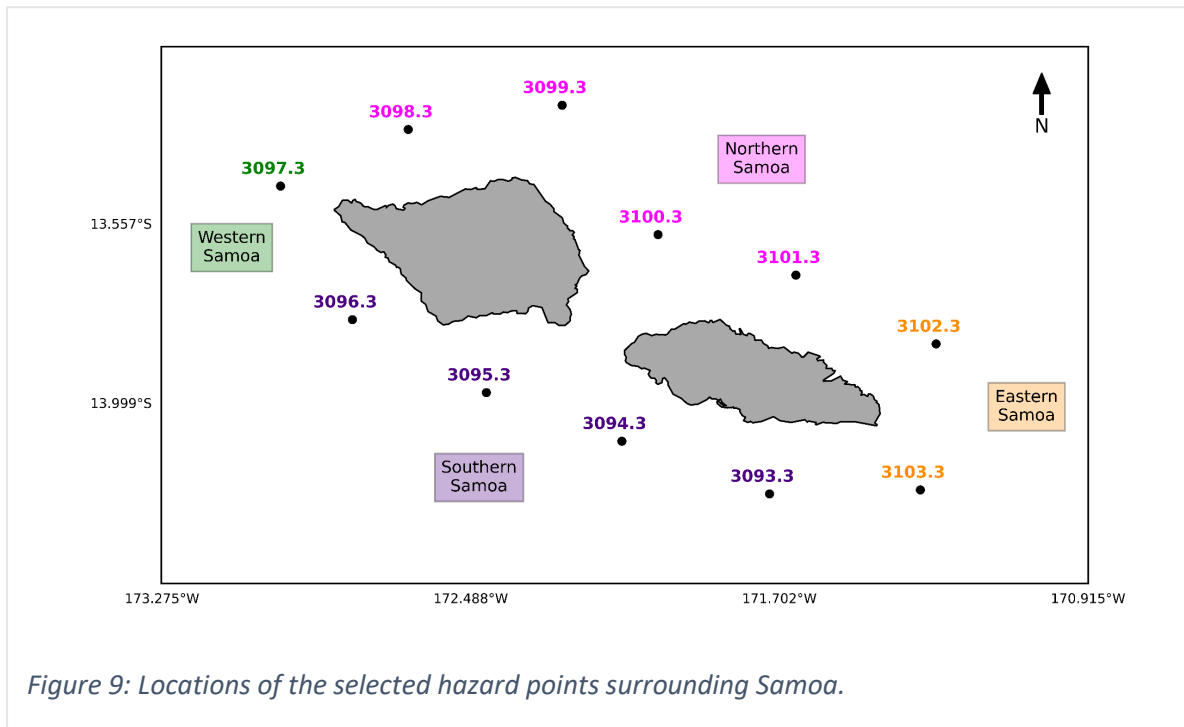


Figure 9: Locations of the selected hazard points surrounding Samoa.

For our case study, 11 hazard points surrounding Samoa were identified (Figure 9, Table 2). Global hazard point locations in PTHA18 (in .csv and .shp format) can be found [as described here](#).

Table 2: Selected hazard point details for the Samoan case study. Text is coloured according to locations specified in Figure 9.

Hazard Point ID	Longitude	Latitude	Elevation
3097.3	187.029	-13.46	-3599.16
3098.3	187.354	-13.32	-3581.93
3099.3	187.746	-13.26	-1153.97
3100.3	187.990	-13.58	-1622.93
3101.3	188.341	-13.68	-2565.69
3012.3	188.698	-13.85	-3599.46
3103.3	188.658	-14.21	-2318.08
3093.3	188.274	-14.22	-3149.01
3094.3	187.898	-14.09	-1733.98
3095.3	187.553	-13.97	-2896.96
3096.3	187.212	-13.79	-2585.94

Once relevant hazard points are identified, they can be specified in the [multi-gauge scenario selection script](#) which will provide the hazard point data that is used for scenario selection. Different earthquake slip types are supported, see Appendix A for more information.

The PTHA18 database sometimes contains repeated points with the same location but different gauge IDs. Any duplicates should be removed as shown in the script, to ensure that each site is only counted once.

Step 2: Source zone selection and earthquake slip type

The PTHA18 models the contribution of each major tsunami **source zone** to the offshore tsunami hazard for every **hazard point**. These model results can be accessed through the hazard point [source deaggregation](#) plots.

Figure 10 provides the source **deaggregation** plots for Samoa hazard point ID 3101.3. After reviewing each source deaggregation plot for the 11 hazard points, a total of 8 sources were subjectively identified for further investigation. These sources were Alaska Aleutians, Izu Mariana, Kermadec Tonga, Kurils Japan, Mexico, New Hebrides, Outer-rise Kermadec Tonga, and South America (most sources shown in Figure 11).

We stress that modellers can apply some judgement at this stage of the analysis; source zones may be included even if the PTHA18 deaggregation suggests they are unimportant. The PTHA18 source-zone deaggregation can vary from hazard point to hazard point, and only reflects the logic-tree-mean scenario occurrence-rate model. We encourage modellers to combine the PTHA18 information with their own experience when selecting source zones to include; final decisions on which scenarios to include will be made later in the workflow, so if in doubt, it is better to include source zones at this point. The capacity for modellers to make these judgements highlights the flexibility of scenario-based approaches, which is one of their most important advantages.

In the [multi-gauge scenario selection script](#), we search each identified source zone for scenarios with a given slip type. In this study **heterogeneous-slip** (HS) scenarios were used, but the script also supports the use of **variable-area-uniform-slip** (VAUS) scenarios.

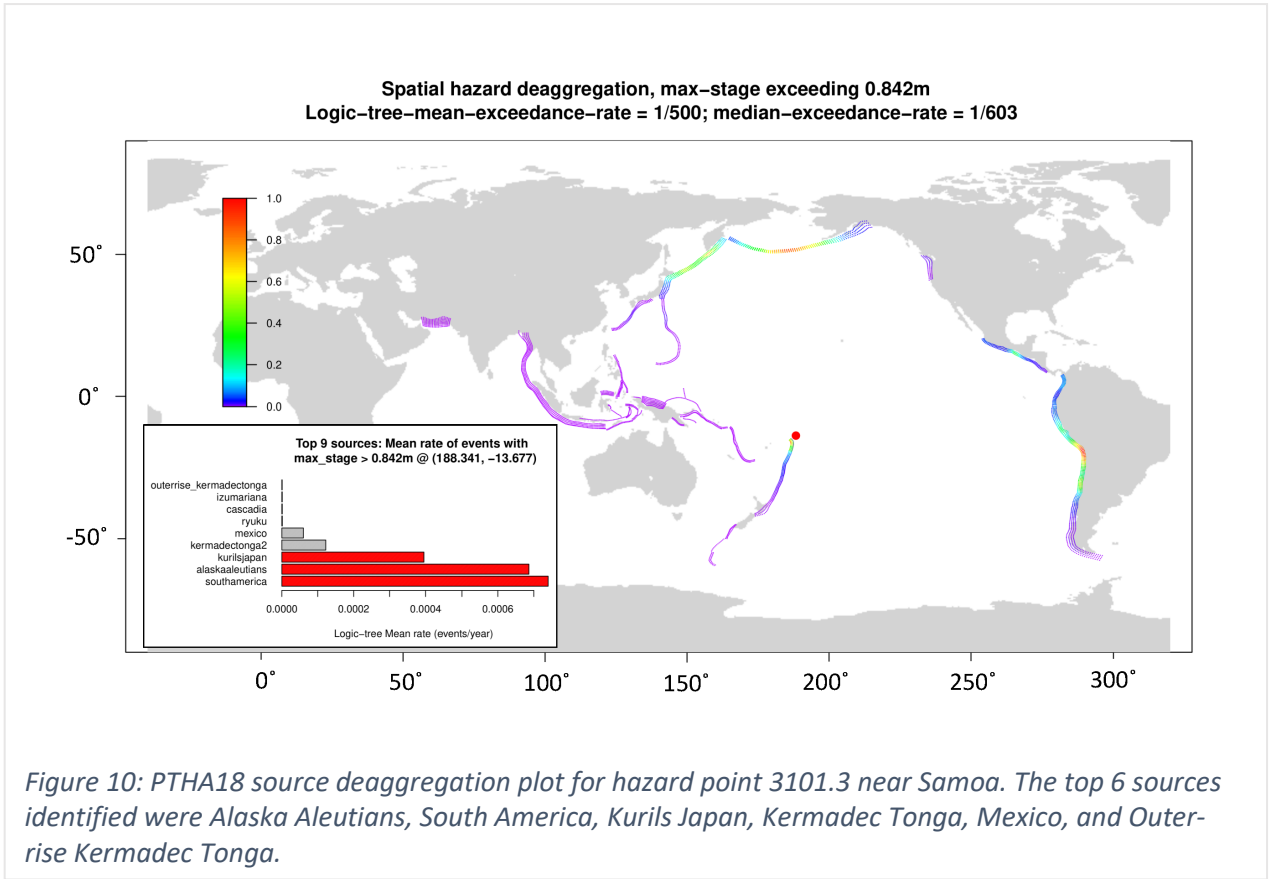


Figure 10: PTHA18 source deaggregation plot for hazard point 3101.3 near Samoa. The top 6 sources identified were Alaska Aleutians, South America, Kurils Japan, Kermadec Tonga, Mexico, and Outer-rise Kermadec Tonga.

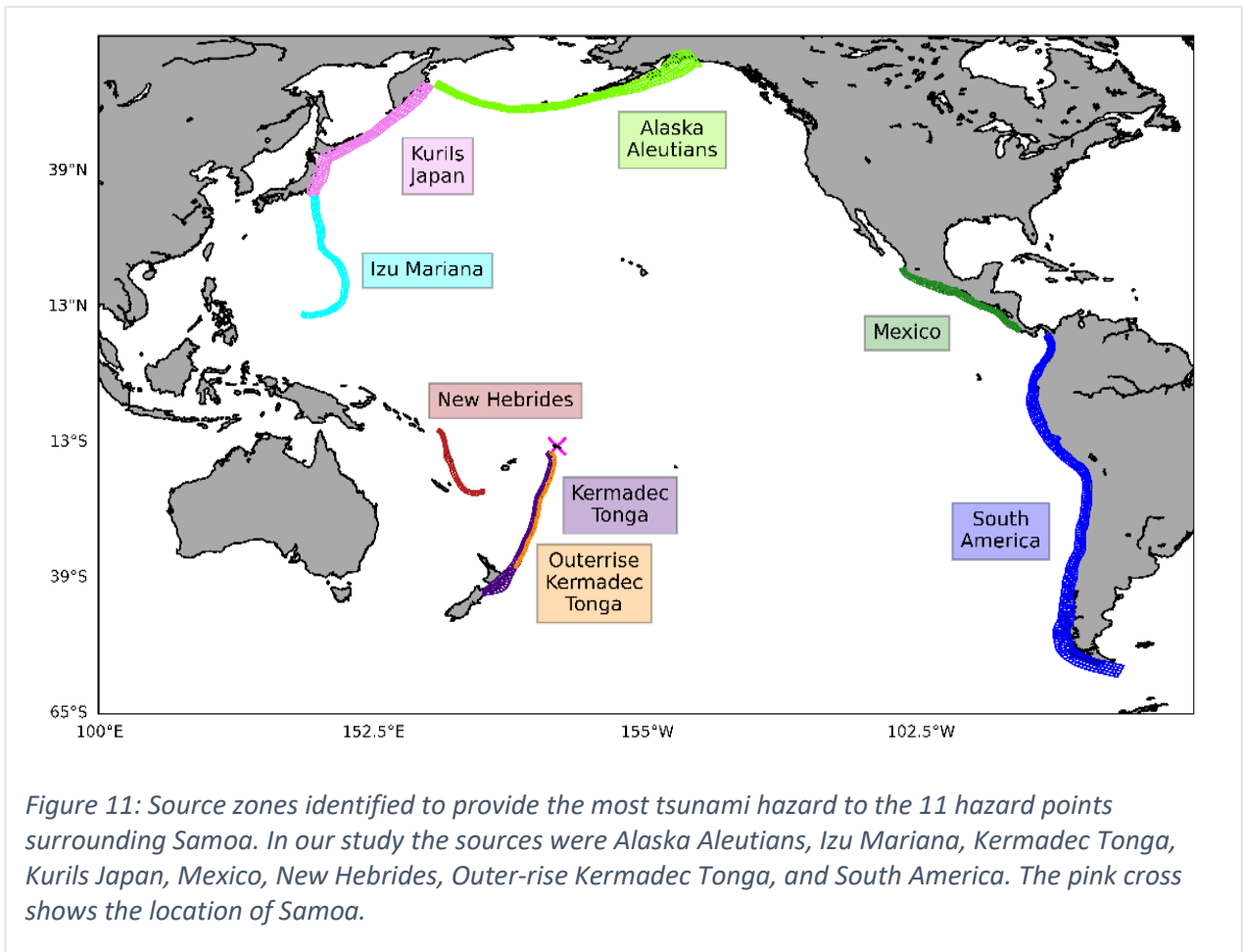


Figure 11: Source zones identified to provide the most tsunami hazard to the 11 hazard points surrounding Samoa. In our study the sources were Alaska Aleutians, Izu Mariana, Kermadec Tonga, Kurils Japan, Mexico, New Hebrides, Outer-rise Kermadec Tonga, and South America. The pink cross shows the location of Samoa.

Step 3: Candidate scenario selection: matching the exceedance-rate and stage tolerance criteria

The **hazard point** source **deaggregation** plots in **Step 2** show the tsunami **maximum-stage exceedance-rate** curves and the associated uncertainty. Figure 12 provides an example. This information helps define the offshore tsunami sizes that are likely to be of interest.

The selection of exceedance rates should be made in consultation with relevant stakeholders and decision-makers in accordance with the intended application. For the Samoa case study, four exceedance rates were chosen (Table 3).

Table 3: Exceedance rate and corresponding ARI values selected for the Samoa scenario-based tsunami hazard assessment.

Exceedance Rate (events/yr)	Average Recurrence Interval (yr)
0.01	100
0.002	500
0.001	1000
0.0004 (84th percentile)	2500 (84th percentile)

A note on uncertainty: The PTHA18 hazard point data is derived from modelling tsunamis from earthquake sources with uncertain frequencies. The uncertainties from these methods are quantified using logic trees and stored with the tsunami frequency and size information for the hazard point. Different percentiles of uncertainty are [available](#) to the user. It is generally advised to use the logic-tree-mean exceedance-rate curves. For a more conservative approach, the 84th percentile may be used.

At rare return periods, we are likely to be considering earthquake scenarios that do not have a 100% chance of being possible according to the PTHA18 (because of uncertainties in maximum magnitudes). Rather, the various exceedance-rate curves provided in PTHA18 represent an attempt to characterise uncertainties in the frequency of large tsunamis from multiple source zones.

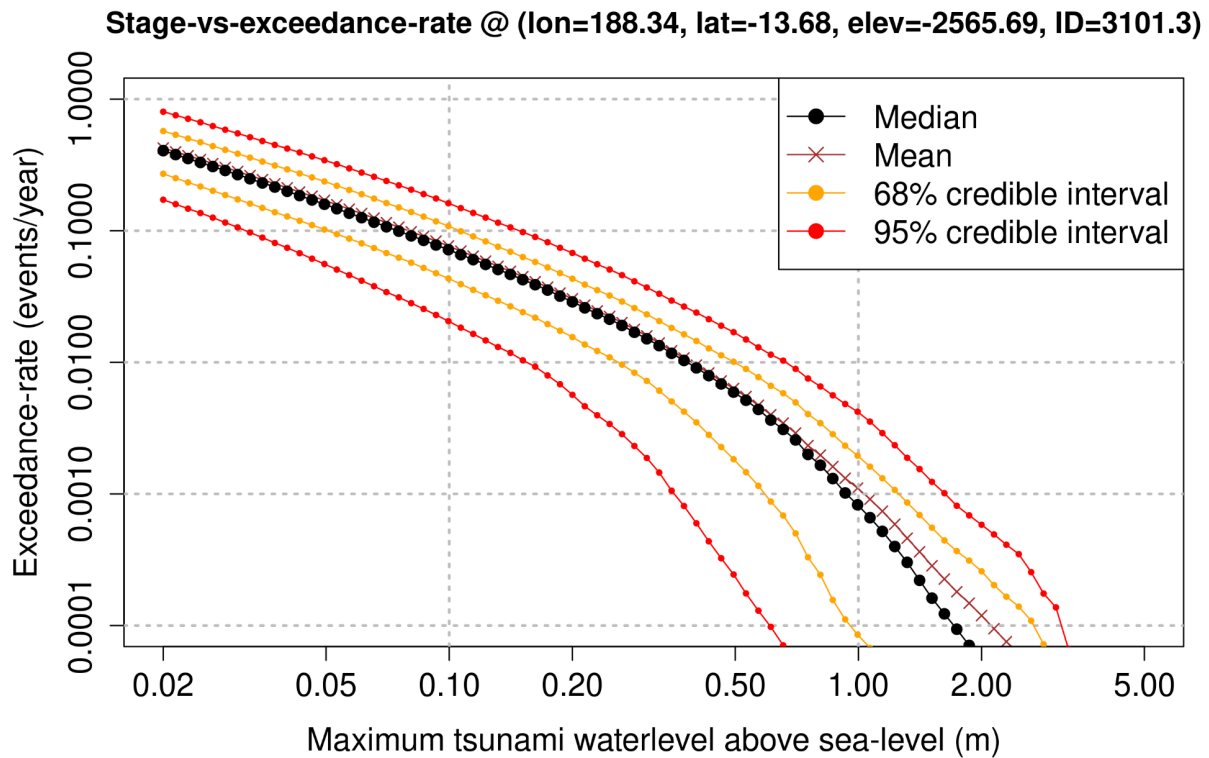


Figure 12: Maximum-stage exceedance rate curve for one of the hazard points used in the Samoa study (gauge ID 3101.3).

For each exceedance rate, we select multiple scenarios from multiple source zones, such that all the offshore gauges of interest have at least one scenario with tsunami maxima close to the desired exceedance rate, without going too far over. The idea is that collectively the maximum inundation from these scenarios should give an indication of the inundation depths at the target exceedance rate. However, we stress that the procedure is necessarily heuristic given the non-monotonic relations between offshore and onshore wave heights, as noted above.

It is unlikely that scenarios exist that exactly match the desired exceedance rate, particularly when multiple gauges are used. Thus a user-defined tolerance is specified to determine how much the included scenarios can deviate from the desired stage level. In the current study we used a value of 4%; this could be increased (or decreased) to generate more (or fewer) candidate scenarios, although it should not be increased too much (to ensure the offshore tsunami maxima is close to the target value). For instance, hazard point ID 3093.3 has a tsunami stage of 0.962 m at a 1/500 year exceedance rate event, and with a 4% tolerance, so we consider a scenario “close” to this if it is between 0.924 m and 1.000 m at that point (Table 4). The code will find scenarios matching the desired stage interval at some specified number of the hazard points simultaneously (which was set to 3 herein), while being smaller at all the other hazard points.

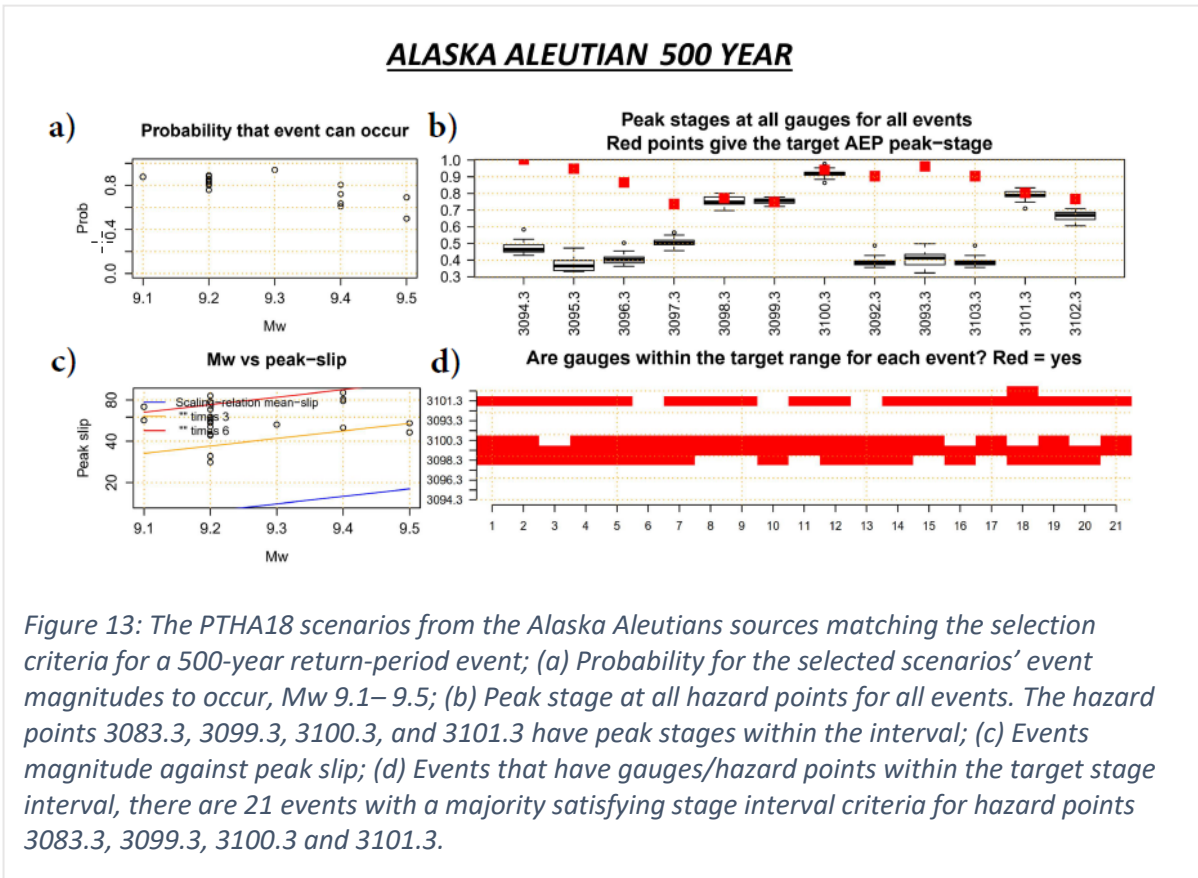
The latter two parameters (tolerance and number of hazard points that must be satisfied simultaneously) affect the number of scenarios that are identified. In practice one can obtain more scenarios by increasing the tolerance or reducing the number of gauges, and vice versa. This should be done to obtain a manageable number of scenarios for further analysis. The code to implement these steps is presented in [this section of the associated tutorial](#).

Table 3: Samoa case study stage interval of 4% for the exceedance rate of 0.002 events/yr or a return period of 500 years for the selected hazard points.

Hazard Point ID	Exceedance Rate (events/yr)	Return Period (yr)	Stage (m)	±4% Stage Interval
3093.3	0.02	500	0.962	0.924–1.000
3094.3	0.02	500	1.004	0.964–1.044
3095.3	0.02	500	0.949	0.911–0.987
3096.3	0.02	500	0.866	0.831–0.901
3097.3	0.02	500	0.737	0.708–0.766
3098.3	0.02	500	0.772	0.741–0.803
3099.3	0.02	500	0.748	0.718–0.778
3100.3	0.02	500	0.941	0.903–0.979
3101.3	0.02	500	0.803	0.771–0.835
3102.3	0.02	500	0.767	0.736–0.798
3103.3	0.02	500	0.903	0.867–0.939

Once the above parameters are set, the [multi-gauge scenario selection script](#) can be used to filter the PTHA18 scenarios based on the chosen criteria. It will also generate a graphical summary with various statistics describing the scenarios (Figure 13, details explained in the [online tutorial](#)). At any hazard point, by construction the scenarios will not greatly exceed the desired stage level (assuming the tolerance specified above is small). However, some scenarios may produce waves much smaller than the desired stage level at some gauges; this is depicted in two different ways in the right-hand panels of Figure 13 (see also the [online tutorial](#)).

At this stage of the analysis, the intention is that the modeller has derived a reasonable set of candidate scenarios. However, not all of these scenarios will typically be used for inundation modelling; rather the modeller should select from among these using subjective judgement.



Step 4: Final scenario selection

Selecting the tsunami scenarios that were filtered in **Step 3** requires some judgement. It should be done so that:

- the selected scenarios produce tsunami maxima that collectively reach the desired exceedance rate at the hazard points of interest. Outputs such as Figure 13d can be helpful to identify scenarios meeting the criteria at particular hazard points.
- the modeller and end-users are otherwise comfortable with the selected scenarios, considering their own subjective judgements as well as the PTHA18 scenario occurrence-rate models.

This step is very flexible. Some factors that modellers may want to consider are shown below.

Is the scenario likely to be possible?

Each scenario has a likelihood that it is possible. This is a different concept to the exceedance rates of the wave heights at offshore locations. Modellers should be careful about over-emphasising scenarios that are unlikely to be possible according to the PTHA18, unless the intention is to run very conservative scenarios.

To understand this concept, recall that PTHA18 treats the maximum magnitude on each source zone as uncertain. Thus, although PTHA18 includes scenarios up to the largest allowed maximum magnitude, they are increasingly unlikely to be possible according to the PTHA18's own scenario occurrence-rate models. Figure 13a depicts the probability that some candidate scenarios can occur according to PTHA18, and similar plots are created in the [online tutorial](#). The probability will be a decreasing function of magnitude because higher magnitudes are more likely to exceed the maximum magnitude. For source zones that include a segmented treatment it will also depend on the earthquake location. All else being equal, scenarios that are likely to be possible should be preferred.

What is the relative likelihood of each scenario occurring?

In general the candidate scenarios will cover a range of earthquake magnitudes. Each PTHA18 earthquake is prescribed an occurrence rate and the largest magnitudes are relatively rare. The selection script [online tutorial](#) includes plots that depict the cumulative distribution of earthquake magnitudes for the selected scenarios, weighted by their occurrence rate.

All else being equal, scenarios with typical magnitudes (i.e. contributing most to the exceedance rate) should be preferred to scenarios with rare magnitudes.

What is the initial potential energy?

A measure of the overall size of the tsunami generated by each earthquake scenario can be inferred by comparing its initial potential energy to that from other scenarios and historical tsunamis (e.g. Nosov et al., 2014; Titov et al., 2016; Davies et al. 2020). For example, if the energy is far greater than that of the 1960 Chile tsunami, then the scenario is clearly very large. If an event is similar to another historical event (e.g. 2010 Maule tsunami) but on a different source, we might describe the scenario as “similar to the 2010 Maule event but in a different location”. Such information can help the user make judgements about the plausibility of different scenarios.

The selection script [online tutorial](#) includes a plot with potential energy information. Note that potential energy does not indicate the size of the tsunami at the hazard points of interest, which also depends on the earthquake scenario location.

What is the maximum slip?

In the PTHA18, maximum slip varies for each earthquake scenario. For **variable-area-uniform-slip** scenarios (see Appendix A), it will depend on the magnitude and rupture area, while for **heterogeneous-slip** scenarios it will depend on these factors as well as the spatial distribution of slip. In addition, scenarios are not permitted to have slip maxima >7.5 times the average slip expected for that magnitude. Such scenarios can be generated but are assigned an occurrence rate of 0; full details are in Section 3.2.3 of Davies and Griffin (2018). The factor 7.5 permits slip maxima that are consistent with some of the higher published values for finite fault inversions for large tsunamigenic earthquakes. In reality such limits on slip maxima are very uncertain.

The selection script [online tutorial](#) creates a plot with information on slip maxima (see also Figure 13c).

Does the tsunami maxima occur many hours after tsunami arrival?

The largest tsunami wave may not be the first wave in the tsunami **wave train**. To check when the largest wave occurs, the wave time series can be extracted from the hazard points (Figure 14). Code for doing this is presented in the scenario selection [online tutorial](#).

In general it is preferable to focus on scenarios where the wave maximum occurs within a few hours of the tsunami arrival, perhaps less than eight. This is advantageous because the inundation model will not need to be run for so long. Furthermore, the PTHA18 models tsunamis without applying friction, meaning that global-scale tsunami dissipation is not well represented. This will reduce the accuracy of very late arriving waves (Davies et al., 2020). Although the latter study presents an approach to correct for this that can be used, it is simpler and computationally cheaper to focus on scenarios where the largest waves occur soon after tsunami arrival.

For the Samoa case study, the scenario selection initially focused on the probability that each scenario is possible according to the PTHA18. For example, based on Figure 13(a) for Alaska Aleutians RP 500 year, magnitudes from 9.1 to 9.4 were considered plausible (>50%), whereas scenarios with magnitude 9.5 were less favoured as the PTHA18 suggests they have <50% chance of occurring. While the latter probabilities refer to the chance of different earthquake magnitudes being possible (over any time frame), it should be noted that the return periods reflect the wave heights for the logic-tree-mean exceedance-rate curve, and do not reflect the return periods of the earthquakes themselves.

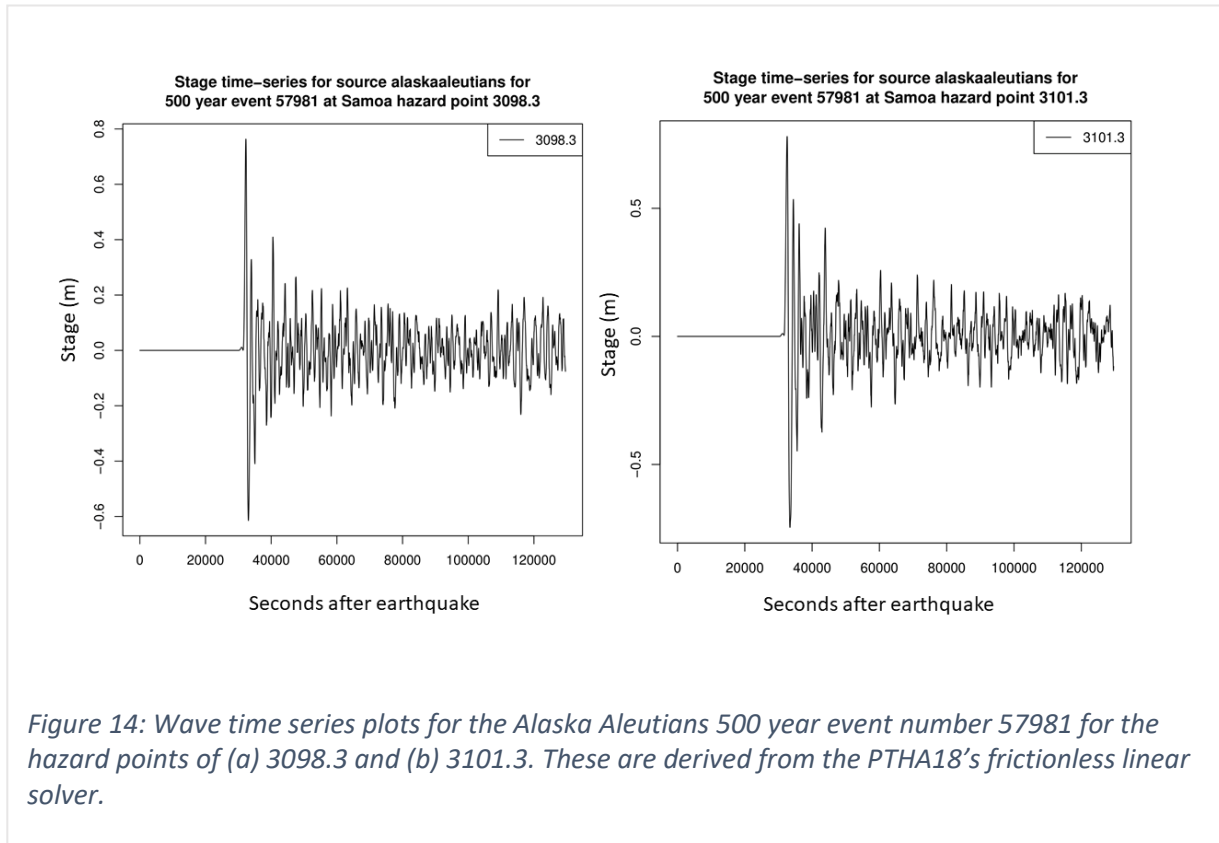


Figure 14: Wave time series plots for the Alaska Aleutians 500 year event number 57981 for the hazard points of (a) 3098.3 and (b) 3101.3. These are derived from the PTHA18's frictionless linear solver.

We also consider the scenario's peak-slip and magnitude. Figure 13(c) has coloured lines used for comparative purposes: the blue line (bottom) shows the average slip for a hypothetical uniform-slip earthquake with the specified magnitude and median scaling-relation area, with orange (middle) and red (upper) lines showing the latter multiplied by 3 and 6 respectively. For variable-area-uniform-slip earthquakes (VAUS), high peak slip values correspond to compact earthquakes and vice versa. For heterogeneous-slip earthquakes (HS), high peak slip values are often associated with compact earthquakes but can more generally indicate that the slip is concentrated on an asperity. We chose to select scenarios with slip maxima between the scaling-relation-based value for a uniform-slip earthquake (blue line, bottom) and 6 times greater (red line, top). For example, this would allow a magnitude 9.1 earthquake to have a peak slip value of at most 65 m. The latter is in the vicinity of slip maxima inverted for the 2011 Tohoku earthquake, an event known for its relatively compact rupture (Lay, 2018).

Subject to the above constraints, a set of scenarios was manually selected for each return period. When combined, the scenarios met the stage interval criteria for most hazard points near sites of interest. For example, the Alaska Aleutians 500-year return period scenarios covered four hazard points (Table 5). Scenarios from other source zones were used to meet the exceedance-rate criteria at other sites. Ultimately 68 tsunami scenarios were selected for inundation simulation in the study. **Deformation grids** for all scenarios were then extracted for use in **hydrodynamic modelling** (Figure 15).

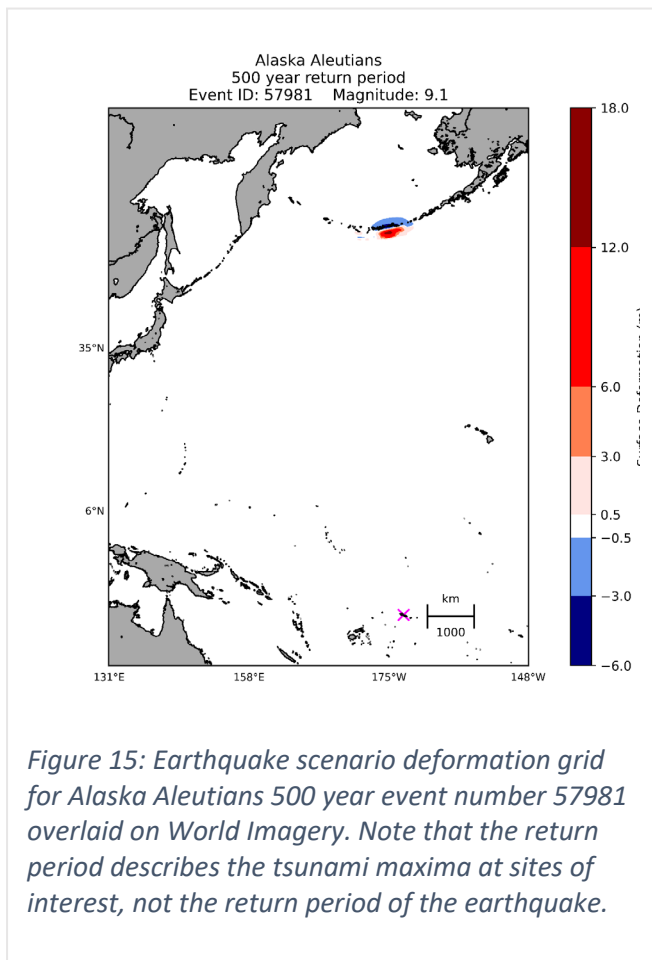


Figure 15: Earthquake scenario deformation grid for Alaska Aleutians 500 year event number 57981 overlaid on World Imagery. Note that the return period describes the tsunami maxima at sites of interest, not the return period of the earthquake.

Step 5: Tsunami inundation modelling

Once the scenarios have been selected, they can be modelled through to **inundation**. For guidelines on tsunami modelling methodologies we refer to Lynett et al. (2016) and AIDR (2018). There are several key factors to consider.

In the Samoan case study, the tsunami was simulated from the earthquake source through to inundation, using the PTHA18 **deformation grids** to define the earthquake-induced ocean surface perturbation for each scenario. The model BG-Flood (Bosserele et al., 2020) was used to solve the nonlinear shallow water equations in spherical coordinates on a series of nested grids, with grid-sizes ranging from 5 km (in the deep ocean) through to 50 m (around all of Samoa), and 5 m at a site of interest (the town of Apia).

Further information on the Samoa hydrodynamic model can be found in the SPC PCRAFI Samoa tsunami hazard assessment report (Giblin, 2022 - in preparation). This covers the model used, the **sensitivity analysis** and **validation**, and the choice of the background sea level to reflect the effects of the tide and sea level rise.

The inundation generated by a tsunami can vary significantly depending on the tide level and other meteorological processes (e.g. sea level anomaly). A common practice is to use a static tide level (e.g. MSL or some other value). As the joint probability of tsunami wave and water level is not considered in this methodology, the modeller should consider using relatively high water levels such as the Mean High Water Spring (MHWS) or even the Highest Astronomical Tide (HAT) to add a degree of conservatism and make it less likely that the model will under-predict the inundation from real tsunamis. We also recommend that inundation hazard assessments consider the intensification of the hazard due to climate change. Sea level rise

(SLR) scenarios, informed by the latest IPCC report and consultation with relevant stakeholders, should be integrated into such assessment.

Further considerations:

Tsunami inundation modelling – what to consider:

1. Is the model you are using well tested/validated?
2. Are you using a grid resolution that will resolve the information you need?
3. Do you have historical data with which to test your model?
4. Do you have sufficient elevation data for a seamless topography/bathymetry grid? (Make sure you know what the vertical reference datum is for all datasets used.)
5. Have you considered tide and other changes to local water levels? Are you using a static or dynamic water level?
6. Have you considered sea level rise due to climate change?
7. Have you consulted local stakeholders about their interests?

Step 6: Results aggregation

After inundation models have been run for all scenarios, the results can be aggregated for each exceedance rate. The various inundation output parameters that are commonly used include maximum flow depth, maximum velocity, and maximum flux. Figure 17 shows an example of aggregated maximum inundation flow depths for Samoa. Other inundation hazard products can be derived from the scenario-based approach, and we refer to the SPC PCRAFI Samoa tsunami hazard assessment report discussed by Giblin (2022, in preparation).

It is important to note the conservative nature of aggregating inundation parameters for each exceedance rate, which is a feature of the scenario-based method. This is a consequence of the fact that offshore wave heights are not a perfect predictor of onshore impacts, as noted above. For example, the wave period and direction will also contribute to variations in the inundation along a given coastline. If the scenarios are combined by taking their point-wise maxima, then if many scenarios are included, we are likely to have at least one that is conservative. This implies that the combined result is also likely to be conservative. Examples of variation in inundation results for different tsunamis with similar offshore wave heights are provided in Appendix C.

***A note on elevation datasets:**

Input data quality can significantly affect results (e.g. Griffin et al., 2015) and both data resolution and accuracy must be considered. Global datasets such as [GEBCO](#) can be suitable for regional scale tsunami modelling but are not suitable for modelling at a local scale.

Higher resolution datasets may be required and can often be obtained from online databases such as [AusSeabed](#). Multiple datasets can then be compiled, and gaps can be interpolated (e.g. Wilson & Power, 2018). If no data is available, elevation data collection can be commissioned. We encourage the release of elevation data under creative commons licensing to facilitate further study.

In general terms, a grid size of less than 5 m can be considered high resolution; 5–50 m, mid-level; and greater than 50 m, low resolution.

Elevation data grid resolution must also be reflected in the model setup. Figure 16 shows an example of tsunami modelling at different resolutions:

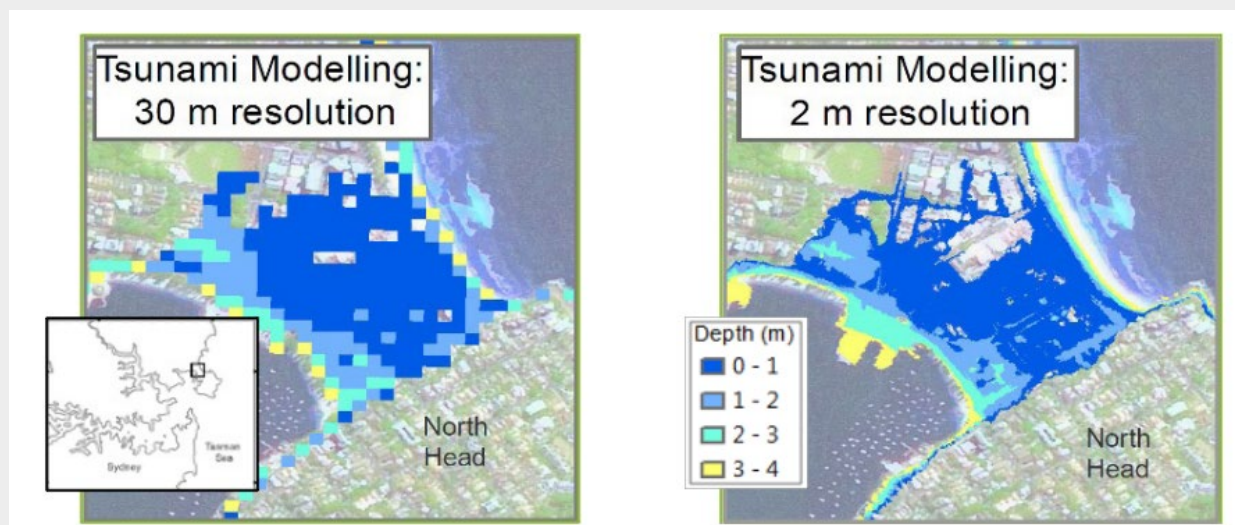
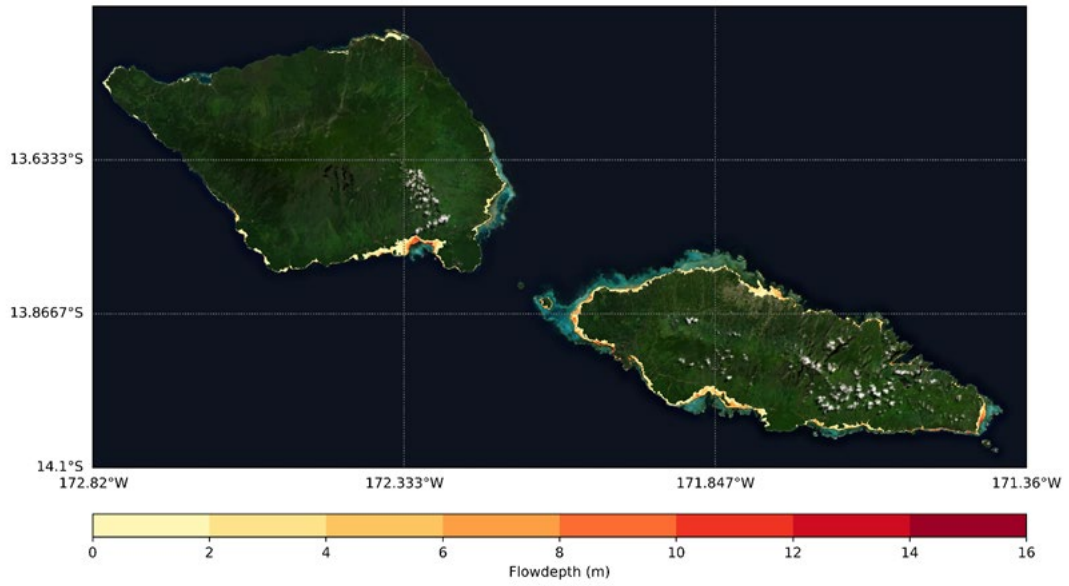


Figure 16: Comparison of maximum inundation depth resulting from tsunami modelling using different elevation data and model resolution (Picard et al., 2019).

a)

Tsunami Inundation of Samoa
Flow depth aggregation per return period
Return Period: 2500 year 84th percentile



b)

Tsunami Inundation of Apia, Samoa
Flow depth aggregation per return period
Return Period: 2500 year 84th percentile

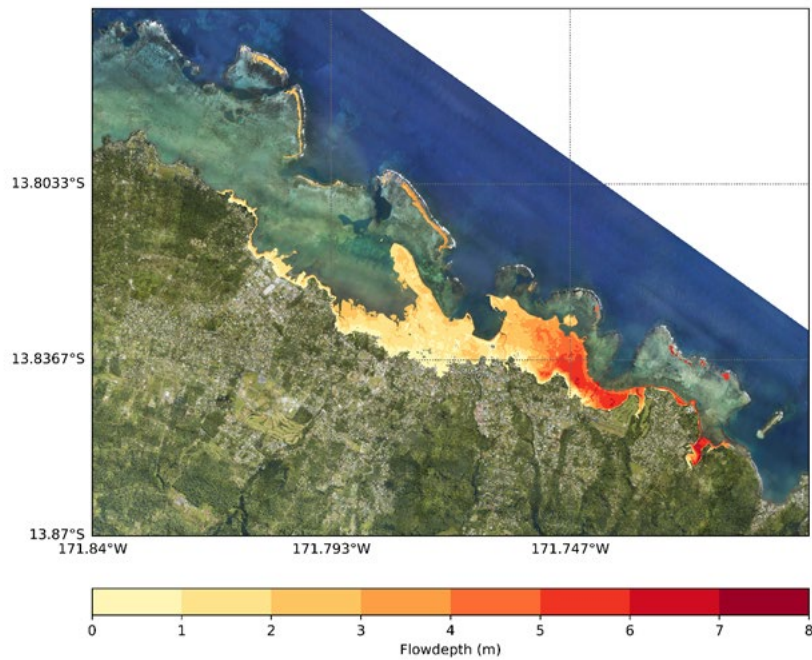


Figure 17: Aggregated maximum flow depth inundation at return period 2500 year 84th percentile for (a) Samoa at 50 m resolution national scale, and (b) Apia at 5 m resolution.

6.2 Method 2: Monte Carlo sampling and application in PNG and Tonga

The scenario-based method presented above (**Method 1**) provides a practical approach to onshore tsunami hazard assessment. The main shortcoming is that results will not necessarily match those that would be obtained if we simulated every scenario in the offshore PTHA (the “all-scenarios solution”). Further it is difficult to know how large the differences could be. Such limitations are fundamental to scenario-based approaches; they are not specific to tsunami hazard assessment. For example, the same issues arise in flood hazard assessment (Ball et al. 2019).

In this section we present an alternative approach to using offshore PTHA for onshore hazard assessment, based on Monte Carlo sampling. The Monte Carlo approach enables rigorous approximation of the “all-scenarios solution”. It also enables uncertainties in the offshore PTHA to be fully represented onshore. In this regard it is superior to the scenario-based approach.

But these benefits of Monte Carlo methods come at significant cost. The number of scenarios for which inundation modelling is required will vary from case to case, but the range is in the order of 100 to 10,000 (e.g. De Risi and Goda, 2017; Williamson et al., 2020; Gonzalez et al., 2021). Thus, the method will typically require access to **high-performance-computing (HPC)** resources and associated technical skill sets, making it infeasible in some situations. But for applications that warrant rigorous translation of the offshore PTHA results onshore, with full representation of uncertainties, it is worth considering a Monte Carlo approach.

Monte Carlo methods approximate the onshore hazard by using a large random sample of scenarios. Inundation is only simulated for the random scenarios. If the entire Monte Carlo sample represents just a small fraction of all the offshore PTHA scenarios, then the technique is much more computationally efficient than simulating all scenarios (while approximating the same result).

The key challenge is that, because not all scenarios are simulated, there is some **approximation error** (or Monte Carlo error) in the exceedance rates that needs to be controlled. The statistical properties of these errors are well understood for a variety of Monte Carlo methods, making it possible to control the errors in practice (Davies et al., 2021). The **root-mean-square error** can always be reduced by simulating more scenarios, and typically scales with the inverse square-root of the number of random scenarios. For example, to halve the expected error, we should increase the number of scenarios by a factor of four.

While effective, the management of Monte Carlo errors by using larger random samples quickly becomes computationally prohibitive. However, a range of Monte Carlo sampling methods exist, and in the context of PTHA, some have much greater accuracy than others for equivalent sampling effort.

For offshore-to-onshore PTHA, the most common Monte Carlo sampling techniques are synthetic catalogues, and **stratified sampling by magnitude**. We recommend that modellers use variants of stratified sampling by magnitude, including the techniques discussed below

to better represent scenarios with large waves near the site of interest. Although not recommended here, discussion of synthetic catalogues is provided in Appendix D. Further detail and equations for all methods are provided in Davies et al. (2021), and a tutorial that shows how to implement the calculations is [available online here](#).

Checklist – what do I need?

- High performance computing resources
- [PTHA18 report](#)
- [PTHA18 source code](#)
- An understanding of the relevant source zones for my area of interest (see PTHA18 report)
- [Tsunami history](#) for the area
- PTHA18 global [hazard point locations](#)
- The [source deaggregation plot](#) to see which sources contribute most to the hazard at the selected hazard points
- This [tutorial](#) explaining how to perform various kinds of stratified sampling by magnitude in the context of PTHA18
- This [tutorial](#) explaining how to calculate the **variance** that would result from repeated Monte Carlo at PTHA18 hazard points.

Outcomes – what will this method provide me with?

- Estimates of the tsunami inundation depth and frequency at all locations in the model domain.
- Quantified uncertainty for the onshore tsunami hazard results, similar to that available in the offshore PTHA.

Limitations of Monte Carlo sampling for onshore PTHA

Compared with scenario-based methods, Monte Carlo methods are less flexible because they aim to approximate the “all-scenarios” PTHA result. This means it is more difficult to integrate user judgements about tsunami sources (e.g. maximum magnitudes) that are not already implicit in the offshore PTHA.

Monte Carlo sampling tends to be computationally expensive, and the calculations are more technically challenging to implement than are scenario-based approaches.

The tutorials linked in these guidelines show how to implement scenario sampling, so modellers do not need to write their own sampling code; however, we cannot provide code to run all the inundation models or integrate their results. This component will vary with the specific inundation model used in each study and modellers need to be able to implement this themselves.

Steps – how to do it

The steps below describe **stratified sampling by magnitude**, which is a common Monte Carlo technique for estimating exceedance rates in offshore-to-onshore PTHA (e.g. De Risi and Goda, 2017; Williams et al., 2020). A tutorial explaining how to perform stratified sampling by magnitude, optionally with modifications that improve the representation of large tsunamis near the site of interest, is [available online here](#). For a more detailed explanation see Appendix E and Davies et al. (2021).

In practice we suggest that modellers employ modified variants of stratified sampling (discussed in the next section), which can more efficiently represent large tsunamis near the site of interest. These are modifications of the basic stratified sampling technique, which is described below.

Step 1: Stratify the PTHA18 scenarios

The PTHA18 scenarios are first stratified (or grouped) into separate magnitude bins, denoted $M_{w,b}$. In PTHA18 the scenario earthquake magnitudes range from 7.2 to 9.6 in increments of 0.1, and the [online tutorial](#) calculations use these magnitudes as unique bins.

Each magnitude bin $M_{w,b}$ should be thought of as representing a set of scenarios (containing all the offshore PTHA scenarios with the associated magnitude).

Step 2: Sample the scenarios from each magnitude bin.

A chosen number of scenarios $N(M_{w,b})$ is randomly sampled from each magnitude bin using **weighted random sampling with replacement**. Within each magnitude bin the chance of sampling each scenario should be proportional to the **scenario occurrence rate**. The latter constraint will be relaxed in the modified sampling methods below, to facilitate better representation of large waves near the site of interest.

For example, we might sample 12 scenarios per magnitude bin (i.e. $N(M_{w,b}) = 12$). As PTHA18 contains 25 magnitude bins, this will lead to 300 random scenarios in total. We denote the set of random scenarios that were sampled from magnitude bin $M_{w,b}$ as $E_{b,SS}$.

Often the number of selected scenarios $N(M_{w,b})$ is the same (uniform) in each magnitude bin. But this is not essential, and below we suggest **non-uniform sampling** methods that can be more efficient.

Step 3: Calculate exceedance rates from the Monte Carlo sample

The exceedance-rate calculation requires knowing the quantity of interest $Q(e)$ for each random scenario, and the overall occurrence rate of earthquakes in each magnitude bin $M_{w,b}$, denoted $\lambda_i(M_{w,b})$. The latter can be calculated directly from PTHA18 by summing the occurrence rates of all earthquakes in that bin (including all scenarios, whether or not they were randomly sampled). The quantity of interest can be calculated from the inundation model results, or at offshore hazard points by using the PTHA18 wave time series.

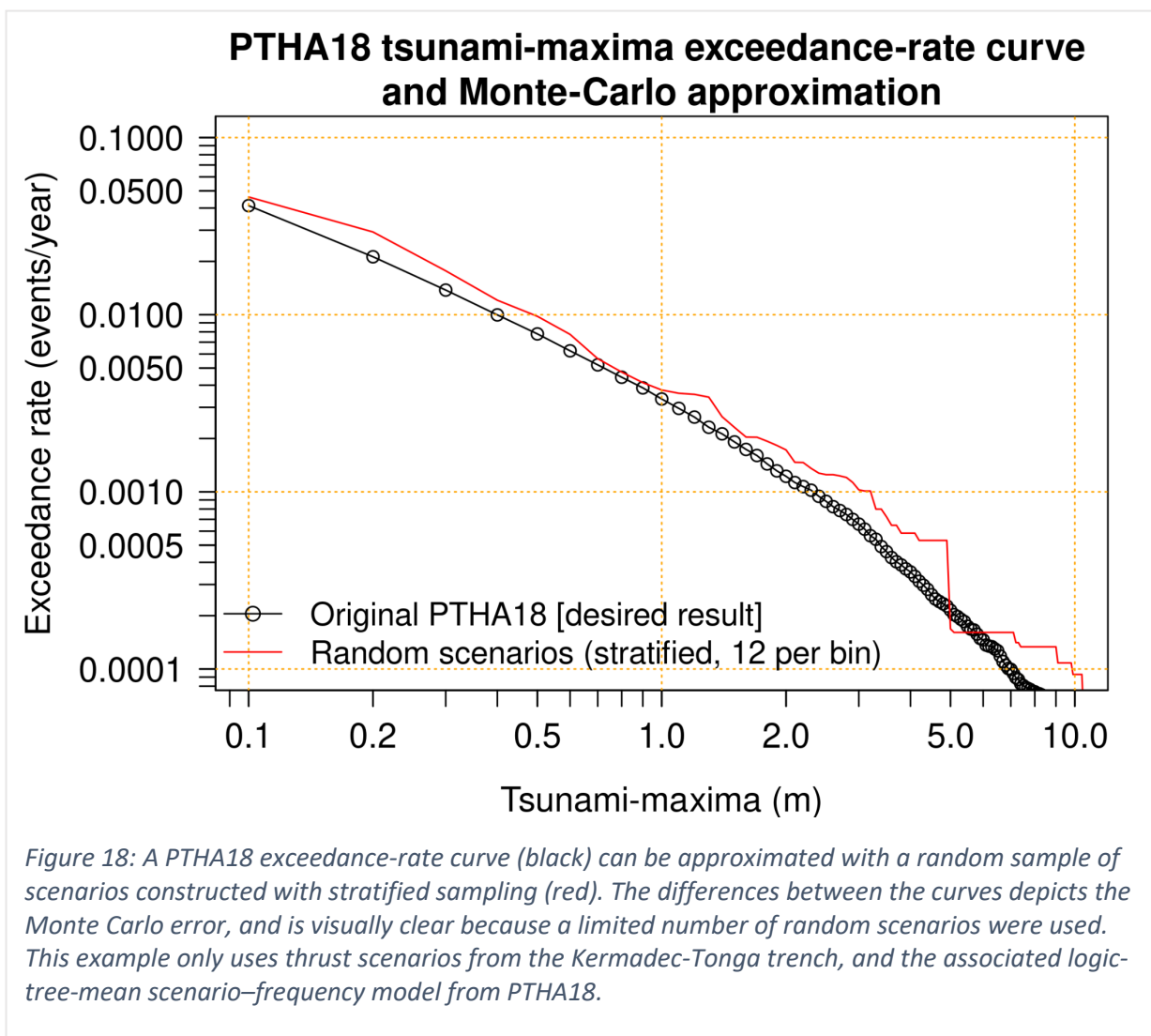
The exceedance rates can then be approximated from the Monte Carlo sample as:

Equation 2

$$\lambda_i(Q > Q^T) \approx \sum_{M_{w,b} \in \{ \text{All magnitude bins} \}} \lambda_i(M_{w,b}) \left(\sum_{e \in E_{b,SS}} \left[\frac{1_{(Q(e) > Q^T)}}{N(M_{w,b})} \right] \right)$$

where the notation in Equation 2 follows that used in Equation 1. The calculations are demonstrated in the [online tutorial](#).

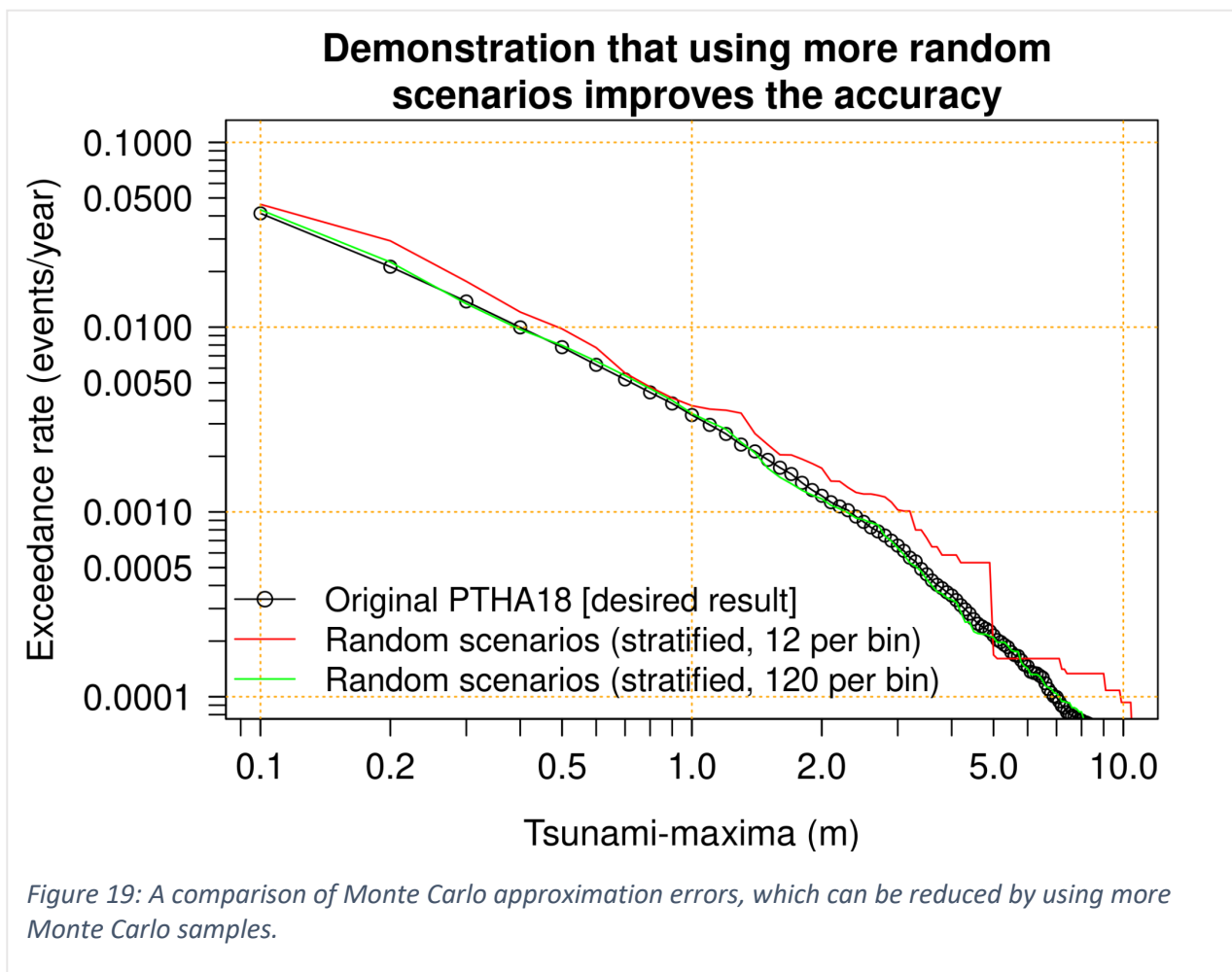
Figure 18 illustrates one Monte Carlo approximation to an exceedance-rate curve, computed using stratified sampling and Equation 1. While there is clearly some approximation error, the advantage is that for inundation hazard assessment we only need to simulate inundation for a limited number of random scenarios (300 in this case).



Managing approximation errors by selecting an appropriate sample size

The key challenge of Monte Carlo methods is in managing the approximation errors, such as those visible in Figure 19. How much error is acceptable will vary depending on the application. The significance of approximation errors should be considered in comparison to the epistemic uncertainties (Figure 5). If approximation errors are much smaller than epistemic uncertainties, then so long as the epistemic uncertainties are accounted for when interpreting the model results, the approximation errors will be of minor significance and can largely be ignored.

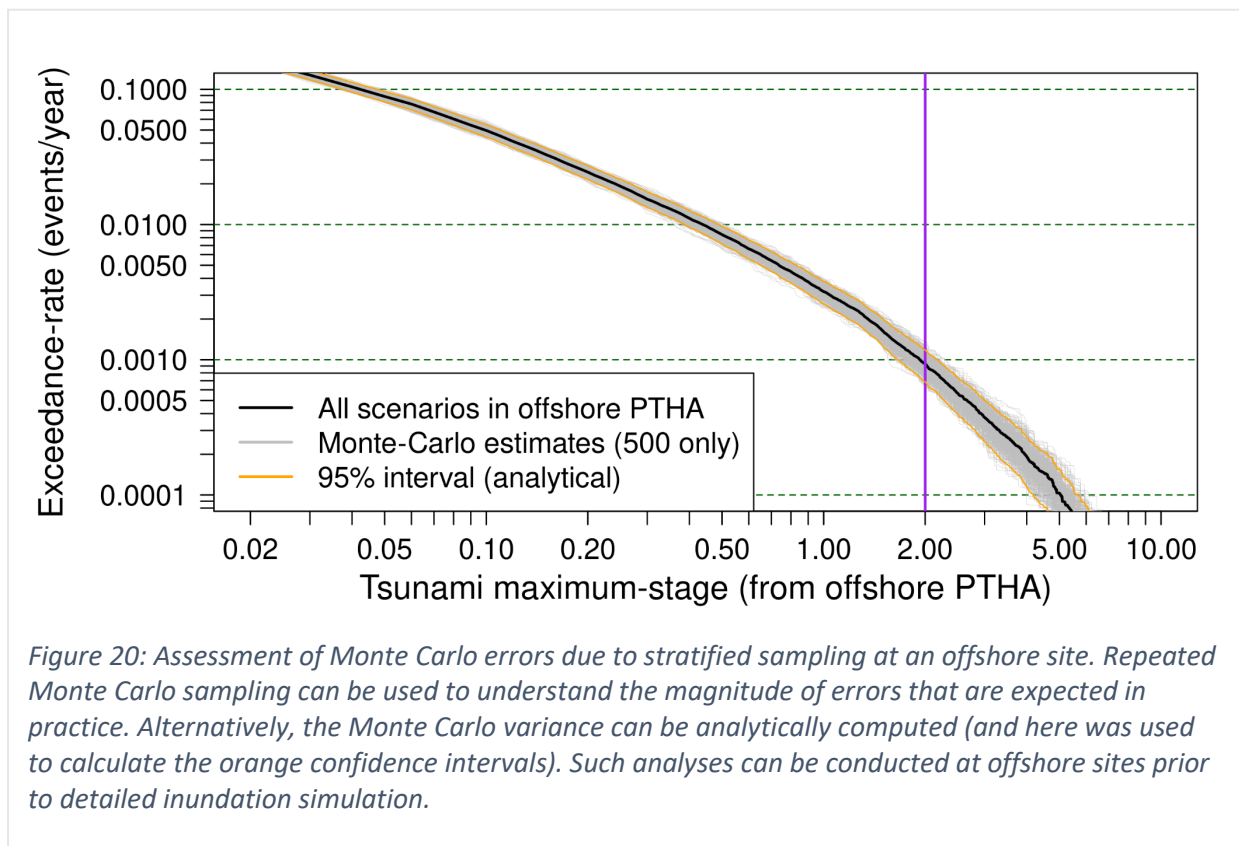
The simplest way to reduce Monte Carlo errors is to increase the number of random samples. Figure 19 compares the results using sample sizes of 12 and 120 per magnitude bin. It is clear that use of 120 scenarios per magnitude bin has substantially reduced the Monte Carlo error. But in practice, the sample sizes that are used will be constrained by the efficiency of the inundation model and available computational resources.



To help choose the Monte Carlo sample size, we suggest that modellers pick a range of feasible sizes and then check the associated Monte Carlo accuracy at PTHA18 hazard points, as outlined below. This does not require inundation modelling because PTHA18 provides the modelled waves. It allows modellers to quantify the **approximation errors** that are expected

for a given Monte Carlo sample size, at the hazard points. If the errors are found to be large at offshore hazard points close to the onshore site of interest, they are likely also to be large at the onshore site of interest. In that case the modeller should revise the sampling scheme.

One way to compute the approximation errors is to generate many Monte Carlo samples and examine the spread of the exceedance-rate curves (e.g. Figure 20). This spread gives an idea of the errors that will be expected from a single Monte Carlo sample. A useful fact is that, at offshore hazard points, the variance of these curves can be calculated from theory without doing Monte Carlo sampling. This provides a fast method of quantifying approximation errors at offshore sites. Full details are provided in Davies et al. (2021), and calculations using PTHA18 are demonstrated in [this online tutorial](#) (specifically [this section](#)).



The simplest way to reduce approximation errors is to increase the sampling effort, if that is computationally feasible. It is also likely that the errors can be reduced without additional **computational effort** by using the techniques in the next section.

Once the offshore errors have been checked and judged reasonable, the onshore analysis proceeds by simulating inundation for all sampled tsunami scenarios.

Step 4: Results aggregation

Once inundation has been simulated for the random scenarios, the exceedance-rate calculations can then be implemented anywhere in the inundation model domain using Equation 2. This enables depth-vs-exceedance-rate curves to be computed at any site. By doing this at multiple sites we can map the exceedance rate for any inundation depth, or the inundation depth for any exceedance rate. Figure 21 provides an example for Vanimo in Papua New Guinea, which was derived using stratified sampling via the workflow above. In this case 660 scenarios were used, with 30 scenarios in each magnitude bin from magnitudes 7.5 to 9.6.

A note on high performance computing (HPC)

The computational resources needed for inundation hazard assessment tend to be dominated by the time required for inundation simulation. If N scenarios are to be simulated, and each takes T CPU-core hours, then the computational resources will be approximately NT . The time required for one inundation simulation will vary greatly from study to study. It is sensitive to the spatial and temporal extent for which high-resolution simulation is needed, and the grid size in the inundation zone. For most models if the grid size is coarsened by a factor of 2, the CPU time will decrease by (roughly) a factor of 8. Considering that inundation models use grid sizes as fine as 1 m, or as coarse as several tens of metres, the model run times can vary enormously.

For example in the Tongatapu inundation study (presented later), the majority of the island was simulated with a 7.5 m grid resolution. Each inundation simulation took approximately 1.5 hours when using four CPUs (96 cores) of the NCI Gadi supercomputer. Given the Monte Carlo sample size of 1200 scenarios (containing some repeated samples), about 150,000 CPU-core hours were needed. This would be difficult to implement without supercomputing. However the time could be substantially reduced by using a coarser grid in the inundation zone, or a smaller high-resolution area, if testing indicated this was adequate for the study purpose.

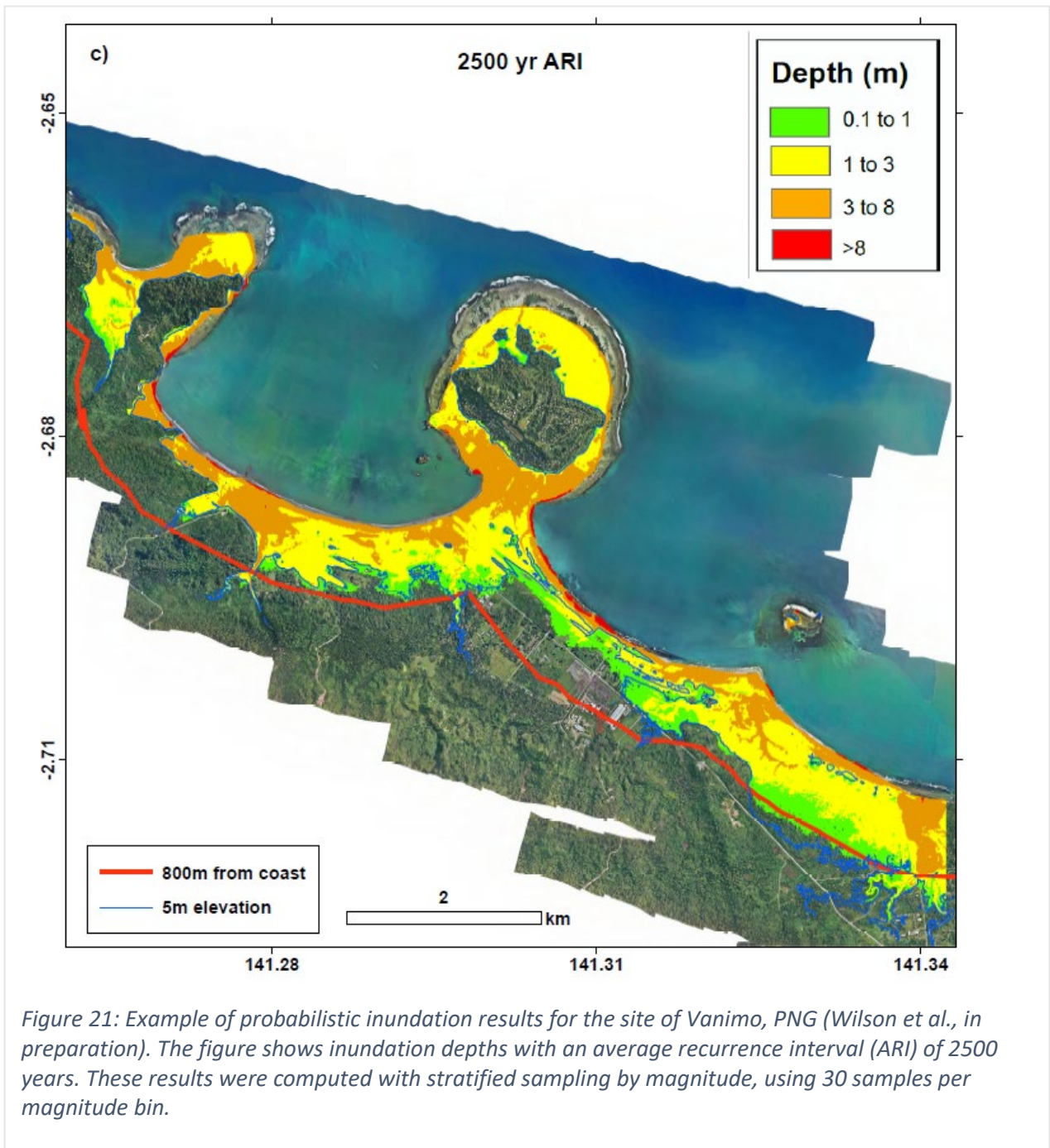
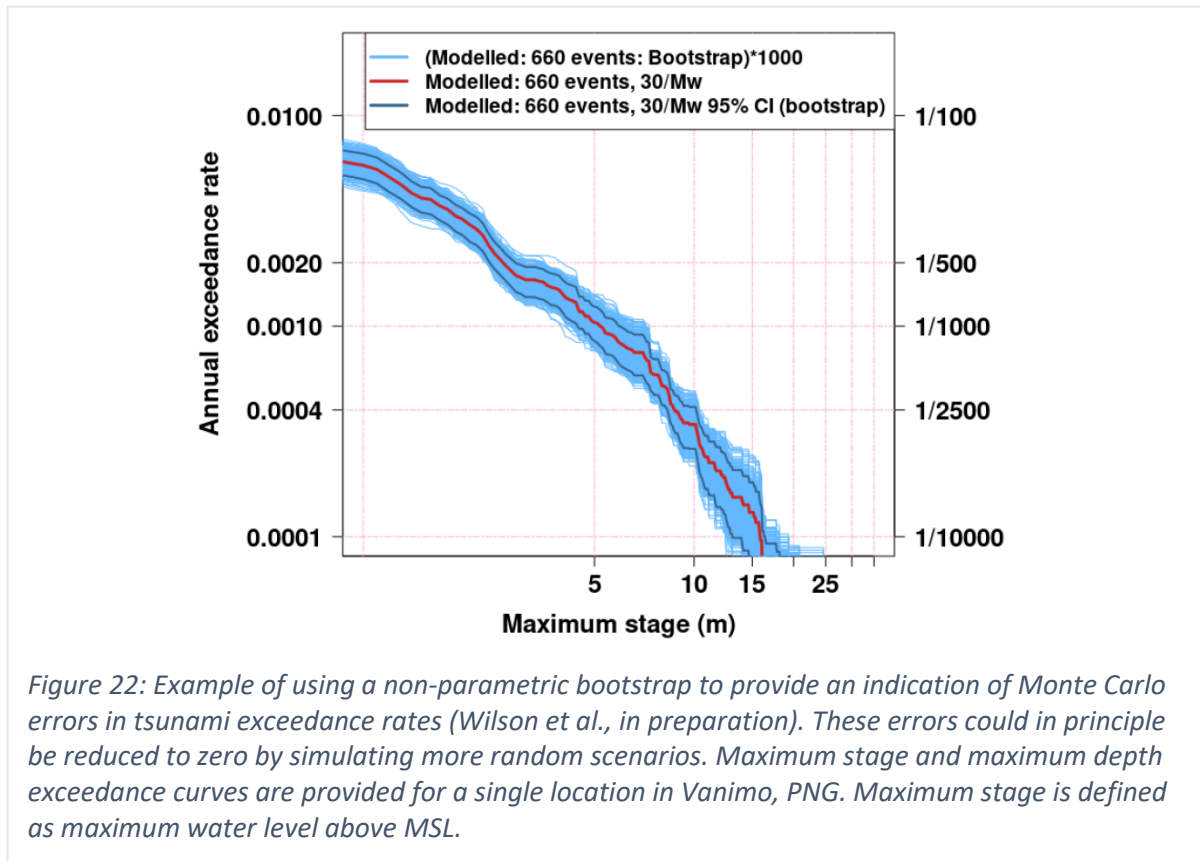


Figure 21: Example of probabilistic inundation results for the site of Vanimo, PNG (Wilson et al., in preparation). The figure shows inundation depths with an average recurrence interval (ARI) of 2500 years. These results were computed with stratified sampling by magnitude, using 30 samples per magnitude bin.

After the tsunami simulations have been completed and onshore hazard results have been derived (Figure 21), it is good practice to estimate the remaining Monte Carlo errors at sites of interest. This gives an indication of how much the results might change if we had simulated all scenarios in the PTHA18, rather than just the random Monte Carlo sample.

One approach is to use a **non-parametric percentile bootstrap** (e.g. Davison and Hinkley, 1997) to derive an approximate confidence interval for the true exceedance-rate curve (Figure 22). With this approach, one repeatedly resamples $N(M_{w,b})$ scenarios with

replacement from the sampled scenarios in each magnitude bin. Each repetition produces a new “bootstrap sample”. For each bootstrap sample the exceedance-rate curve is recomputed. When repeated many times this leads to a family of bootstrap exceedance-rate curves that reflect the Monte Carlo uncertainties (blue curves in Figure 22). The interval containing 95% of these curves is an approximate 95% confidence interval for the true exceedance rate and gives an indication of the Monte Carlo errors that remain.



Another approach to calculating onshore confidence intervals involves using the random scenarios to estimate the variance of the Monte Carlo exceedance rate (Davies et al., 2021). Assuming the exceedance-rate errors are approximately normally distributed, an approximate confidence interval for the true exceedance rate can be constructed without resampling. A tutorial on this technique is [available here](#) while the theory and equations are presented in Davies et al. (2021).

We stress that the above uncertainty calculations only quantify the approximation errors that are due to use of a limited Monte Carlo sample. This is important for quality control (to ensure that enough scenarios have been simulated), but the confidence intervals do not quantify the epistemic uncertainties (which cannot be reduced by simulating more tsunami scenarios).

Improving the efficiency of stratified sampling

In the stratified sampling technique presented above, only the earthquake magnitudes and scenario occurrence rates were used to inform the sampling method. The sampling was

independent of the offshore PTHA tsunami wave heights. In some situations this technique will sample many scenarios with small tsunamis at the site of interest. Such scenarios are usually unimportant for disaster risk management. This can be a source of inefficiency because, for a given computational budget, it reduces the number of scenarios that have hazardous waves near the site of interest and are simulated through to inundation. As a result, the hazard is less accurately characterised.

Several techniques can increase the efficiency by leveraging offshore PTHA wave-height information near the site of interest (Davies et al., 2021). The idea is to better focus Monte Carlo sampling on scenarios with large waves near the site of interest, without introducing bias. There are two basic strategies, described here, which can be applied in combination or separately: **Stratified/Importance sampling within each magnitude bin** and **Non-uniform sampling of different magnitude bins**. These are both covered in the [online tutorial](#), along with methods to [quantify their uncertainties](#). An additional method that involves ignoring small events is presented in Appendix F. In practical applications these techniques should be seriously considered to help manage the computation effort.

Stratified/importance sampling within each magnitude bin

This Monte Carlo method alters **Step 2** of stratified sampling to over-represent some scenarios, such as those with large waves at the nearest hazard point. In practice we select a hazard point near the site of interest, and adjust the scenario sampling weights in **Step 2** in proportion to the scenario tsunami maxima. As a result, scenarios with large tsunamis are more likely to be sampled. On its own this would introduce bias, but the theory of importance sampling enables weighting of the scenarios to produce unbiased exceedance-rate estimates. This leads to a modified equation for the exceedance rate in **Step 4** (in place of Equation 2).

Stratified/importance-sampling shares all the key properties of stratified sampling discussed above, but can greatly reduce the Monte Carlo approximation errors near a site of interest. This is because it can better represent tsunamis that are large (and thus of more relevance to the hazard) near the site of interest.

A tutorial on demonstrating stratified/importance sampling is provided [here](#), in particular in [this subsection](#), while the theory is presented in Davies et al. (2021).

Non-uniform sampling of different magnitude bins

Non-uniform sampling can be used to better resolve magnitude bins that are more important for a hazard assessment.

For example, if small magnitudes contribute little to the hazard at the site of interest, they do not have to be sampled, or may be assigned very few scenarios. That will increase the errors associated with those magnitude bins, but if their contribution is known at the outset to be very small, then the errors do not matter in practice. The sampling effort is better spent on magnitude bins that do contribute.

Some judgement is required to choose a good non-uniform sampling effort. A theoretically optimal solution can be computed at an offshore hazard point for a given tsunami maxima threshold and source–frequency model (Davies et al., 2021). In practice a range of such optimal solutions should be considered at offshore sites near the site of interest. These can be combined to determine non-uniform sampling effort, although the final choice remains somewhat subjective.

A tutorial on non-uniform sampling of different magnitude bins is provided [here](#), in particular in [this subsection](#). This technique can be applied in conjunction with stratified/importance sampling. In applications, that combination is likely to be the most efficient of all the approaches discussed here.

Below we present an application of non-uniform stratified/importance-sampling (i.e. the combination of both of the above techniques) to Tongatapu, the main island of Tonga. The main purpose is to illustrate the efficiency improvements that can be obtained. Full details of this example are presented in Davies et al. (2021), and a tutorial demonstrating the calculations is [here](#).

The first step is to check the performance of the Monte Carlo scheme at offshore sites. Figure 23 compares the performance of uniform stratified sampling with non-uniform stratified/importance-sampling at a PTHA18 hazard point near Tongatapu. Given the computational resources available for our study, it was feasible to simulate inundation for 1200 scenarios, and so we tested the Monte Carlo techniques using this many scenarios. For large tsunamis Figure 23 shows that non-uniform stratified/importance-sampling substantially reduces the Monte Carlo errors, compared with the basic approach. At a maximum stage of 2 m it reduces the variance of the Monte Carlo errors by a factor of about six (Figure 23). Similar results were obtained at other nearby sites. This highlights the efficiency improvements that can be obtained in practice (Davies et al., 2021).

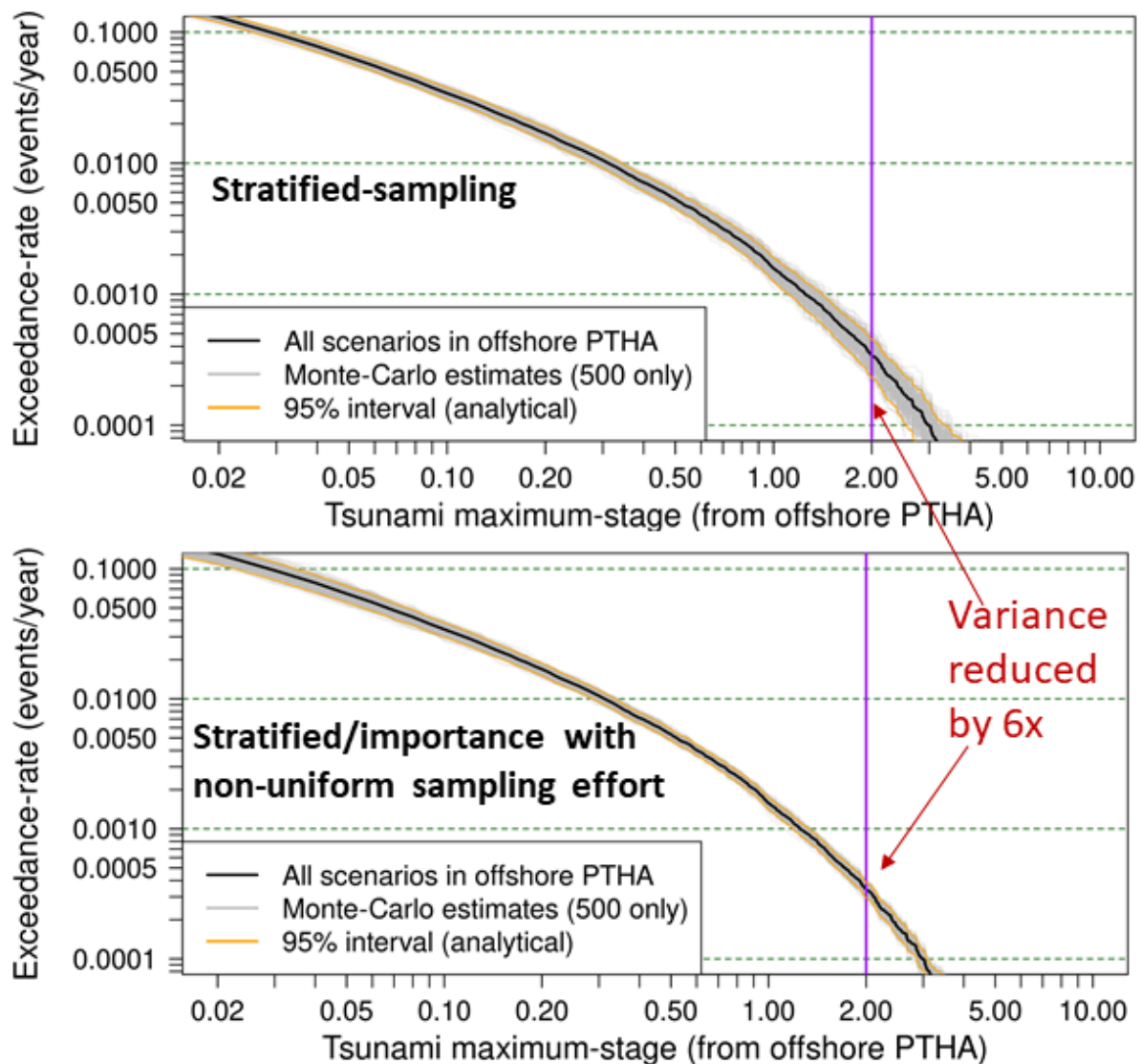
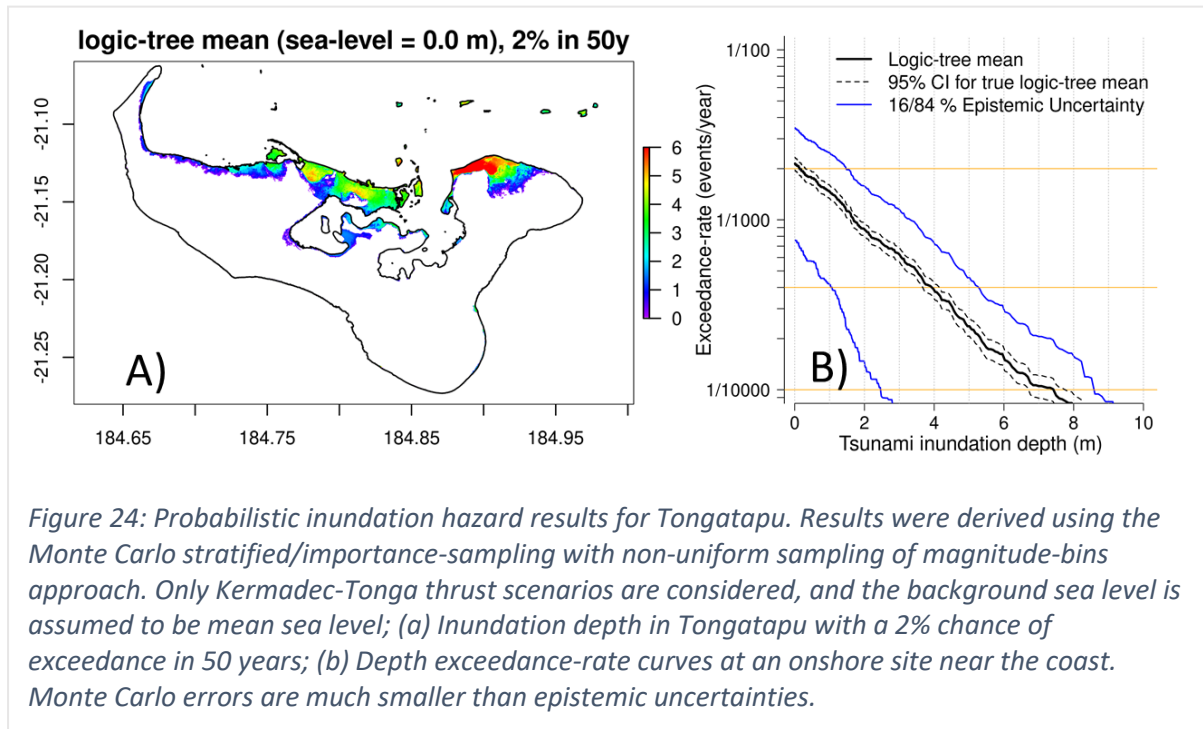


Figure 23: Comparison of the Monte Carlo accuracy of stratified sampling (top panel) with the modified sampling techniques (bottom panel) at a deep-ocean site south of Tongatapu (results at other sites are shown in Davies et al., 2021). Only thrust earthquake scenarios on the Kermadec-Tonga source zone in PTHA18 are used. The grey regions in each figure represent 500 different Monte Carlo samples so give an idea of the typical Monte Carlo errors. The black line represents the solution obtained using all scenarios in the PTHA, which the Monte Carlo technique is trying to estimate. The 95% confidence interval (in orange) was computed using the analytical variance of the Monte Carlo exceedance rates and captures the random variability of the Monte Carlo results well.

Tsunami inundation hazard results derived using non-uniform stratified/importance Monte Carlo sampling are presented in Figure 24. The tsunami simulations considered thrust scenarios on the Kermadec-Tonga trench and assume a background sea level matching the mean sea level. In practice we should also consider higher sea levels, but that is not depicted here. Figure 24a shows the estimated inundation depths with a 2% chance of exceedance in 50 years (Davies et al., 2021).

Figure 24b shows depth-vs-exceedance-rate curves at one onshore site in the model domain with a 95% confidence interval for the logic-tree-mean exceedance-rate curve. The 16th and 84th percentiles of the epistemic uncertainty distribution are also presented. It is clear that the epistemic uncertainties are far greater than the Monte Carlo errors. The epistemic uncertainties are large because the potential of the Kermadec-Tonga trench to host large magnitude thrust earthquakes is very uncertain, which is also reflected in the literature and surveys of expert opinion (e.g. Berryman et al., 2015; UNESCO/IOC, 2020).



7 Summary and Conclusions

These guidelines are designed to support Pacific island countries in using the PTHA18 to produce tsunami inundation hazard information. The document provides strategies for using the PTHA18 for scenario design in tsunami inundation hazard assessments. Guidance is provided on two practical approaches with different strengths and weaknesses.

Scenario-based: This approach is less computationally demanding than Monte Carlo sampling and is very flexible. While offering useful information, the approach does not provide probabilistic onshore results.

Monte Carlo sampling: This approach allows for mathematically rigorous translation of the offshore PTHA18 to onshore results. Outputs provide onshore tsunami hazard data with exceedance rate and uncertainty information. It is, however, more challenging to implement due to the significant computational expense of modelling a large number of scenarios.

We hope this contribution facilitates further work to reduce tsunami risk across the Pacific.

We stress that these guidelines are not intended to be overly prescriptive, or restrict the application of innovative methodologies to offshore-to-onshore PTHA, which remains a subject of research. In the longer term there is a need for further research into PTHA methodologies, coupled with efforts at standardisation that involve a broader cross-section of the community of scientists working on tsunami hazard assessment. Thus we expect the guidelines should evolve as technology advances and scientific knowledge increases.

References

- AIDR (Australian Institute of Disaster Resilience). (2018). Tsunami hazard modelling guidelines. <https://knowledge.aidr.org.au/media/5640/tsunami-planning-guidelines.pdf>
- Allen, T., & Hayes, G. P. (2017). Alternative rupture-scaling relationships for subduction interface and other offshore environments. *Bulletin of the Seismological Society of America*, *107*(3), 1240-1253. doi: 10.1785/0120160255
- Allgeyer, S., & Cummins, P. (2014). Numerical tsunami simulation including elastic loading and seawater density stratification. *Geophysical Research Letters*, *41*(7), 2368-2375. doi: 10.1002/2014GL059348
- An, C., Liu, H., Ren, Z., & Yuan, Y. (2018). Prediction of tsunami waves by uniform slip models. *Journal of Geophysical Research: Oceans*, *123*(11), 8366-8382. doi: 10.1029/2018JC014363
- Atwater, B. F., Nelson, A. R., Clague, J. J., Carver, G. A., Yamaguchi, D. K., Bobrowsky, P. T., Bourgeois, J., Darienzo, M. E., Grant, W. C., Hemphill-Haley, E., Kelsey, H. M., Jacoby, G. C., Nishenko, S. P., Palmer, S. P., Peterson, C. D. & Reinhart, M. A. (1995). Summary of Coastal Geologic Evidence for past Great Earthquakes at the Cascadia Subduction Zone. *Earthquake Spectra*, *11*(1), 1-18. doi: 10.1193/1.1585800
- Baba, T., Allgeyer, S., Hossen, J., Cummins, P. R., Tsushima, H., Imai, K., Yamashita, K. & Kato, T. (2017). Accurate numerical simulation of the far-field tsunami caused by the 2011 Tohoku earthquake, including the effects of Boussinesq dispersion, seawater density stratification, elastic loading, and gravitational potential change. *Ocean Modelling*, *111*, 46-54. doi: 10.1016/j.ocemod.2017.01.002
- Basili, R., Brizuela, B., Herrero, A., Iqbal, S., Lorito, S., Maesano, F. E., Murphy, S., Perfetti, P., Romano, F., Scala, A., Selva, J., Taroni, M., Tiberti, M. M., Thio, H. K., Tonini, R., Volpe, M., Glimsdal, S., Harbitz, C. B., Løvholt, F., Baptista, M. A., Carrilho, F., Matias, L. M., Omira, R., Babeyko, A., Hoechner, A., Gürbüz, M., Pekcan, O., Yalçiner, A., Canals, M., Lastras, G., Agalos, A., Papadopoulos, G., Triantafyllou, I., Benchekroun, S., Agrebi Jaouadi, H., Ben Abdallah, S., Bouallegue, A., Hamdi, H., Oueslati, F., Amato, A., Armigliato, A., Behrens, J., Davies, G., Di Bucci, D., Dolce, M., Geist, E., Gonzalez Vida, J. M., González, M., Macías Sánchez, J., Meletti, C., Ozer Sozdinler, C., Pagani, M., Parsons, T., Polet, J., Power, W., Sørensen, M. & Zaytsev, A. (2021). The Making of the NEAM Tsunami Hazard Model 2018 (NEAMTHM18). *Frontiers in Earth Science*, *8*. doi: 10.3389/feart.2020.616594
- Behrens, J., Løvholt, F., Jalayer, F., Lorito, S., Salgado-Gálvez, M. A., Sørensen, M., Abadie, S., Aguirre-Ayerbe, I., Aniel-Quiroga, I., Babeyko, A., Baiguera, M., Basili, R., Belliazzi, S., Grezio, A., Johnson, K., Murphy, S., Paris, R., Ralifiana, I., De Risi, R., Rossetto, T.,

- Selva, J., Taroni, M., Del Zoppo, M., Armigliato, A., Bureš, V., Cech, P., Cecioni, C., Christodoulides, P., Davies, G., Dias, F., Bayraktar, H. B., González, M., Gritsevich, M., Guillas, S., Harbitz, C. B., Kânoğlu, U., Macías, J., Papadopoulos, G. A., Polet, J., Romano, F., Salamon, A., Scala, A., Stepinac, M., Tappin, D. R., Thio, H. K., Tonini, R., Triantafyllou, I., Ulrich, T., Varini, E., Volpe, M. & Vyhmeister, E. (2021). Probabilistic Tsunami Hazard and Risk Analysis: A Review of Research Gaps. *Frontiers in Earth Science*, 9. doi: 10.3389/feart.2021.628772
- Berryman K., W. L., Hayes G., Bird P., Wang K., Basili R., Lay T., Pagani M., Stein R., Sagiya T., Rubin C., Barreintos S., Kreemer C., Litchfield N., Stirling M., Gledhill K., Haller K., Costa C. (2015). The GEM Faulted Earth Subduction Interface Characterisation Project. Global Earthquake Model Foundation.
- Bosserelle, C., Williams, S., Cheung, K. F., Lay, T., Yamazaki, Y., Simi, T., Roeber, V., Lane, E., Paulik, R. & Simanu, L. (2020). Effects of Source Faulting and Fringing Reefs on the 2009 South Pacific Tsunami Inundation in Southeast Upolu, Samoa. *Journal of Geophysical Research: Oceans*, 125(12), e2020JC016537. doi: 10.1029/2020JC016537
- Burbidge, D., Cummins, P., & Thio, H. (2009). A Probabilistic Tsunami Hazard Assessment for Western Australia (Vol. 165, pp. 2059-2088).
- Butler, R., Frazer, L. N., & Templeton, W. J. (2016). Bayesian probabilities for Mw 9.0+ earthquakes in the Aleutian Islands from a regionally scaled global rate. *Journal of Geophysical Research: Solid Earth*, 121(5), 3586-3608. doi: 10.1002/2016JB012861
- Butler, R., Walsh, D., & Richards, K. (2017). Extreme tsunami inundation in Hawai'i from Aleutian–Alaska subduction zone earthquakes. *Natural Hazards*, 85(3), 1591-1619. doi: 10.1007/s11069-016-2650-0
- Camus, P., Menéndez, M., Méndez, F. J., Izaguirre, C., Espejo, A., Cánovas, V., Pérez, J., Rueda, A., Losada, I. J. & Medina, R. (2014). A weather-type statistical downscaling framework for ocean wave climate. *Journal of Geophysical Research: Oceans*, 119(11), 7389-7405. doi: 10.1002/2014JC010141
- Cardno. (2013). NSW Tsunami Inundation Modelling and Risk Assessment. NSW State Emergency Service and the Office of Environment and Heritage. <https://www.ses.nsw.gov.au/media/2593/nswtsunamiinundationmodellingriskassessment-report.pdf>
- Chock, G. (2016). Design for Tsunami Loads and Effects in the ASCE 7-16 Standard. *Journal of Structural Engineering*, 142, 04016093. doi: 10.1061/(asce)st.1943-541x.0001565
- Chock, G. Y. K. (2015). The ASCE 7 Tsunami Loads and Effects Design Standard. *Structures Congress 2015*, 1446-1456. doi: 10.1061/9780784479117.124
- Clarke, S. L., Hubble, T. C. T., Miao, G., Airey, D. W., & Ward, S. N. (2019). Eastern Australia's submarine landslides: implications for tsunami hazard between Jervis Bay and Fraser Island. *Landslides*, 16(11), 2059-2085. doi: 10.1007/s10346-019-01223-6
- Cummins, P. (2004). Small threat, but warning sounded for tsunami research. *AusGeo News*, 75, 4-7.
- Davies, G. (2019). Tsunami variability from uncalibrated stochastic earthquake models: tests against deep ocean observations 2006–2016. *Geophysical Journal International*, 218(3), 1939-1960. doi: 10.1093/gji/ggz260
- Davies, G., Weber, R., Wilson, K. & Cummins, P. (2021). From offshore to onshore probabilistic tsunami hazard assessment via efficient Monte Carlo sampling. Unpublished preprint submitted to EarthArxiv. doi: 10.31223/X5J04W
- Davies, G., & Griffin, J. (2018). The 2018 Australian Probabilistic Tsunami Hazard

- Assessment. Record 2018/41. Canberra: Geoscience Australia.
- Davies, G., & Griffin, J. (2020). Sensitivity of Probabilistic Tsunami Hazard Assessment to Far-Field Earthquake Slip Complexity and Rigidity Depth-Dependence: Case Study of Australia. *Pure and Applied Geophysics*, 177(3), 1521-1548. doi: 10.1007/s00024-019-02299-w
- Davies, G., Griffin, J., Lovholt, F., Glimsdal, S., Harbitz, C., Thio, H. K., Lorito, S., Basili, R., Selva, J., Geist, E. & Baptista, M. A. (2017). A global probabilistic tsunami hazard assessment from earthquake sources. *Geological Society, London, Special Publications*, 456, 219-244. doi: 10.1144/sp456.5
- Davies, G., Romano, F., & Lorito, S. (2020). Global Dissipation Models for Simulating Tsunamis at Far-Field Coasts up to 60 hours Post-Earthquake: Multi-Site Tests in Australia. *Frontiers in Earth Science*, 8. doi: 10.3389/feart.2020.598235
- Davison, A., & Hinkley, D. (1997). Bootstrap Methods and Their Application. *Journal of the American Statistical Association*, 94. doi: 10.2307/1271471
- De Risi, R., & Goda, K. (2017). Simulation-Based Probabilistic Tsunami Hazard Analysis: Empirical and Robust Hazard Predictions. *Pure and Applied Geophysics*, 174(8), 3083-3106. doi: 10.1007/s00024-017-1588-9
- England, P. (2018). On Shear Stresses, Temperatures, and the Maximum Magnitudes of Earthquakes at Convergent Plate Boundaries. *Journal of Geophysical Research: Solid Earth*, 123(8), 7165-7202. doi: 10.1029/2018JB015907
- Fritz, H., & Kalligeris, N. (2008). Ancestral heritage saves tribes during 1 April 2007 Solomon Islands tsunami. *Geophysical Research Letters*, 35, L01607. doi: 10.1029/2007gl031654
- Geist, E., Titov, V., Arcas, D., Pollitz, F., & Bilek, S. (2007). Implications of the 26 December 2004 Sumatra-Andaman Earthquake on Tsunami Forecast and Assessment Models for Great Subduction-Zone Earthquakes. *Bulletin of the Seismological Society of America*, 97, 249-270. doi: 10.1785/0120050619
- Gibbons, S. J., Lorito, S., Macías, J., Løvholt, F., Selva, J., Volpe, M., Sánchez-Linares, C., Babeyko, A., Brizuela, B., Cirella, A., Castro, M. J., de la Asunción, M., Lanucara, P., Glimsdal, S., Lorenzino, M. C., Nazaria, M., Pizzimenti, L., Romano, F., Scala, A., Tonini, R., Manuel González Vida, J. & Vöge, M. (2020). Probabilistic Tsunami Hazard Analysis: High Performance Computing for Massive Scale Inundation Simulations. *Frontiers in Earth Science*, 8. doi: 10.3389/feart.2020.591549
- Giblin, J., Damlamian, H. & Davies, G. (2022). Tsunami Hazard Assessment: Samoa Case Study. Unpublished manuscript.
- Gica, E., Teng Michelle, H., Liu Philip, L. F., Titov, V., & Zhou, H. (2007). Sensitivity Analysis of Source Parameters for Earthquake-Generated Distant Tsunamis. *Journal of Waterway, Port, Coastal, and Ocean Engineering*, 133(6), 429-441. doi: 10.1061/(asce)0733-950x(2007)133:6(429)
- Goff, J. (2011). Evidence of a previously unrecorded local tsunami, 13 April 2010, Cook Islands: implications for Pacific Island countries. *Natural Hazards and Earth System Sciences*, 11(5), 1371-1379. doi: 10.5194/nhess-11-1371-2011
- Goff, J., & Terry, J. (2015). Tsunamigenic slope failures: the Pacific Islands 'blind spot'? *Landslides*. doi: 10.1007/s10346-015-0649-3
- González, M., Álvarez-Gómez, J. A., Aniel-Quiroga, Í., Otero, L., Olabarrieta, M., Omira, R., Luceño, A.; Jelinek, R.; Krausmann, E.; Birkman, J.; Baptista, M. A.; Miranda, M. & Aguirre-Ayerbe, I. (2021). Probabilistic Tsunami Hazard Assessment in Meso and

- Macro Tidal Areas. Application to the Cádiz Bay, Spain. *Frontiers in Earth Science*, 9. doi: 10.3389/feart.2021.591383
- Grezio, A., Babeyko, A., Baptista, M. A., Behrens, J., Costa, A., Davies, G., Geist, E. L., Glimsdal, S., González, F. I., Griffin, J., Harbitz, C. B., LeVeque, R. J., Lorito, S., Løvholt, F., Omira, R., Mueller, C., Paris, R., Parsons, T., Polet, J., Power, W., Selva, J., Sørensen, M. B. & Thio, H. K. (2017). Probabilistic Tsunami Hazard Analysis: Multiple Sources and Global Applications. *Reviews of Geophysics*, 55(4), 1158-1198. doi: 10.1002/2017RG000579
- Griffin, J., Latief, H., Kongko, W., Harig, S., Horspool, N., Hanung, R., Rojali, A., Maher, N., Fuchs, A., Hossen, J., Upi, S., Dewanto, S. E., Rakowsky, N & Cummins, P. (2015). An evaluation of onshore digital elevation models for modeling tsunami inundation zones. *Frontiers in Earth Science*, 3. doi: 10.3389/feart.2015.00032
- Jankaew, K., Atwater, B. F., Sawai, Y., Choowong, M., Charoentitirat, T., Martin, M. E., & Prendergast, A. (2008). Medieval forewarning of the 2004 Indian Ocean tsunami in Thailand. *Nature*, 455(7217), 1228-1231. doi: 10.1038/nature07373
- Johnston, D., Pettersson, R., Downes, G., Paton, D., Leonard, G., Pishief, K., & Bell, R. (2008). Developing an effective tsunami warning system: Lessons from the 1960 Chile earthquake tsunami for New Zealand coastal communities. *Kōtuitui: New Zealand Journal of Social Sciences Online*, 3(2), 105-120. doi: 10.1080/1177083x.2008.9522436
- Kagan, Y. Y., & Jackson, D. D. (2013). Tohoku Earthquake: A Surprise? *Bulletin of the Seismological Society of America*, 103(2B), 1181-1194. doi: 10.1785/0120120110
- Koshimura, S., & Shuto, N. (2015). Response to the 2011 Great East Japan Earthquake and Tsunami disaster. *Philosophical Transactions of the Royal Society A: Mathematical, Physical and Engineering Sciences*, 373(2053), 20140373. doi: 10.1098/rsta.2014.0373
- Lane, E. M., Gillibrand, P. A., Wang, X., & Power, W. (2013). A Probabilistic Tsunami Hazard Study of the Auckland Region, Part II: Inundation Modelling and Hazard Assessment. *Pure and Applied Geophysics*, 170(9), 1635-1646. doi: 10.1007/s00024-012-0538-9
- Lane, E. M., Mountjoy, J. J., Power, W. L., & Mueller, C. (2016). Probabilistic Hazard of Tsunamis Generated by Submarine Landslides in the Cook Strait Canyon (New Zealand). *Pure and Applied Geophysics*, 173(12), 3757-3774. doi: 10.1007/s00024-016-1410-0
- Lay, T. (2018). A review of the rupture characteristics of the 2011 Tohoku-oki Mw 9.1 earthquake. *Tectonophysics*, 733, 4-36. doi: <https://doi.org/10.1016/j.tecto.2017.09.022>
- Li, L., Switzer, A. D., Chan, C.-H., Wang, Y., Weiss, R., & Qiu, Q. (2016). How heterogeneous coseismic slip affects regional probabilistic tsunami hazard assessment: A case study in the South China Sea. *Journal of Geophysical Research: Solid Earth*, 121(8), 6250-6272. doi: 10.1002/2016JB013111
- Løvholt, F., Fraser, S., Salgado-Gálvez, M., Lorito, S., Selva, J., Romano, F., Suppasri, A., Mas, E., Polet, J., Behrens, J., Canals, M., Papadopoulos, G. A., Schaefer, A. M., Zamora, N., Chacon, S., Wood, N., Aguirre-Ayerbe, I., Aniel-Quiroga Zorilla, I., Gonzalez Rodriguez, M., Johnson, D., Leonard, G., Paris, R., Guillas, S., Dias, F. & Baptista, M. (2019). Global trends in advancing tsunami science for improved hazard and risk understanding. Contributing Paper to GAR 2019 Global Assessment Report on Disaster Risk Reduction. <https://www.undrr.org/publication/global-trends->

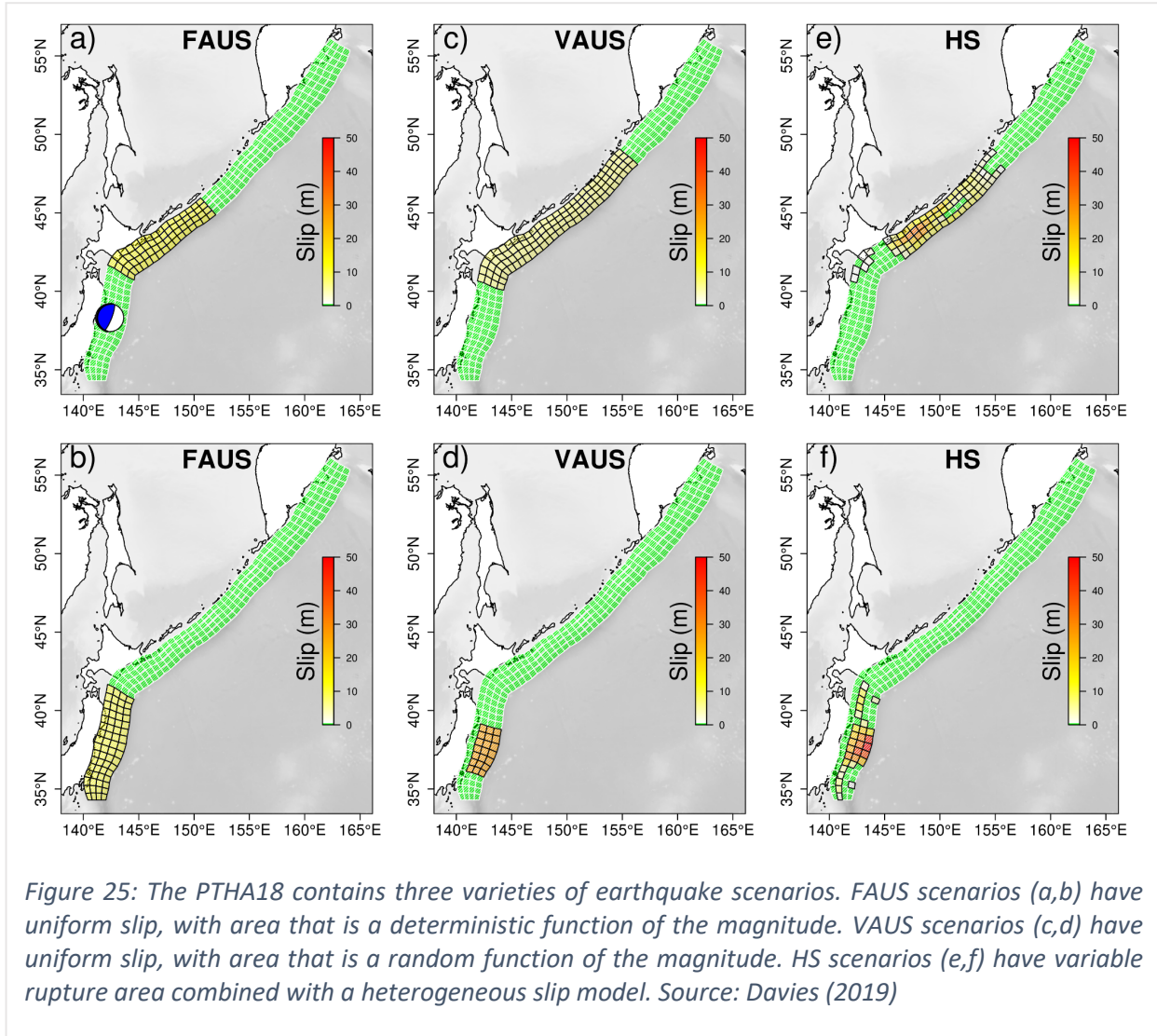
- advancing-tsunami-science-improved-hazard-and-risk-understanding
- Løvholt, F., Setiadi, N. J., Birkmann, J., Harbitz, C. B., Bach, C., Fernando, N., Kaiser, G. & Nadim, F. (2014). Tsunami risk reduction – are we better prepared today than in 2004? *International Journal of Disaster Risk Reduction*, *10*, 127-142. doi: 10.1016/j.ijdrr.2014.07.008
- Lynett, P., Wei, Y. & Arcas, D. (2016). Tsunami Hazard Assessment: Best Modeling Practices and State-of-the-Art Technology. Office of Nuclear Regulatory Research. <https://www.nrc.gov/docs/ML1635/ML16357A270.pdf>
- Martínez-Asensio, A., Wöppelmann, G., Ballu, V., Becker, M., Testut, L., Magnan, A. K., & Duvat, V. K. E. (2019). Relative sea-level rise and the influence of vertical land motion at Tropical Pacific Islands. *Global and Planetary Change*, *176*, 132-143. doi: 10.1016/j.gloplacha.2019.03.008
- Melgar, D., Williamson, A. L., & Salazar-Monroy, E. F. (2019). Differences between heterogenous and homogenous slip in regional tsunami hazards modelling. *Geophysical Journal International*, *219*(1), 553-562. doi: 10.1093/gji/ggz299
- Montoya, L., Lynett, P., Kie Thio, H., & Li, W. (2017). Spatial Statistics of Tsunami Overland Flow Properties. *Journal of Waterway, Port, Coastal, and Ocean Engineering*, *143*(2), 04016017. doi: 10.1061/(asce)ww.1943-5460.0000363
- Mueller, C., Power, W., Fraser, S., & Wang, X. (2015). Effects of rupture complexity on local tsunami inundation: Implications for probabilistic tsunami hazard assessment by example. *Journal of Geophysical Research: Solid Earth*, *120*(1), 488-502. doi: 10.1002/2014JB011301
- NGDC/WDS (National Geophysical Data Center / World Data Service). (2021). NCEI/WDS Global Historical Tsunami Database. NOAA National Centers for Environmental Information. doi:10.7289/V5PN93H7
- Nosov, M. A., Bolshakova, A. V., & Kolesov, S. V. (2014). Displaced Water Volume, Potential Energy of Initial Elevation, and Tsunami Intensity: Analysis of Recent Tsunami Events. *Pure and Applied Geophysics*, *171*(12), 3515-3525. doi: 10.1007/s00024-013-0730-6
- NTHMP (National Tsunami Hazard Mitigation Program). (2012). Proceedings and Results of the 2011 NTHMP Model Benchmarking Workshop. NOAA Special Report, National Tsunami Hazard Mitigation Program.
- Okal, E. A. (2015). The quest for wisdom: lessons from 17 tsunamis, 2004–2014. *Philosophical Transactions of the Royal Society A: Mathematical, Physical and Engineering Sciences*, *373*(2053), 20140370. doi: 10.1098/rsta.2014.0370
- Okal, E. A., Fritz, H. M., Synolakis, C. E., Borrero, J. C., Weiss, R., Lynett, P. J., Titov, V. V., Foteinis, S., Jaffe, B. E., Liu, P. L. F. & Chan, I. C. (2010). Field Survey of the Samoa Tsunami of 29 September 2009. *Seismological Research Letters*, *81*(4), 577-591. doi: 10.1785/gssrl.81.4.577
- Pakoksung K., Suppasri A., Imamura F. (2021) Probabilistic Tsunami Hazard Analysis of Inundated Buildings Following a Subaqueous Volcanic Explosion Based on the 1716 Tsunami Scenario in Taal Lake, Philippines. *Geosciences*. 11:92. doi: 10.3390/geosciences11020092
- Paris, R., Ulvrova, M., Selva, J., Brizuela, B., Costa, A., Grezio, A., Lorito S. & Tonini R. (2019). Probabilistic hazard analysis for tsunamis generated by subaqueous volcanic explosions in the Campi Flegrei caldera, Italy. *Journal of Volcanology and Geothermal Research*, *379*:106-116. doi: 10.1016/j.jvolgeores.2019.05.010
- Picard, K., Judge, M., Ferrini, V., Snaith, H., Raineault, N., Gee, L., Woelf, A. K., Wilson, K.,

- Power, H. E. (2019). Seabed Mapping: The missing link to complete and improved ocean observations. Hawaii: OceanObs.
- Pilarczyk, J. E., Sawai, Y., Namegaya, Y., Tamura, T., Tanigawa, K., Matsumoto, D., . . . Vane, C. H. (2021). A further source of Tokyo earthquakes and Pacific Ocean tsunamis. *Nature Geoscience*, *14*(10), 796-800. doi: 10.1038/s41561-021-00812-2
- Power, W., Mountjoy, J., Lane, E., Popinet, S., & Wang, X. (2016). Assessing landslide-tsunami hazard in submarine canyons, using the Cook strait canyon system as an example. *Science of Tsunami Hazards*, *35*, 145-166.
- Power, W., Wang, X., Wallace, L., Clark, K., & Mueller, C. (2018). The New Zealand Probabilistic Tsunami Hazard Model: development and implementation of a methodology for estimating tsunami hazard nationwide. *Geological Society, London, Special Publications*, *456*(1), 199. doi: 10.1144/sp456.6
- Rousselet, G. A., Pernet, C. R., & Wilcox, R. R. (2021). The Percentile Bootstrap: A Primer With Step-by-Step Instructions in R. *Advances in Methods and Practices in Psychological Science*, *4*(1), 2515245920911881. doi: 10.1177/2515245920911881
- Rueda Zamora, A., Cagigal, L., Pearson, S., Antolinez, J. A. A., Storlazzi, C., van Dongeren, A., Camus, P. & Mendez, F. (2019). HyCReWW: A Hybrid Coral Reef Wave and Water level metamodel. *Computers & Geosciences*, *127*. doi: 10.1016/j.cageo.2019.03.004
- Sannikova, N. K., Segur, H., & Arcas, D. (2021). Influence of Tsunami Aspect Ratio on Near and Far-Field Tsunami Amplitude. *Geosciences*, *11*(4). doi: 10.3390/geosciences11040178
- Satake, K., & Atwater, B. F. (2007). Long-Term Perspectives on Giant Earthquakes and Tsunamis at Subduction Zones. *Annual Review of Earth and Planetary Sciences*, *35*(1), 349-374. doi: 10.1146/annurev.earth.35.031306.140302
- Selva, J., Lorito, S., Volpe, M., Romano, F., Tonini, R., Perfetti, P., Bernardi, F., Taroni, M., Scala, A., Babeyko, A., Løvholt, F., Gibbons, S. J., Macias, J., Castro, M. J., González-Vida, J. M., Sánchez-Linares, C., Bayraktar, H. B., Basili, R., Maesano, F. E., Tiberti, M. M., Mele, F., Piatanesi, A. & Amato, A. (2021). Probabilistic tsunami forecasting for early warning. *Nature Communications*, *12*(1), 5677. doi: 10.1038/s41467-021-25815-w
- Sepúlveda, I., Liu, P. L. F., & Grigoriu, M. (2019). Probabilistic Tsunami Hazard Assessment in South China Sea With Consideration of Uncertain Earthquake Characteristics. [<https://doi.org/10.1029/2018JB016620>]. *Journal of Geophysical Research: Solid Earth*, *124*(1), 658-688. doi: <https://doi.org/10.1029/2018JB016620>
- Synolakis, C., & Kânoğlu, U. (2015). The Fukushima accident was preventable. *Philosophical Transactions of the Royal Society A: Mathematical, Physical and Engineering Sciences*, *373*(2053), 20140379. doi: 10.1098/rsta.2014.0379
- Synolakis, C. E., Bardet, J.-P., Borrero, J. C., Davies, H. L., Okal, E. A., Silver, E. A., . . . Tappin, D. R. (2002). The slump origin of the 1998 Papua New Guinea Tsunami. *Proceedings of the Royal Society of London. Series A: Mathematical, Physical and Engineering Sciences*, *458*(2020), 763-789. doi: 10.1098/rspa.2001.0915
- Titov, V., Song, Y. T., Tang, L., Bernard, E. N., Bar-Sever, Y., & Wei, Y. (2016). Consistent Estimates of Tsunami Energy Show Promise for Improved Early Warning. *Pure and Applied Geophysics*, *173*(12), 3863-3880. doi: 10.1007/s00024-016-1312-1
- Tonini, R., Di Manna, P., Lorito, S., Selva, J., Volpe, M., Romano, F., Basili, R., Brizuela, B., Castro, M. J., de la Asunción, M., Di Bucci, D., Dolce, M., Garcia, A., Gibbons, S. J., Glimsdal, S., González-Vida, J. M., Løvholt, F., Macías, J., Piatanesi, A., Pizzimenti, L.,

- Sánchez-Linares, C. & Vittori, E. (2021). Testing Tsunami Inundation Maps for Evacuation Planning in Italy. *Frontiers in Earth Science*, 9. doi: 10.3389/feart.2021.628061
- UNESCO/IOC. (2020). Experts Meeting on Tsunami Sources, Hazards, Risk and Uncertainties Associated with the Tonga-Kermadec Subduction Zone. <https://oceanexpert.org/document/26988>
- Ward, S. N., & Day, S. (2003). Ritter Island Volcano—lateral collapse and the tsunami of 1888. *Geophysical Journal International*, 154(3), 891-902. doi: 10.1046/j.1365-246X.2003.02016.x
- Williamson, A. L., Rim, D., Adams, L. M., LeVeque, R. J., Melgar, D., & González, F. I. (2020). A Source Clustering Approach for Efficient Inundation Modeling and Regional Scale Probabilistic Tsunami Hazard Assessment. [Original Research]. *Frontiers in Earth Science*, 8. doi: 10.3389/feart.2020.5916
- Wilson, K. M., Davies, G., Weber, R. The Tsunami Threat to northern Papua New Guinea: A probabilistic inundation assessment with a near-field earthquake source. Manuscript in preparation.
- Wilson, K. M., & Power, H. E. (2018). Seamless bathymetry and topography datasets for New South Wales, Australia. *Scientific Data*, 5(1), 180115. doi: 10.1038/sdata.2018.115
- Yuan, Y., Li, H., Wei, Y., Shi, F., Wang, Z., Hou, J., . . . Xu, Z. (2021). Probabilistic Tsunami Hazard Assessment (PTHA) for Southeast Coast of Chinese Mainland and Taiwan Island. *Journal of Geophysical Research: Solid Earth*, 126(2), e2020JB020344. doi: 10.1029/2020JB020344

Appendix A: PTHA18 earthquake source details

The PTHA18 database contains around 750,000 hypothetical scenarios, all generated by major earthquake source zones in the Indian and Pacific Oceans. Three alternative methods are provided for representing earthquake scenarios (Figure 25):



1. Fixed-area-uniform-slip (FAUS) scenarios have uniform slip and a rupture area that is a deterministic function of the magnitude, based on the scaling relation of Strasser et al. (2010).
2. Variable-area-uniform-slip (VAUS) scenarios have uniform slip but a stochastic rupture area, which aim to represent the observed variability in earthquake magnitude-vs-area relationships (Figure 4). For a given earthquake magnitude a range of scenarios exist, varying between compact-area-high-slip scenarios, to large-area-low-slip scenarios.

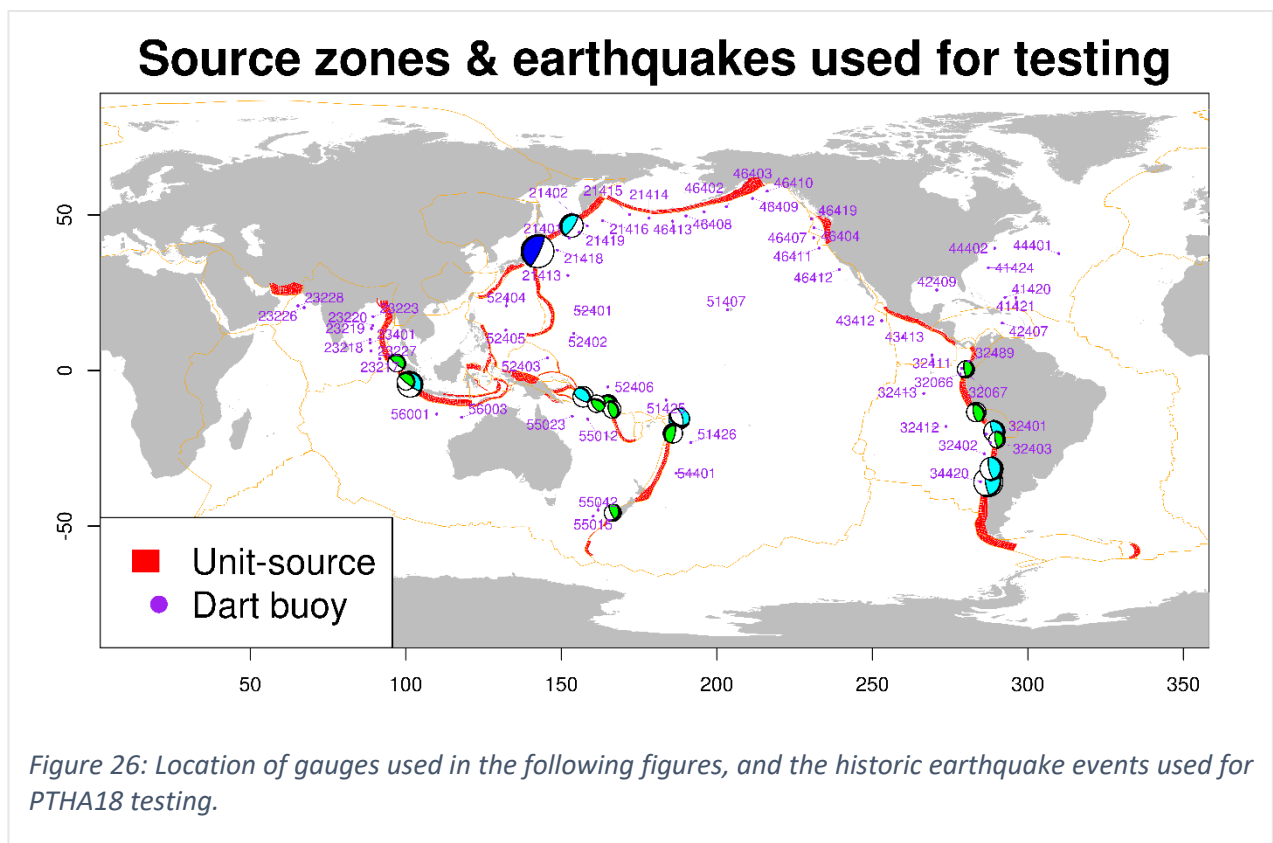
3. Heterogeneous-slip (HS) scenarios have a variable rupture area (like VAUS) as well as spatially variable slip. Real earthquakes exhibit spatially variable slip, and the HS model aims to simulate that.

Only the HS and VAUS scenarios are recommended for use in any applications. The FAUS scenarios play an important role in the implementation of the PTHA tsunami modelling, but based on the testing shown in Appendix B are not recommended for general use.

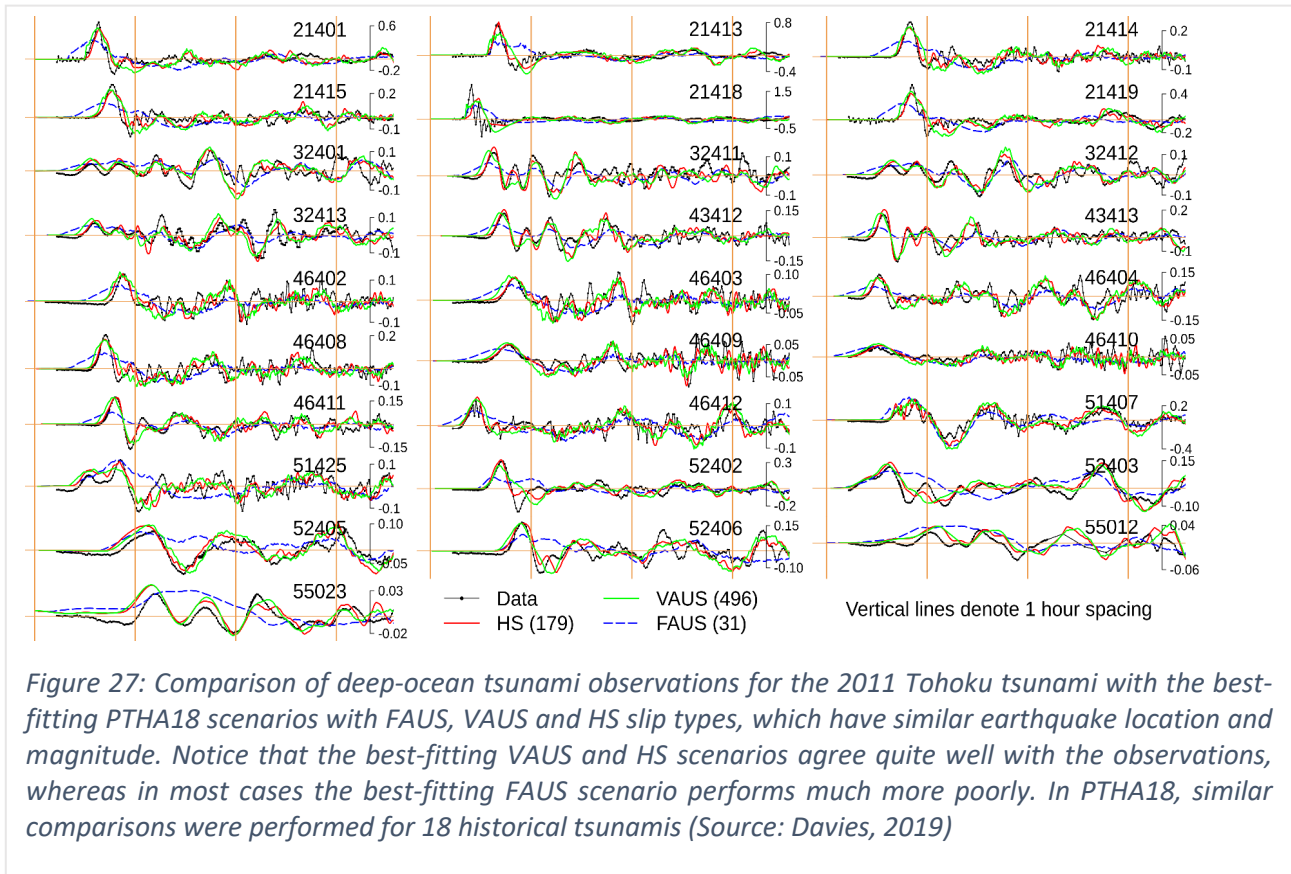
For all scenarios, the resulting tsunami is modelled globally for 36 hours of propagation time on a 1 arcmin² grid and the wave time series are stored at the hazard points in Figure 2a. Time series can be extracted from the PTHA18 database. The initial water surface deformation is also provided for all scenarios, which enables the tsunami to be simulated from source. A family of scenario occurrence-rate models is provided, along with associated source deaggregation and average recurrence interval information.

Appendix B: Testing of the PTHA18

The capacity of PTHA18 scenarios to represent real earthquake tsunamis was tested by comparison with deep-ocean observations of 18 tsunamis in 2006–2016 (Davies, 2019; Figure 26, Figure 27, Figure 28). To compare the statistical properties of modelled tsunamis with observations, for each historical event a “corresponding family of model scenarios” was defined to include all PTHA18 scenarios with earthquake magnitude and location “similar” to the observed earthquake (technical details in Davies, 2019). The core idea is that if the “corresponding family of model scenarios” gives an unbiased representation of real tsunamis,



then the 18 observed tsunamis should appear statistically like a random sample with one event drawn from each of these 18 sets of modelled scenarios. This gives a “null hypothesis” from which statistical tests can be derived to test for biases in the modelled tsunamis.



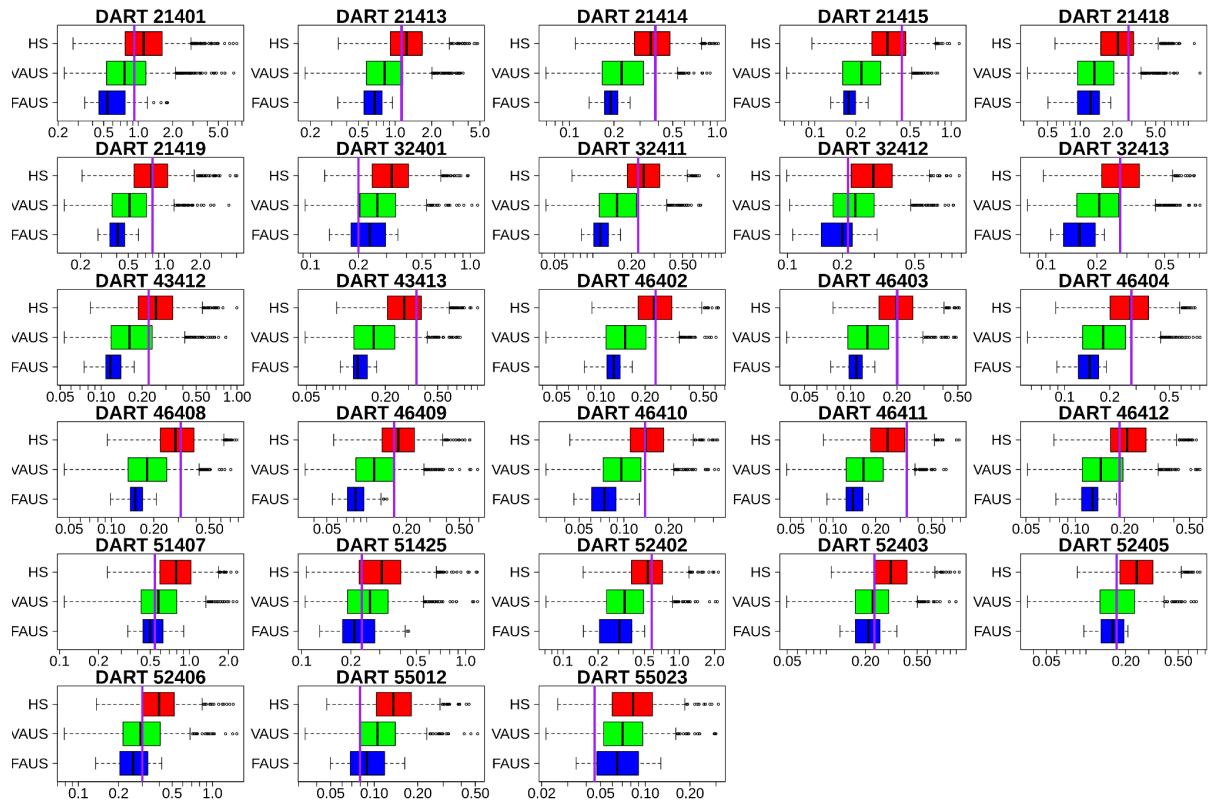


Figure 28: Comparison of a single observed tsunami and the statistical properties of random tsunami scenarios in PTHA (Davies, 2019). The 2011 Tohoku “tsunami size” is depicted at a range of deep-ocean sites with a vertical purple line (one site per panel). The tsunami size is defined as the difference between the observed water-level maxima and minima after removal of tides. The box-plots depict the modelled distribution (without bias adjustment) for PTHA18 tsunami scenarios in the “corresponding family of model scenarios” (precisely defined in Davies, 2019). At most sites, the FAUS scenarios predict tsunamis much smaller than were observed, without overlapping the observations. The VAUS scenarios overlap the observations but tend to be smaller. The HS scenarios also overlap the observations, and are not consistently smaller or larger. By repeating analysis like this for 18 historical tsunami events, PTHA18 tested for bias in the FAUS, VAUS and HS earthquake models (Source: Davies, 2019).

Based on this testing, it was found that both the HS and VAUS models have similar capacity to represent observed deep-ocean tsunamis, whereas the FAUS model performs poorly in some cases (such as for the 2011 Tohoku tsunami). This is because it neglects variations in the earthquake rupture area and average slip. The FAUS scenarios showed a statistical tendency for downward bias in tsunami wave heights, with the 2011 Tohoku tsunami being a particularly clear example (Figure 27). For this reason, FAUS scenarios in the PTHA18 database are not recommended for general use.

The PTHA18 testing also identified some biases in the tsunamis produced by random VAUS scenarios (although these biases were subsequently corrected). The VAUS scenarios that best matched observed tsunamis tended to be relatively compact (i.e. small area, high slip) compared to random scenarios, and the latter also exhibited a downward bias in tsunami wave heights (Davies, 2019). These issues were addressed with a bias adjustment that increases the occurrence rate of compact VAUS scenarios, with corresponding reductions for less compact scenarios (Davies and Griffin, 2020). Interestingly, a separate analysis by An et

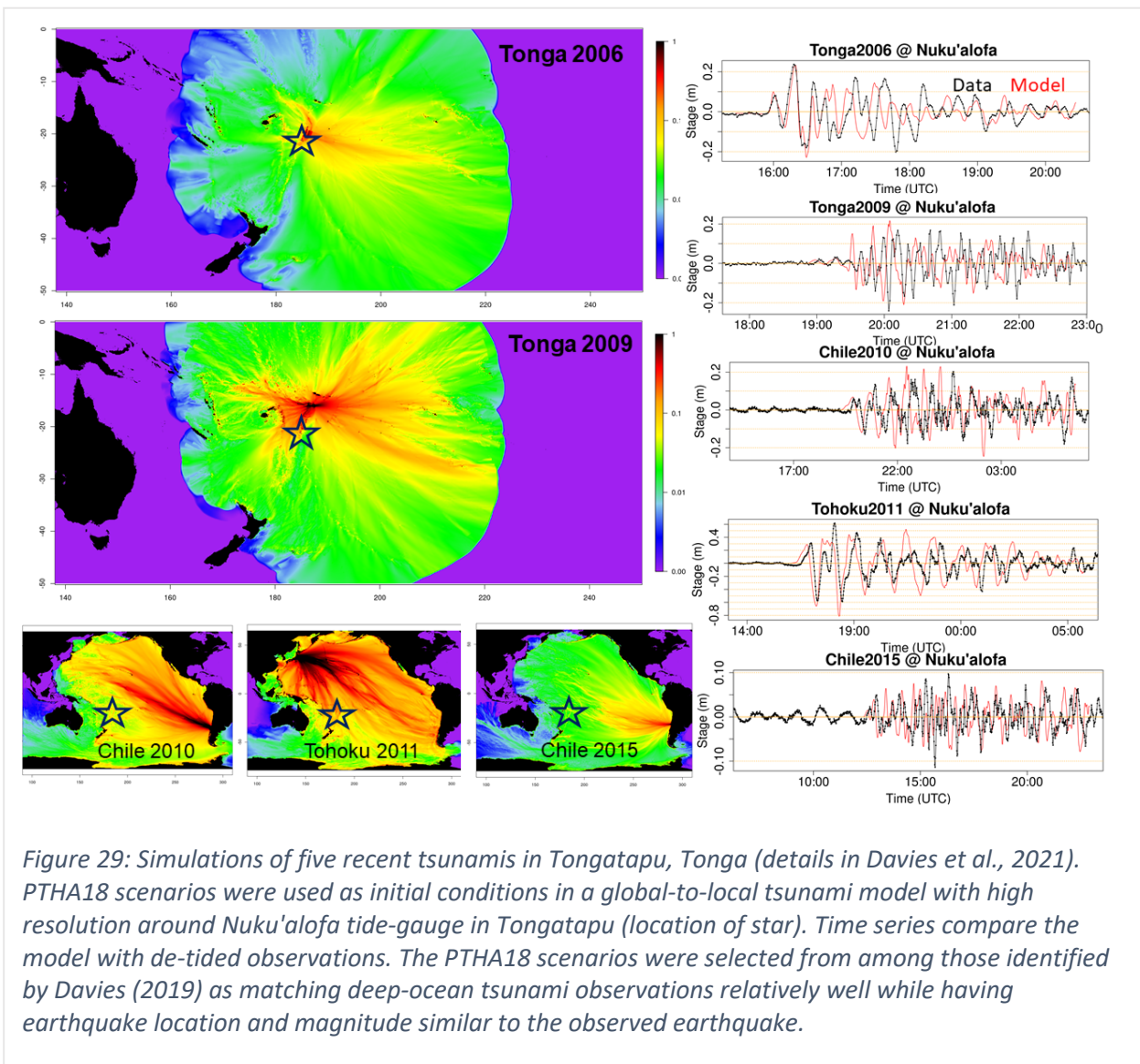
al. (2018) also favours the use of compact uniform slip for representing real earthquake tsunamis. Compact scenarios tend to produce larger tsunamis by virtue of their greater average slip. This bias adjustment is integrated into the PTHA18 scenario-occurrence-rate models, and leads to better agreement with the statistical properties of observed tsunamis (Davies, 2019; Davies and Griffin, 2020).

A similar bias analysis was conducted for the HS scenarios. In this case the bias adjustment was small. With these bias adjustments, testing to date suggests that both the VAUS and HS scenarios perform reasonably well in practice.

The above testing is restricted to deep-ocean tsunamis. The PTHA18 hydrodynamic model solves the frictionless linear shallow water equations on a nearly global 1-arcmin² grid, and while sufficient for simulating long waves in the deep ocean, it cannot directly simulate nearshore waves or inundation. However, the PTHA18 scenarios can be used to force a high-resolution nonlinear tsunami model, either using the earthquake coseismic displacement as an initial condition or using the wave time series at hazard points as a boundary condition. The initial-condition approach is generally applicable. The boundary condition approach is only possible when enough hazard points exist near the site of interest. Caution should also be applied if using the boundary condition approach to simulate tsunamis for many hours after tsunami arrival, because the frictionless linear solver does not capture late-time tsunami dissipation (Davies et al., 2020). The latter study compared modelled and observed nearshore tsunamis at 16 Australian tide gauges, and found the neglect of friction was unimportant for about 8 hours following tsunami arrival, but slowly grew in importance thereafter, with clear effects 36–60 hours post-earthquake. However, a simple transformation of the frictionless model can be applied and leads to better performance even at late times (Davies et al., 2020).

Figure 29 depicts nested-grid tsunami simulations, based on the nonlinear shallow water equations, which use initial conditions from PTHA18 to simulate nearshore waves. The hydrodynamic model has high resolution around Tongatapu in Tonga where the model is compared with nearshore tsunami observations (Figure 29). The PTHA18 scenarios were selected from among those identified by Davies (2019) as similar to some historical events (based on deep-ocean tsunami observations), but the scenarios were not otherwise tuned to force good agreement with data. However, the modelled waves give a reasonable representation of the observations at Nuku'alofa tide gauge. For the far-field events, we expect that the model will arrive slightly earlier than the observation, as seen in these

examples. This is due to the neglect of loading and seawater density stratification (Allgeyer and Cummins, 2014; Baba et al., 2017).



The other core component of PTHA18 is the scenario occurrence-rate model. This was derived by combining models of earthquake magnitude–frequencies at the source-zone level, and models that relate the scenario conditional probabilities to spatial variations in the tectonic convergence rate and also implement the aforementioned bias adjustments (details in Davies and Griffin, 2018, 2020). The scenario occurrence-rate models were constrained with a range of data, including earthquake catalogues, tectonic-plate convergence rates, and expert opinion in the 2015 GEM Faulted Earth Subduction Interface Characterisation Project (Berryman et al., 2015). The latter in part reflects knowledge of historical and paleo-tsunami data that is otherwise difficult to formally integrate into large-scale PTHAs. Bayesian techniques were used to weight the alternative models.

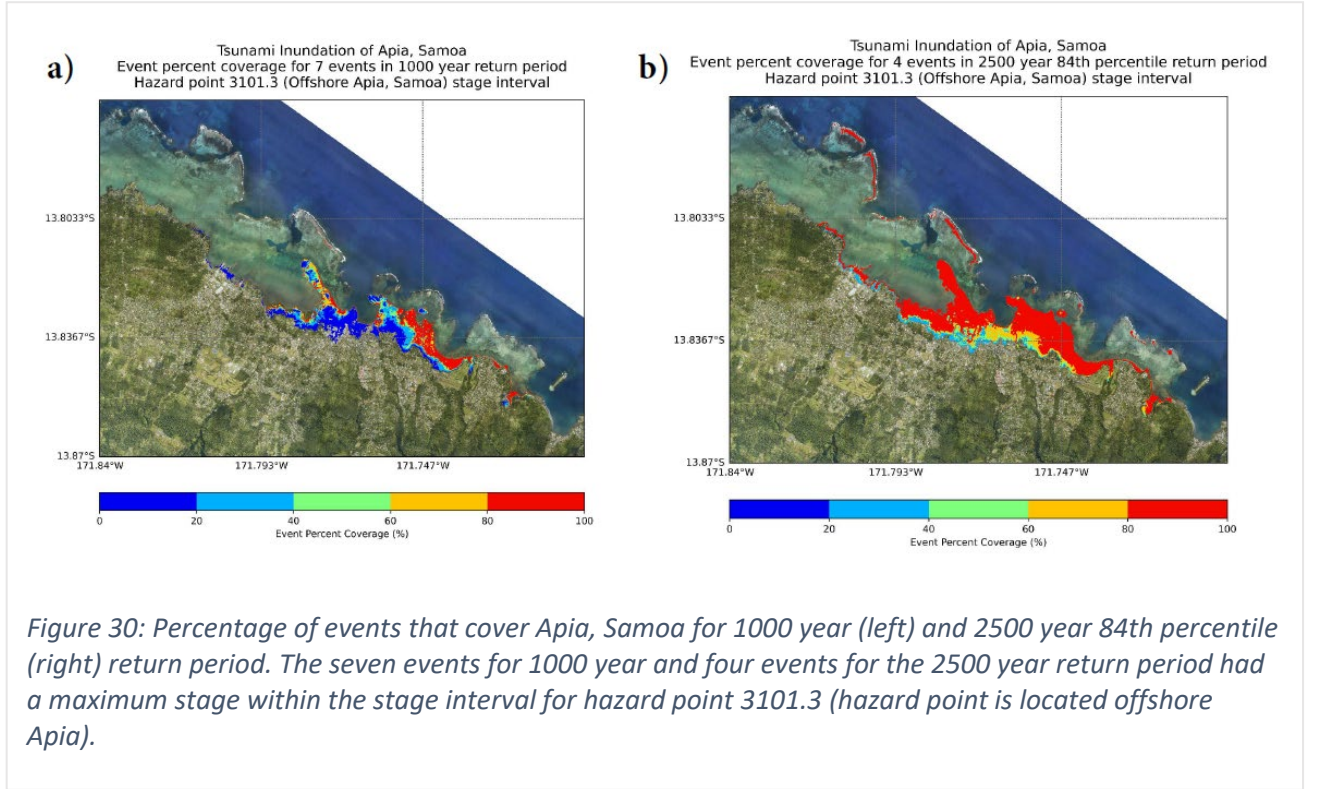
The magnitude-frequency models in PTHA18 were tested by comparison against global integrated seismicity observations (Davies and Griffin, 2018, 2020). This is a useful test because it can identify systematic biases that are not evident at the level of individual source-zones due to lack of data (e.g. Bird and Kreemer, 2015). In addition, the scenario occurrence-rate models were tested separately at seven specific sites where longer-term historical and paleoseismic data exist. The model exhibited reasonable performance considering the uncertainties (Davies and Griffin, 2020).

The information above provides only a brief summary of the PTHA18 products and testing; further details are available in the cited references and source-code repository.

Appendix C: Inundation differences for tsunamis with similar offshore wave heights.

Figure 30 provides an example that illustrates the variability of inundation between scenarios with the same offshore wave heights. The two figure panels give the percentage of scenarios inundating each site at RP 1000 year and RP 2500 year (both 84th percentile); all included scenarios had maximum stage values within the tolerance interval for hazard point 3101.3 (located offshore Apia, Samoa). Even though the offshore tsunami maxima were similar in each case, the onshore inundation extents vary. For RP 1000 year, the seven events came from three source zones: Alaska Aleutians (two events), Kurils Japan (three events) and South America (two events). The RP 2500 year had three events from Alaska Aleutians and one event from South America. The difference in the onshore inundation reflects the imperfect correlations between offshore wave heights and onshore impacts. By aggregating multiple scenarios from various source zones we expect the combined result to be conservative.

Another specific example is that outer rise normal faults may produce significantly more inundation than subduction zone sources that have a similar hazard point maximum stage value. This can happen because outer-rise sources tend to produce particularly prominent troughs (minimum stage values), which influence the wave run-up but may not be captured by the deep-water maximum stage.



Appendix D: Synthetic catalogues

Synthetic catalogues are random time series of scenarios with a given time duration D (e.g. $D = 100,000$ years). If the occurrence rate of *any* scenario in the offshore PTHA is R (events/year), and the scenario timings are independent, then the number of scenarios that occur in time duration D behaves like a random sample from a Poisson distribution with mean (RD) . Denoting the random number of scenarios as N , the synthetic catalogue may be constructed by randomly sampling N scenarios from the offshore PTHA using weighted random sampling with replacement. Here the sampling weights are proportional to the scenario occurrence rates. This leads to a synthetic catalogue containing a set of random scenarios, denoted E_{SC} below.

Once a synthetic catalogue has been created, the inundation can be simulated for each random scenario. At any site, an estimate of the average number of scenarios in any year that meets some criteria relevant to the hazard (e.g. inundation depth greater than a given threshold, such as 1 m, or 5 m) can then be computed by counting the number of such scenarios in the synthetic catalogue and dividing by D :

$$\lambda_i(Q > Q^T) \approx \sum_{e \in E_{SC}} 1_{(Q(e) > Q^T)} / D$$

where the above equation above gives an estimate of the exceedance rate that would have been obtained with the “all scenarios” approach. Although it is approximate, the advantage

is that it only requires inundation simulation for random scenarios in the synthetic catalogue (rather than every scenario in the offshore PTHA).

Synthetic catalogues lead to unbiased estimates of exceedance rates. This means that even though Monte Carlo errors may be significant in any particular synthetic catalogue, if the sampling were repeated infinitely many times then the average error would be zero. Furthermore, if the sampling were repeated many times, the standard deviation of their Monte Carlo errors would be inversely proportional to the square-root of the catalogue duration D (Davies et al., 2021). This is equivalent to the errors being inversely proportional to the square root of the average number of random scenarios in each catalogue, which as noted above, is typical for Monte Carlo techniques.

In the context of inundation PTHA, synthetic catalogues suffer from a number of inefficiencies that are not shared by the other Monte Carlo techniques discussed below. In PTHA18 and most other large-scale PTHAs, earthquake magnitude-frequency distributions have a Gutenberg–Richter type form, with low-magnitude earthquakes being much more common than high-magnitude earthquakes. Thus synthetic catalogues tend to be dominated by lower magnitude earthquakes, and as a result the Monte Carlo errors tend to be relatively large for high-magnitude earthquakes, although the latter are often more significant for hazard applications (Sepulveda et al., 2019; Williams et al., 2020). Another weakness of synthetic catalogues arises in the context of epistemic uncertainty quantification, where we wish to consider multiple scenario occurrence-rate models $i \in I$. In that case a separate synthetic catalogue should be simulated for each, which can lead to rapid growth of the number of scenarios requiring inundation simulation.

These issues are particularly challenging in the context of inundation PTHA because onshore tsunami simulations are expensive. They are much less of an issue in other contexts where tsunami simulation is not expensive, such as in some large-scale PTHAs where unit-sources and other approximations are used for tsunami computation (e.g. Li et al., 2016; Power et al., 2017). But for onshore hazard assessment, for efficiency reasons we encourage use of the techniques discussed below in preference to synthetic catalogues.

Appendix E: Stratified sampling by magnitude equations

Stratified sampling by magnitude is another common Monte Carlo approach for estimating $\lambda_i(Q > Q^T)$ in offshore-to-onshore PTHA (e.g. De Risi and Goda, 2017; Williams et al., 2020). For site-specific onshore hazard assessments, the basic stratified sampling method can also be modified to further improve the efficiency (discussed in the next section). This section presents uniform stratified sampling, because it is common and provides a basis for the other techniques.

In stratified sampling the PTHA scenarios are first *stratified* (or grouped) into separate magnitude bins. This can be done in a variety of ways. While equally spaced bins are often used, non-uniform spacing can equally well be used (e.g. Basili et al., 2021). In PTHA18 the scenario earthquake magnitudes range from 7.2 to 9.6 in increments of 0.1, and these provide a natural set of 25 different magnitude bins $M_{w,b}$:

$$M_{w,b} \in \{ (7.15, 7.25], (7.25, 7.35], \dots, (9.55, 9.65] \}$$

where each magnitude bin contains all the offshore PTHA scenarios with the associated magnitude; we denote the set of all scenarios in bin $M_{w,b}$ as E_b .

In uniform stratified sampling, a chosen number of scenarios $N(M_{w,b})$ is randomly sampled from E_b using weighted random sampling with replacement. We denote this set of random scenarios in magnitude bin $M_{w,b}$ as $E_{b,SS}$. The chance of sampling each scenario should be proportional to the scenario conditional probability within the magnitude bin, or equivalently the scenario occurrence rate $r_i(e)$. The latter are equivalent because the sampling is applied to each magnitude bin separately. For example, we might sample 12 scenarios per bin to produce 25 sets of random scenarios $E_{b,SS}$, leading to $12 \times 25 = 300$ scenarios in total. Often the number of selected scenarios $N(M_{w,b})$ is the same in each magnitude bin, like in this example, although this is not essential and below we suggest alternatives that can be more efficient.

From the offshore PTHA, for any scenario frequency model the occurrence rate of earthquakes in each magnitude bin (denoted $\lambda_i(M_{w,b})$) can be computed by summing the occurrence rates $r_i(e)$ over all PTHA scenarios in E_b . This information is readily available in the offshore PTHA. Using the random scenarios, exceedance rates for any quantity of interest Q can be approximated at any threshold Q^T as:

$$\lambda_i(Q > Q^T) \simeq \sum_{M_{w,b} \in \{ \text{All magnitude bins} \}} \lambda_i(M_{w,b}) \left(\sum_{e \in E_{b,SS}} \left[\frac{1_{(Q(e) > Q^T)}}{N(M_{w,b})} \right] \right)$$

where the equation above approximates the solution that would be obtained by simulating all scenarios. Although approximate, it has the advantage that we only need to know the quantity of interest $Q(e)$ for the random scenarios, instead of every scenario in the PTHA. In the context of inundation hazard assessment this can lead to substantial computational savings, because inundation only needs to be simulated for the random scenarios.

As compared with synthetic catalogues, a benefit of stratified sampling is that the number of scenarios in each magnitude bin does not need to mirror the occurrence rates of those magnitudes. This makes it easier to give a good representation of all magnitude bins in the analysis, even if lower magnitudes are much more common (as implied by Gutenberg–Richter type magnitude-frequency relations). Fundamentally this is because in synthetic catalogues, the sampled scenarios are themselves used to represent the scenario frequencies, whereas in stratified sampling, the sampled scenarios represent the within-magnitude-bin scenario conditional probabilities, with each bin being weighted to produce the final result.

A related advantage of stratified sampling arises when representing epistemic uncertainties using many scenario–frequency models $i \in I$. In the case of synthetic catalogues, it was noted above that many different random catalogues would be required to represent epistemic uncertainties. But for stratified sampling the same random sample can be used for

all cases, as long as all alternative models $i \in I$ imply the same within-magnitude-bin scenario conditional probabilities (i.e. within each magnitude bin, the relative frequency of each scenario is the same for all alternative models). This constraint holds for many offshore PTHAs including PTHA18, except that in PTHA18 the partially segmented source zones need to be treated on a segment-by-segment basis (full details are presented in Davies et al., 2021). As a result, for stratified sampling, random scenarios can be reused to a very large extent for epistemic uncertainty calculations. If epistemic uncertainties should be quantified, this leads to substantial computational savings compared to synthetic catalogues.

Appendix F: Excluding small scenarios based on offshore wave heights

Whatever Monte Carlo technique is used, scenarios with “small” offshore wave heights will probably be selected. In some applications, modellers will be confident that these scenarios do not contribute to the hazard at onshore sites of interest. To reduce the computational effort it may be desirable to remove “small” scenarios prior to inundation modelling. After simulating inundation for the remaining scenarios, exceedance-rate calculations can proceed by assuming $1_{(Q(e) > Q^T)} = 0$ for the “small” scenarios. The latter is correct if the “small” tsunamis are always beneath the thresholds of interest.

This requires a strategy to identify “small” scenarios prior to inundation modelling, and needs to be implemented with care to prevent bias. It is natural to exclude all scenarios with PTHA tsunami maxima below some threshold at a chosen offshore site; if the latter is near the onshore site of interest, it should be roughly indicative of the onshore tsunami impacts. The threshold used to discard scenarios could be specified from judgement, or equivalently chosen so that only the largest N scenarios are included, such as the largest 100 or 300 (Lane et al., 2012).

While this can be a useful technique it must be stressed that there are risks of introducing negative bias in the onshore hazard results, because tsunami maxima at the onshore site of interest will not be perfectly correlated with offshore wave heights. To illustrate why this can occur, Figure 31 depicts a hypothetical example with imperfect correlation between offshore and nearshore tsunami maxima. Suppose that, based on the offshore tsunami maxima, the largest 300 scenarios are selected for inundation modelling; these scenarios fall to the right of the solid vertical line in Figure 31a. Although many of these scenarios also have large nearshore tsunami maxima, they do not represent the largest 300 nearshore tsunamis; there is a tsunami maxima downward bias due to the imperfect correlation with the offshore wave heights (Figure 31). For instance, in this example the smallest selected nearshore tsunami maximum is 1.5 m, whereas the 300th ranked nearshore tsunami maxima is 2.6 m (Figure 31b). Thus, irrespective of the Monte Carlo method used, any nearshore exceedance-rate calculation for thresholds around these tsunami maxima would have substantial downward bias. The bias will vanish for sufficiently large nearshore tsunamis (>5 m in this example), once all nearshore tsunamis above that size are included in the selected scenarios (Figure 31b).

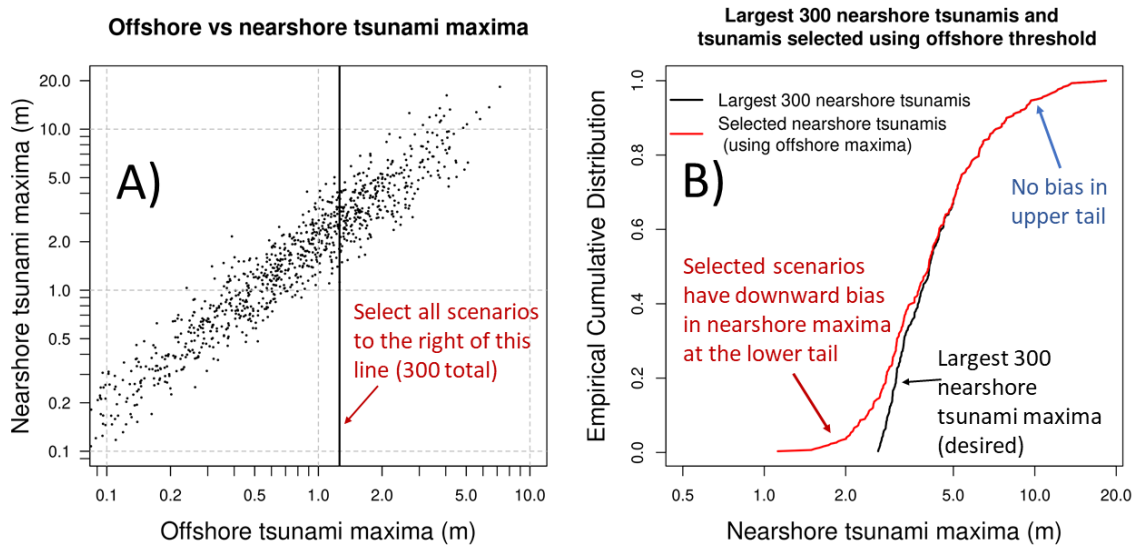


Figure 31: Hypothetical example of how biases can be introduced by discarding scenarios that are small at an offshore site: (a) Suppose we select the largest 300 scenarios based on their offshore tsunami maxima (available in an offshore PTHA). The nearshore tsunami maxima for those scenarios are generally unknown without detailed modelling, but will be imperfectly correlated with the offshore maxima; (b) Comparison of the nearshore tsunami maxima distributions for the selected scenarios, and the 300 scenarios with the largest nearshore tsunami maxima. The former differs from the latter in the lower tail. This difference is a potential source of bias in exceedance-rate calculations.

To mitigate the bias in practice, the offshore threshold must be low enough that all of the nearshore scenarios of interest are included. Just how low will depend on the degree of correlation between the offshore and nearshore tsunami size. If the latter exhibit a zero rank correlation, then any threshold would introduce bias; conversely if they exhibit a perfect rank correlation there will never be any bias. In real applications this is not known a priori, and so choosing the threshold requires careful judgement. We recommend using thresholds substantially lower than the wave heights of interest while accepting that this will come with significant additional computational expense; that is the price of avoiding biases in the final results.

Appendix G: Procuring a tsunami inundation assessment

Undertaking tsunami hazard assessments requires significant expert knowledge, and some countries may procure consultancy services to undertake these assessments on their behalf. There are known issues in the Pacific, as well as other locations around the world, with data access and copyright on assessments undertaken by consultants, as well as the difficulty in determining whether a quality product has been provided. To this end we propose a non-exhaustive checklist, largely based on the AIDR (2018) guidelines, to support governments of the Pacific Island countries and territories to procure tsunami inundation hazard assessment studies that are fit for purpose.

Key points that should be investigated to support the procurement of tsunami inundation hazard assessment study are given below.

Define the purpose of the study

The purpose of the study should be clearly identified by the procurer to help guide some key decisions in the formulation of the terms of reference, the methodology used by the consultant and the treatment of copyright. For example, the purpose of the study should guide the selection of scenarios and the resolution of the inundation model. If one purpose of the assessment is to support evacuation planning and establishment of evacuation centres, the end-user should consider the inclusion of very rare to near-unlikely events (depending on the end-user's views on the appropriate level of conservatism). Similarly, it is expected that the resolution of the inundation model would differ, depending on the risk management decision that it informs. A coarser inundation product could be procured to broadly understand tsunami risk at an island or national scale (e.g. for a pre-feasibility study) but may be less suitable to support evacuation mapping in an urban setting.

Establish an advisory or steering committee group

To ensure that the final product caters to an appropriate range of end-users, we recommend that a multidisciplinary advisory or steering committee be established to guide the study design. Whenever relevant, we suggest that governments/procurers call upon a relevant regional public servant at SPC to provide technical expert guidance through the advisory committee. Alternatively, a relevant expert from partner agencies (e.g. GA, NIWA, GNS, etc.) could also be invited.

Determine who will provide third-party Peer review

The procurer should consider seeking third party peer review to validate the quality of the assessment. This task could be sought from a relevant expert group at SPC or from relevant development partner agencies (e.g. GA, NIWA, GNS, etc.).

Determine which exceedance rates will be used

Both of the methodologies presented in this document involve the selection of exceedance rates. While applications exist for which exceedance-rate information is not needed, if it is to be used, then the choice of exceedance rates should be informed by the purpose of the study. If the terms of reference do not include a fixed set of exceedance rates to be investigated, it

is expected that a decision will be made in the early phase of the assignment in consultation with the procurer. If considering very rare exceedance rates, it is important to keep in mind that, due to maximum-magnitude uncertainties, they will likely describe scenarios that have a significant chance of being impossible.

Select the appropriate earthquake scenario

The procurer should require the consultant to follow these guidelines (or some other appropriate methodology) to ensure that the method is clearly communicated and reproducible. The approach taken (e.g. Monte Carlo or scenario-based approach) should be clearly specified by the consultant. While the Monte Carlo approach offers a more rigorous representation of tsunami frequencies and uncertainties, it is expected to be a more expensive service and could significantly reduce the pool of service providers. Hybrid approaches (e.g. Camus et al., 2014; Rueda et al., 2019) are not currently addressed in these guidelines but could also be considered. While these guidelines do not intend to be overly prescriptive about how this is done, it is important that decisions related to scenario selection are appropriately communicated by the consultant and understood by key end-users.

Select the appropriate hydrodynamic model

There are various models that can be selected to perform tsunami inundation modelling. A bid cannot be properly assessed without clear information on the numerical model that will be used. Hydrodynamic models solving the nonlinear shallow-water equations are commonly used for such assessment. The model should also enable friction, wetting and drying, and output parameters tailored to the client's need (e.g. velocities, and forces on structures). Importantly, the model selected must have been successfully tested against common benchmark tests (e.g. NTHMP, 2011). Finally, it is highly recommended for the procurer to require the use of an open source model, which will help to ensure that future tsunami studies can be built upon the work.

Validate the model

The model should be compared with historical events to provide the necessary confidence in its ability to satisfactorily reproduce real events. If nearshore and inundation datasets are available for the study sites from known tsunamigenic earthquakes, the procurer should require the consultant to validate the model against these. For sites with no local data, the client could require that the model be validated against DART buoy data (if the tsunami is modelled from the source).

Select appropriate model resolution

It is good practice for the consultant to undertake convergence testing to select the most appropriate resolution. Resolution of the model offshore typically ranges from hundreds of metres to a few kilometres, whereas it should range from one metre to tens of metres in the coastal zone. It may also depend on the purpose of the study; for example a coarser inundation product may be sufficient to broadly understand tsunami risks at an island or national scale (e.g. for a pre-feasibility study), but may be less suitable to support analysis of

loads on structures. The approach to determining the model resolution should be agreed upon by the consultant and procurer of the study in the initial study design phase.

Ensure baseline data is available

To ensure the product delivery is fit for purpose, the procurer must ensure that adequate bathymetry and topography is available for the study site before undertaking such procurement. Vertical datums must be known to accurately combine different datasets. If only relatively coarse and low accuracy datasets are available for the study site (e.g. global elevation datasets), it is expected that the resulting tsunami inundation product would carry significant uncertainty. In this situation the procurer should carefully consider whether inundation modelling will add value. Procurers are highly recommended to first invest in the procurement of appropriate baseline data.

Include structures

The consultant should also consider the inclusion of small-scale structures that could affect the tsunami inundation assessment, including the natural (e.g. beach berm) and man-made (e.g. seawall) coastal defences. Structures such as buildings and bridges could also be included. However, with large uncertainties in their ability to withstand tsunami-driven forces, these structures are commonly omitted, resulting in a more conservative inundation product.

Stipulate the friction coefficient

Friction (or roughness) coefficients are used to control how the flow energy is dissipated by interacting with the landscape and can lead to significant changes in the resulting inundation. The methodology used to define friction coefficient(s) should be clearly stipulated by the consultant. Friction coefficients can vary spatially (e.g. depending on land coverage, sea/land area), or be set as a constant value.

Determine the tide level

The tide level can play a significant role in the resulting tsunami inundation. To account for the uncertainties inherent in tsunami hazard assessment, the procurer might consider a conservative approach and require a high tide value (e.g. MHWS or HAT).

Take account of sea level rise projection scenarios and vertical land motion

If the modelling is to be used to inform long-term development strategies or infrastructure with a long lifetime, we recommend the procurer includes sea level rise scenarios in the tsunami inundation hazard assessment. These scenarios could be sourced from the latest IPCC report. Ideally, there should be a consistent approach to climate change scenario selection across the various hazard assessment studies to support multi-hazard mapping.

In addition, some Pacific islands are experiencing uplift and/or subsidence due to various reasons which affect the relative sea level.

Ensure ownership of copyrights and license agreements

Ensure that all deliverables are open access, and that the ownership belongs with the government/procurer. Government ownership is of paramount importance to ensure future projects can fully capitalise on the commissioned assessment.

Stipulate delivery formats

Ensure that all the derived products are delivered and in a format that is compatible with your own systems and following international standards and best practices. This includes:

- a. final report (digital and hard copy)
- b. all model set-up and input files
- c. inundation products (digital format and maps).

Produced by the Pacific Community (SPC)
Pacific Community
B.P.D5 - 98848 Noumea Cedex, New Caledonia
Telephone: +687 262 000
Email: spc@spc.int
Website: www.spc.int
© Pacific Community (SPC) 2022

